Theses and Dissertations   1. Thesis and Dissertation Collection, all items

2012-03

Climatological Factors Affecting Electromagnetic Surface Ducting in the Aegean Sea Region

Raptis, Konstantinos

Monterey, California. Naval Postgraduate School

https://hdl.handle.net/10945/6857

NAVAL POSTGRADUATE SCHOOL

MONTEREY, CALIFORNIA

THESIS

CLIMATOLOGICAL FACTORS AFFECTING ELECTROMAGNETIC SURFACE DUCTING IN THE AEGEAN SEA REGION

by

Konstantinos Raptis

March 2012

Thesis Co-Advisors:	Peter Guest
	Tom Murphree

Approved for public release; distribution is unlimited

THIS PAGE INTENTIONALLY LEFT BLANK

<table>
<tr><td colspan="3" align="center">**REPORT DOCUMENTATION PAGE**</td><td>*Form Approved OMB No. 0704-0188*</td></tr>
</table>

REPORT DOCUMENTATION PAGE			*Form Approved OMB No. 0704-0188*

Public reporting burden for this collection of information is estimated to average 1 hour per response, including the time for reviewing instruction, searching existing data sources, gathering and maintaining the data needed, and completing and reviewing the collection of information. Send comments regarding this burden estimate or any other aspect of this collection of information, including suggestions for reducing this burden, to Washington headquarters Services, Directorate for Information Operations and Reports, 1215 Jefferson Davis Highway, Suite 1204, Arlington, VA 22202-4302, and to the Office of Management and Budget, Paperwork Reduction Project (0704-0188) Washington DC 20503.

1. AGENCY USE ONLY *(Leave blank)*	**2. REPORT DATE** March 2012	**3. REPORT TYPE AND DATES COVERED** Master's Thesis

4. TITLE AND SUBTITLE Climatological Factors Affecting Electromagnetic Surface Ducting in the Aegean Sea Region	**5. FUNDING NUMBERS**
6. AUTHOR(S) Konstantinos Raptis	

7. PERFORMING ORGANIZATION NAME(S) AND ADDRESS(ES) Naval Postgraduate School Monterey, CA 93943-5000	**8. PERFORMING ORGANIZATION REPORT NUMBER**

9. SPONSORING /MONITORING AGENCY NAME(S) AND ADDRESS(ES) N/A	**10. SPONSORING/MONITORING AGENCY REPORT NUMBER**

11. SUPPLEMENTARY NOTES The views expressed in this thesis are those of the author and do not reflect the official policy or position of the Department of Defense or the U.S. Government. IRB Protocol number: N/A

12a. DISTRIBUTION / AVAILABILITY STATEMENT Approved for public release; distribution is unlimited	**12b. DISTRIBUTION CODE**

13. ABSTRACT (maximum 200 words)

We have studied the conditions that affect atmospheric electromagnetic surface ducts in the Aegean Sea region and how those conditions are related to regional and global scale climate variations. As a primary source for our calculations, we used radiosonde soundings from three different stations situated around the Aegean Sea, analyzing a 20-year period, from 1991 to 2010. We derived statistics on ducting parameters and correlated them with the seasonal means of selected climate system variables. We focused on seasonal and interannual variations in surface ducting frequency, height, and strength gradient.

We found that variations in low level atmospheric moisture were a dominant factor governing variations in surface ducting conditions. The moisture variations were mainly associated with fluctuations in: (1) moisture advection associated with mid-latitude cyclones in winter; and (2) local and regional evaporation in summer. The frequency of surface ducts in the summer was twice that for the winter due to larger amounts of atmospheric moisture in the summer. Variations in large-scale subsidence did not seem to significantly affect surface ducting variations. From an interannual perspective, the years that were characterized by increased moisture amounts also tended to exhibit stronger and more frequent ducting conditions for both winter and summer. We found significant correlations between Aegean surface ducting conditions and: (1) local and regional moisture($r = 0.85$ with significance level $p = 99\%$); and,(2) climate variations that affect local and regional moisture, such as those associated with the Arctic Oscillation (AO), North Atlantic Oscillation (NAO), and south Asian monsoon conditions ($r > 0.60$ with $p > 95\%$). As a by-product, we also discovered significant correlations (ranging from $r = 0.67$ to $r = 0.96$ with $p > 95\%$) between ducting parameters and the vertical resolution of the radiosonde data, indicating that differences in data collection procedures need to be accounted for when conducting ducting analyses based on radiosonde data.

14. SUBJECT TERMS Surface ducts, Ducting Conditions, Modified Refractivity, Aegean Sea, Mediterranean, Frequency, Height, Strength Gradient, Arctic Oscillation, North Atlantic Oscillation, Azores High, Indian Thermal Low, Etesian Winds, Mixing Ratio, Seasonal Variability, Interannual Variability, Radiosonde Soundings,Resolution	**15. NUMBER OF PAGES** 191
	16. PRICE CODE

17. SECURITY CLASSIFICATION OF REPORT Unclassified	**18. SECURITY CLASSIFICATION OF THIS PAGE** Unclassified	**19. SECURITY CLASSIFICATION OF ABSTRACT** Unclassified	**20. LIMITATION OF ABSTRACT** UU

NSN 7540-01-280-5500

Standard Form 298 (Rev. 2-89)
Prescribed by ANSI Std. 239-18

THIS PAGE INTENTIONALLY LEFT BLANK

**CLIMATOLOGICAL FACTORS AFFECTING ELECTROMAGNETIC
SURFACE DUCTING IN THE AEGEAN SEA REGION**

Konstantinos Raptis
Lieutenant Commander, Hellenic Navy
B.S., Hellenic Naval Academy, 1995

Submitted in partial fulfillment of the
requirements for the degree of

**MASTER OF SCIENCE IN METEOROLOGY
AND PHYSICAL OCEANOGRAPHY**

from the

**NAVAL POSTGRADUATE SCHOOL
March 2012**

Author: Konstantinos Raptis

Approved by: Dr. Peter Guest
                 Co-Advisor

                 Dr. Tom Murphree
                 Co-Advisor

                 Dr. Wendell A. Nuss
                 Chair, Department of Meteorology

iii

THIS PAGE INTENTIONALLY LEFT BLANK

ABSTRACT

We have studied the conditions that affect atmospheric electromagnetic surface ducts in the Aegean Sea region and how those conditions are related to regional and global scale climate variations. As a primary source for our calculations, we used radiosonde soundings from three different stations situated around the Aegean Sea, analyzing a 20-year period, from 1991 to 2010. We derived statistics on ducting parameters and correlated them with the seasonal means of selected climate system variables. We focused on seasonal and interannual variations in surface ducting frequency, height, and strength gradient.

We found that variations in low level atmospheric moisture were a dominant factor governing variations in surface ducting conditions. The moisture variations were mainly associated with fluctuations in: (1) moisture advection associated with mid-latitude cyclones in winter; and (2) local and regional evaporation in summer. The frequency of surface ducts in the summer was twice that for the winter due to larger amounts of atmospheric moisture in the summer. Variations in large-scale subsidence did not seem to significantly affect surface ducting variations. From an interannual perspective, the years that were characterized by increased moisture amounts also tended to exhibit stronger and more frequent ducting conditions for both winter and summer. We found significant correlations between Aegean surface ducting conditions and: (1) local and regional moisture($r = 0.85$ with significance level $p = 99\%$); and,(2) climate variations that affect local and regional moisture, such as those associated with the Arctic Oscillation (AO), North Atlantic Oscillation (NAO), and south Asian monsoon conditions ($r > 0.60$ with $p > 95\%$). As a by-product, we also discovered significant correlations (ranging from $r = 0.67$ to $r = 0.96$ with $p > 95\%$) between ducting parameters and the vertical resolution of the radiosonde data, indicating that differences in data collection procedures need to be accounted for when conducting ducting analyses based on radiosonde data.

THIS PAGE INTENTIONALLY LEFT BLANK

TABLE OF CONTENTS

LIST OF FIGURES

x

LIST OF TABLES

LIST OF ACRONYMS AND ABBREVIATIONS

ABL	Atmospheric Boundary Layer
AO	Arctic Oscillation
AP	Anomalous Propagation
CPC	Climate Prediction Center
DJF	December – January – February
E	Eastern
EM	Electromagnetic
ESRC	Earth System Research Laboratory
FMA	February – March – April
hPa	hectoPascal
JJA	June – July – August
ML	Modified refractivity Lower
MU	Modified refractivity Upper
MW	Meridional Wind
N	Northern
NAO	North Atlantic Oscillation
NCEP	National Centers for Environmental Prediction
NOAA	National Oceanic and Atmospheric Administration
NWS	National Weather Service
PR	Precipitation Rate
PSD	Physical Sciences Division
RAOBS	Radiosonde Observations
RH	Relative Humidity
SLP	Sea Level Pressure
SST	Sea Surface Temperature
UTC	Coordinated Universal Time
VW	Vector Wind
WMO	World Meteorological Organization
Z	Zulu time
ZW	Zonal Wind

THIS PAGE INTENTIONALLY LEFT BLANK

ACKNOWLEDGMENTS

THIS PAGE INTENTIONALLY LEFT BLANK

I. INTRODUCTION

A. ANOMALOUS PROPAGATION AND REFRACTIVTY

Electromagnetic (EM) radiation is photon energy propagating in the form of waves, and has both electric and magnetic field components, which oscillate in phase perpendicular to each other and perpendicular to the direction of energy propagation. In a vacuum, the waves propagate at the speed of light, whereas in the atmosphere, they propagate at slightly lower speeds. The atmosphere can have a strong effect on the propagation characteristics of EM radiation.

Variations in temperature, humidity, and pressure in the atmosphere cause changes in atmospheric density, which in turn lead to alterations in the speed of EM waves. These changes in speed induce changes in the propagation direction, or refraction, of the waves. In particular, EM waves are refracted as they cross from one medium with a given density to another medium with a different density. Refraction is always such that the waves turn toward the medium in which they travel more slowly, as they pass from a less dense medium into a denser one (Petty 2006). This is the case shown in Figure 1, where an EM ray is shown traveling through medium 1, with a relatively low density, into medium 2, with a relatively high density. The propagation speed is greater in medium 1 than in medium 2, and so the ray bends toward medium 2, as shown in Figure 1.
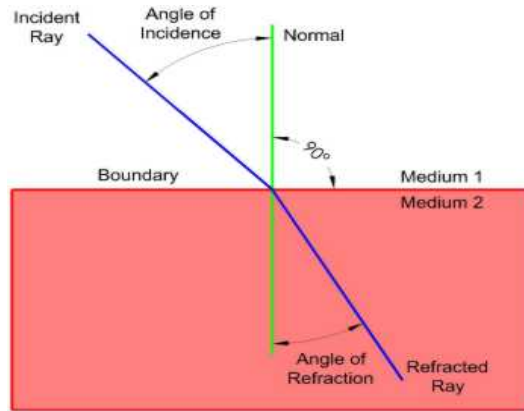
Figure 1.   Schematic depiction of an EM ray being refracted as it travels through different media. Medium 1 denotes a less dense material than medium 2. (From http://www.mysundial.ca/tsp/refraction_of_light.html, accessed January 2012)

Some refraction of EM waves is almost always present in the atmosphere. When the structure of the atmosphere causes unusual bending of EM waves, *anomalous* propagation occurs. Anomalous propagation takes place when the vertical distribution of temperature, pressure, and, most importantly, humidity in the atmosphere is significantly different from average or standard atmosphere conditions (Wallace 2006). In Figure 2, a cartoon shows examples of normal and anomalous propagation (AP) for EM radiation emitted by a radar. The AP sectors indicate regions where EM radiation is present due to unusual refractive conditions. As shown in Figure 2, AP can significantly extend or reduce the range of the emitting radar at various elevations. Therefore, anomalous propagation, denotes EM refraction outside of the norm.
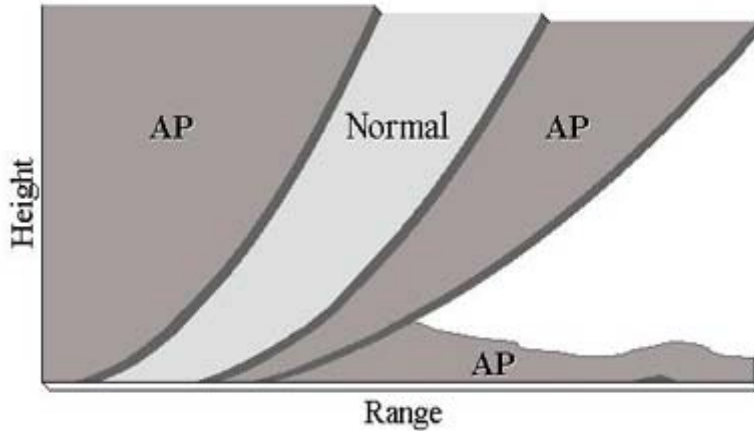
Figure 2.   Two dimensional cartoon showing how the EM energy propagates under normal and abnormal atmospheric conditions. (From http://www.idga.org/views-analysis/articles/fundamentals-of-rf-propagation-in-electronic-warfa/, accessed January 2012)

The index of refraction is a measure of the phase speed of EM radiation in a medium compared to the phase speed in a vacuum, and quantifies the refraction. The index of refraction, n, for a particular medium is defined as the ratio of the phase speed of EM radiation in vacuum, c, (i.e., the speed of light) divided by the phase speed in the medium, v, (Equation 1.1).

$$n = \frac{c}{v} \tag{1.1}$$

Because the phase speed of light is lower in the atmosphere than in a vacuum, n is greater than one. EM waves travel faster in mediums with indices of refraction closer to one for which v is relatively close to c. At Earth's surface, the index of refraction for the atmosphere has an average value of 1.000315. To avoid using values that are very close to one, a quantity called refractivity, N, is used (Equation 1.2) (Guest 2010).

$$N = (n-1)10^6 \tag{1.2}$$

This results in easy-to-use numbers (such as 315, instead of 1.000315). The refractivity, N, for EM waves in the radio frequency range depends on atmospheric pressure $P(hPa)$, Temperature $T(K)$ and water vapor pressure $e(hPa)$, according to the following formula (Guest 2010).

$$N = 77.6\frac{P}{T} - 5.6\frac{e}{T} + 3.73 \times 10^5 \frac{e}{T^2} \tag{1.3}$$

The refractivity (also known as the refractivity index), N, equals 315 at sea level in standard or average conditions. The vertical gradient of N determines the way EM energy propagates through the atmosphere in relation to the horizontal. From a ray perspective, the ratio dN/dz (N gradient) determines the amount that EM rays curves in an absolute (e.g., space) reference frame. If dN/dz is such that the ray's curvature is significantly different from what would occur in standard atmosphere conditions, then anomalous propagation arises. The amount of this departure determines the type and the amount of the anomalous propagation, as described in the following paragraphs.

A modified refractivity term, M, which includes the effect of Earth's curvature, has been adopted for practical purposes and is given as:

$$M = N + 0.157z \tag{1.4}$$

Where N is the refractivity index from (1.3) and z is the height above the surface in meters. M is dimensionless and is expressed in M-units. The second term accounts for Earth's curvature, so that the value of M represents ray curvature with respect to Earth's surface. In a standard atmosphere, because the pressure and the water vapor pressure decrease with height rapidly, while temperature decreases slowly, N decreases with altitude. On the other hand, M increases with altitude in a standard atmosphere, as depicted in Figure 3.
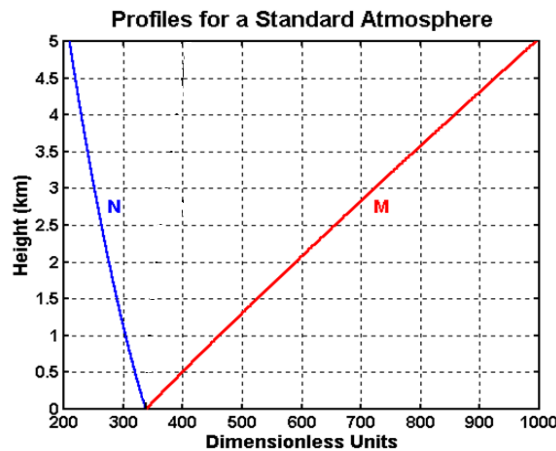
Figure 3.   Vertical profiles of N and M for a standard atmosphere (After: Guest 2010)

4

A synopsis of different types of anomalous conditions is given in Table 1. These conditions depend on how rapidly N or M varies with altitude, in response to temperature and humidity variations.

Table 1.   Types of refractive conditions and the attendant N and M gradients
(From: Turk 2010)

Refractive condition	dN/dz (N-units/km)	dM/dz (M-units/km)	Distance to Surface Horizon
Subrefraction	$0 < N$	$157 < M$	Reduced
Normal	$-79 < N < 0$	$78 < M < 157$	Standard
Super refraction	$-157 < N < -79$	$0 < M < 78$	Increased
Trapping	$N < -157$	$M < 0$	Greatly Increased

Figure 4 shows, schematically, how the different types of refractive conditions lead to alterations of the EM energy paths and, consequently, to different ranges.
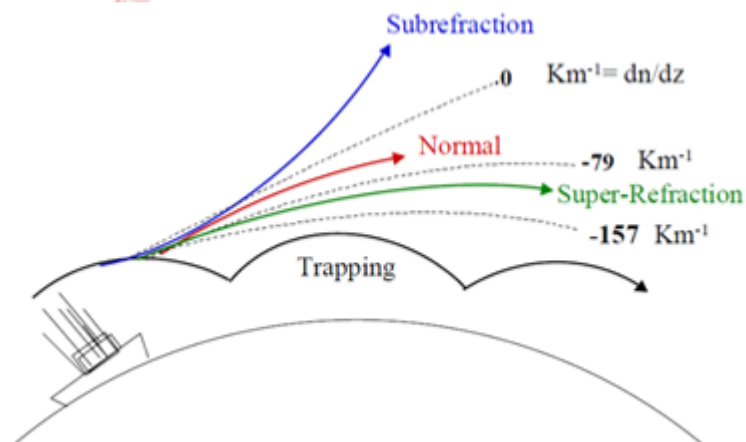
Figure 4.   Cartoon showing the different paths along which EM energy propagates under the effects of different atmospheric refractive conditions (From: Guest 2010).

This study focuses on the very last type of anomalous refractive conditions noted in Table 1, that of trapping, or ducting, as explained in the next section.

B. DUCTING CONDITIONS AND DUCTING FORMATION MECHANISMS

Ducts appear whenever the refractive conditions are such that EM energy is confined and channeled within a trapping layer located somewhere in the atmosphere. The EM signal in this case is forced to propagate, in general, within the duct boundaries. In order for these specific trapping conditions and, by extension, for ducting conditions to occur, the vertical gradient of M must be negative somewhere in its profile.

1. Ducting Formation Mechanisms

Several atmospheric circumstances lead to ducting and non-standard propagation conditions. The basic principle that is required in order for a duct to exist is that M decreases with height; conducive conditions are large decreases of humidity (water vapor pressure e) with height. Within the atmospheric boundary layer (ABL), a variety of processes can produce the necessary conditions for ducting, such as horizontal differential advection, nocturnal radiation cooling, surface fluxes, weather fronts, convective processes, and vertical variations imposed by complex terrain.

The magnitude and the duration of these processes will eventually determine their ability to form ducts and characteristics (e.g., frequency, height, strength). The existence of duct-generating mechanisms can depend on phenomena on a variety of spatial scales. Global and synoptic scale environmental conditions interact with local effects to regulate the final details of the duct-creation mechanisms.

The large-scale environment has an important effect on the moisture structure of the atmosphere. Water vapor pressure tends to play a major role in M structure (Equation 1.3). The amount of moisture in the lower levels controls the context within which the ducting mechanisms act. These mechanisms become significantly more effective when they operate under a regime of increased moisture. This is explained by the fact that the water vapor pressure e is an exponential function of temperature, as shown in Figure 5.
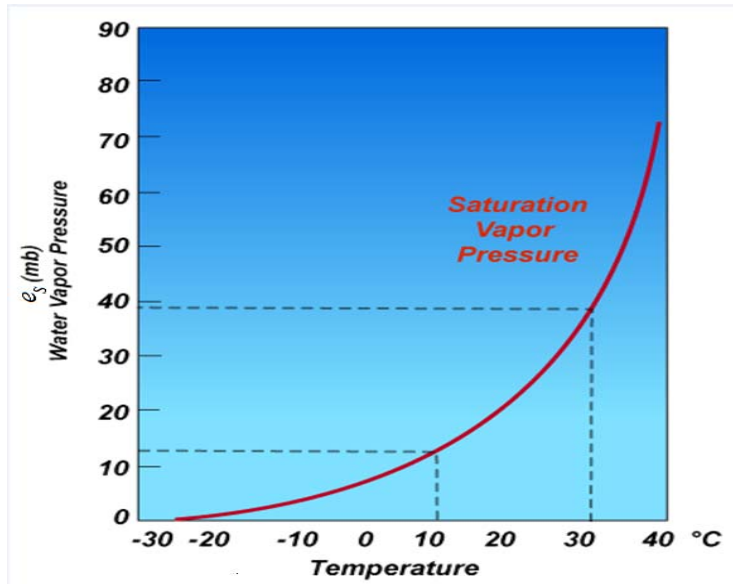
Figure 5.   Variations with temperature of the saturation water vapor pressure over a plane surface of pure water at temperature T. Note, the rapid increase of e_s when the temperature takes on values higher than 10^oC (From: http://apollo/lsc/vsc.edu/classes/met130/notes/chapter4/rh.html, accessed January 2012)

When there is a large amount of moisture in the atmosphere, then the value of the water vapor pressure e is large, and small variations in the relative humidity profile lead to large variations in e and therefore to large variations in the M profile. This effect is particularly enhanced when the air is warm because, in these situations, the e values vary the most with temperature changes. Generally, the duct-formation mechanisms are strongest under a regime of increased moisture. This aspect is explored in more detail in Chapter III, where we see that large difference in ducting occurrence between winter and summer are largely due to different moisture conditions between these two seasons.

2.   Classes of Ducts

Meteorological conditions can cause a trapping layer to occur where the base of the resultant duct is at Earth's surface. There are two types of such ducts, based on the trapping layer's location relative to Earth's surface, referred to as surface ducts and surface-based ducts, as illustrated in Figure 6.
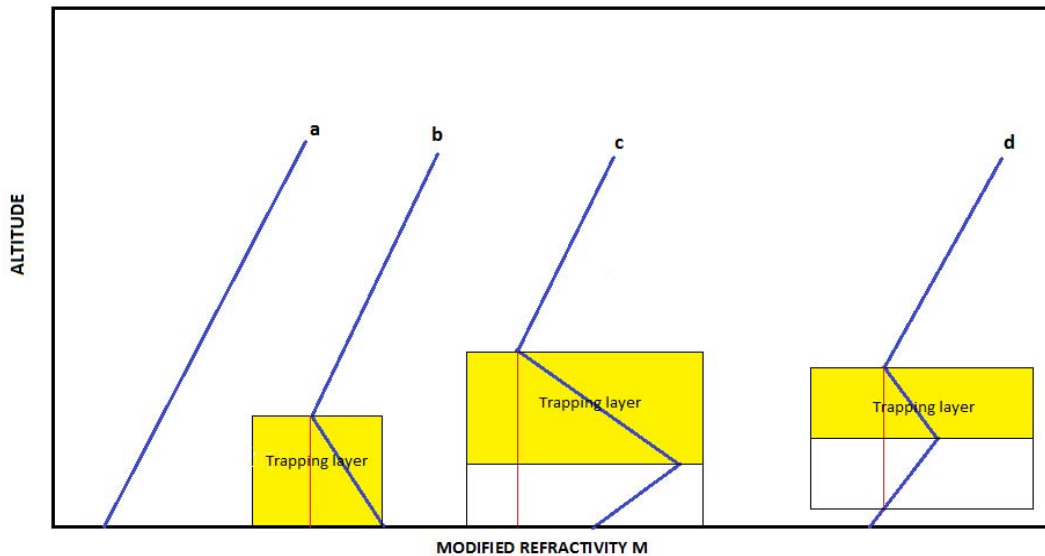
Figure 6.   Illustration of different M profiles along with the different types trapping layers and the ducts that they generate. (a) standard atmosphere – no ducting; (b) surface duct; (c) surface-based duct; and (d) elevated duct. The red line indicates the vertical extent of the ducts.

The first type is a duct created from a surface-based trapping layer (b in Figure 6). This duct is referred to as a "surface duct." The second type of duct is created from an elevated trapping layer (c in Figure 6). This duct is commonly referred to in the literature as a "surface-based duct," although some references call both types "surface ducts." If meteorological conditions cause a trapping layer to occur aloft (d), such that the base of the duct occurs above Earth's surface, then the duct is referred to as an "elevated duct," which can potentially form at any altitude of the atmospheric column. In this study, we focus on surface ducts (b in Figure 6), which are the most common type of the general class of surface ducts (ITU-R 1999a).

C.   DUCTING CLIMATOLOGY STUDIES

Knowledge of the effects of the atmosphere on EM radiation is especially important for operators of systems that use radio frequencies, such as communications and radar systems. For this reason, the study of the factors that affect the propagation of

8

EM energy is an area of active research. As previously explained, ducting conditions are important because they can lead to anomalous propagation, as described in the following quote.

> The existence of ducts is important because they can give rise to anomalous radio wave propagation, particularly on terrestrial or very low angle Earth-space links. Ducts provide a mechanism for radio wave signals of sufficiently high frequencies to propagate far beyond their normal line-of-sight range, giving rise to potential interference with other services. They also play an important role in the occurrence of multipath interference although they are neither necessary nor sufficient for multipath propagation to occur on any particular link. The existence of a duct, even if suitably situated, does not necessarily imply that energy will be efficiently coupled into the duct in such a way that long-range propagation will occur. In addition to satisfying the maximum elevation angle condition above, the frequency of the wave must be above a critical value determined by the physical depth of the duct and by the refractivity profile. Below this minimum trapping frequency, ever-increasing amounts of energy will leak through the duct boundaries. (ITU-R 1999b)

Therefore, understanding ducting enables the users of EM energy propagation to take advantage of atmospheric conditions and use it more effectively in a complicated environment. For this reason, a significant amount of research has been conducted with respect to ducting conditions and climatic factors that affect those conditions.

Ducting climatology studies often involve mapping the ducting conditions around the globe to present the information in an easy-to-understand format. Some of these studies have involved:

- Mapping of M and the associated refractive conditions (Craig et al. 1995).
- Ducting parameters statistics (probability of occurrence, height, thickness, strength, etc.) (Isaakidis et al. 2004; Von Engeln et al. 2004).
- Ducting associated with meteorological parameters (Bech et al. 2002; Zhu et al. 2005).
- Ducting variations based on weather variations (Mentes et al. 2007).
- Identification of areas favorable or unfavorable to ducting conditions (Von Engeln et al. 2004).
- Assessment and validation of data and methods used to derive ducting statistics (Craig et al. 1995; COST 2002).

- Use of satellite imagery to assess ducting variability and climatology (Helvey et al. 1995).

D. MOTIVATION AND PURPOSE OF THIS THESIS

Many of the prior ducting climatology studies have focused on how the existence and characteristics of ducts are affected by weather variations. Research efforts have been performed to derive statistics which reveal the intraseasonal and spatial variability of ducting conditions driven by large scale or synoptic scale variations of weather features (Babin 1996; Bech et al. 2002; Isaakidis et al. 2004; Zhu et al. 2005; Mentes et al. 2007). But to our knowledge, no extensive investigations have explored the connections between interannual variations of ducting and large-scale weather variations.

The main purpose of this study is to derive surface duct statistics for the Aegean Sea, and to examine the long-term variations of these statistics. This study focuses on interannual and interseasonal variations and seeks correlations between these variations and variations of global, regional, and synoptic-scale environmental conditions. A major focus is on explaining why these correlations occur and whether specific physical relationships can be identified that could lead to improved predictions of ducting conditions. Our study also includes an evaluation of the derived statistics based on the accuracy and resolution of the datasets we used in our study.

II. DATASETS AND METHODOLOGY

A. REGION AND PERIOD OF STUDY

We investigated surface ducts in the region around the Aegean Sea. The Aegean Sea is surrounded by four meteorological stations that perform radiosonde measurements and maintain an archive of upper-air data. These stations are Athens (Greece), Heraklion (Greece), Izmir (Turkey), and Thessaloniki (Greece. The focus of our study was on the first three stations for a 20-year period from 1991 through 2010. Figure 7 shows a satellite view of the area of interest and the location of the radiosonde stations.

Figure 7. Map of Aegean Sea region showing the three locations for which we analyzed radiosonde data. (After: Google maps: http://maps.google.com/maps?hl=en&tab=wl, accessed January 2012)

All three stations lie along the coastline, with their distance from it not exceeding a few hundred meters. Their altitudes are 15 m for Athens, 39 m for Heraklion and 29 m for Izmir. A geographical triangle is created by the three stations, with the maximum distance between them being 387 km (Heraklion–Izmir) and the minimum being 296 km

(Athens–Izmir). The relatively short distances between them, their location in the periphery of the same sea, the same proximity to the coastline, and almost similar altitudes render these stations ideal in terms of comparison purposes. These stations are often affected by the same large scale and regional scale weather systems and climate factors, so we can attempt to extract a clear signal of ducting variations, based on synoptic or larger environmental variations, and distinguish these from variability imposed by more local effects.

B.   DATASETS OVERVIEW

Radiosonde sounding datasets are commonly used as a source of data for the meteorological variables needed for the calculation of the modified refractivity, M. We obtained radiosonde datasets for this study from the University of Wyoming, Department of Atmospheric Science. They encompass a span of 20 years for each station. For the needs of this research, the datasets were used in the form of text files, each file containing soundings for an entire month.   More than 35,000 soundings were processed and analyzed in order to compute the respective values of M and, eventually, the corresponding ducting parameters.

For the stations we studied, soundings were taken twice every day, at 00 UTC and 12 UTC. Our ducting analyses were based on meteorological parameter values existing over these specific locations, at these specific times. Quite advantageous for this study is the fact that all of the three stations share the same time zone and the local time leads the UT by two or three hours, depending on the season. Therefore, soundings taken at 00 UTC refer to nighttime and those taken at 12 UTC refer to daytime conditions. The soundings provided a rich record of prevailing meteorological variables throughout the vertical atmospheric column. We focused not only on those parameters necessary for the computation of M, but also on those that were needed to understand the in situ weather conditions. In Figure 8, a segment of a sample sounding record is provided, in which one can notice the provided meteorological variables and the vertical levels at which they are collected. The recorded vertical levels depicted in Figure 8 are just a sample. They differ

from sounding to sounding. Many factors determine the levels at which data is recorded and the spacing between those levels, as discussed in COST Action 255 (2002).

```
16716 LGAT Athinai (Airport) Observations at 00Z 06 Jul 2007
-----------------------------------------------------------------------------
   PRES    HGHT   TEMP   DWPT   RELH   MIXR   DRCT   SKNT   THTA   THTE   THTV
   hPa      m      C      C      %     g/kg   deg    knot    K      K      K
-----------------------------------------------------------------------------
 1005.0     15    27.2   14.2    45   10.22   320     10   299.9  330.2  301.8
 1000.0     51    26.4   11.4    39    8.53   340     13   299.6  324.9  301.1
  998.0     69    26.3   11.4    39    8.54   345     13   299.6  325.0  301.2
  968.0    336    24.8   11.1    42    8.62   350     10   300.8  326.5  302.3
  937.0    621    23.2   10.7    45    8.71    25     18   301.9  328.1  303.5
  925.0    734    22.6   10.6    47    8.75    30     20   302.4  328.7  304.0
  912.0    857    22.1   10.7    49    8.95    30     20   303.1  330.1  304.7
  887.0   1099    21.0   11.0    53    9.37    15     14   304.4  332.8  306.1|
```

Figure 8.   Segment of a full sample sounding recorded from Athens station on July 06, 2007, 00 UTC (After: University of Wyoming, Department of Atmospheric Science, available online at http://www.weather.uwyo.edu/upperair/sounding.html, accessed May 2011)

C.   MODIFIED REFRACTIVITY CALCULATION

For the calculation of M, we used the following formula:

$$M = N + 0.157z = 77.6\frac{P}{T} - 5.6\frac{e}{T} + 3.73x10^5\frac{e}{T^2} + 0.157z \qquad (2.1)$$

The variables that are extracted from the sounding in order to compute M, are P in hPa, T in ^oC and RH in % and z in m. Pressure, P and altitude, z, values are directly inserted in the above formula, without any unit conversion. Temperature T is converted from K to ^oC by using the conversion $T(K) = T(^oC) + 273.15$. For the calculation of water vapor pressure, e, we have used the formula (Isaakidis et al. 2004):

$$e = \frac{RH}{100}e_s \qquad (2.2)$$

where e_s represents the saturation water vapor pressure and is further decomposed according to the expression:

$$e_s = 6.11\exp^{17.2694}\frac{T-273.15}{T-35.85} \qquad (2.3)$$

where T is expressed in K.

13

The outputs of these formulas are computed using MATLAB. The codes are based on Turk's (2010) thesis MATLAB routines. Some of them have been modified and a few new ones have been developed in order to meet the requirements of this study. The codes have been set up to run for each dataset file separately, but they give individual results for each sounding contained inside the file.

The first code used is "preprocess.m." It processes the text file of the raw data to make it readable from MATLAB. The second code used is "load_sounding.m," and is the most important one. It reads the raw data from the text file, computes the M profile, determines ducting conditions throughout the atmospheric column, and, if ducts exist, it calculates the associated ducting parameters. Within this code, two functions are included: the "theta_q.m" function, which computes the potential temperature, Θ and the specific humidity, Q, at each measured level, and the "m_n_profile.m" function, which calculates the profile of the modified refractivity. The next code is the "statistics.m" which derives ducting statistics for the period covered by each file-dataset, a month for our case. The last code used is "decode_and_save_soundings.m." It extracts the variables provided by the sounding, computes the refractivity values again, and finally tabulates all of the products in MATLAB files. Additionally, it computes the vertical resolution of the datasets, as explained in the next chapter. The "plot_all_soundings.m" code is intended for optional use. It plots the profiles of temperature, dew point, and modified refractivity for each sounding, so that one can view at a glance the vertical structure of the atmosphere. These plots are particularly useful in order to identify potentially spurious values. All of these codes are shown in Appendix B.

D. DUCTING PARAMETERS AND RELATED STATISTICS

In this study, we worked only with surface ducts that have their trapping layer attached to the ground (b in Figure 6). Two different seasons were examined: winter, comprised of December, January, and February; and summer, comprised of June, July, and August. Ducting statistics were derived separately for these two seasons. The three ducting parameters that we worked on are frequency of occurrence ("Frequency" from now on), height of duct, and strength gradient of duct.

1.   Definitions

We used the following definitions:

- Frequency: the number of surface ducts occurrence events divided by the total number of recorded soundings under consideration, expressed as a percentage. It gives the probability of occurrence.

- Height: the altitude of the minimum modified refractivity M measured from the mean sea level. It gives the upper boundary of the trapping layer.

- Strength gradient: the difference between M at the bottom and the top of the surface duct divided by the height of the duct. It gives the strength of the ducting structure.

2.   Statistics

The Frequency statistics were based on the available valid observations (soundings) at location, for an entire month. We then averaged the monthly values over a three-month period in order to calculate Frequency for the entire season. For Height and Strength gradient statistics, we used the monthly mean values, and then averaged the monthly means over a three-month period for the season. Tables with the calculated statistics are included in Appendix A.

The same method was used for the derivation of statistics for other meteorological and ducting variables necessary for our study. We created a seasonal time series of the ducting parameters for the period of interest (1991–2010) in order to monitor the yearly variations.

E.   METEOROLOGICAL VARIABLES

Various meteorological variables that can either directly or indirectly affect the ducting parameters were examined. Annual, multi-annual, and long-term seasonal means and anomalies of these variables were used to calculate correlations between them and the ducting parameters. The main source of the meteorological data was acquired from the NOAA/ESRL/PSD reanalysis datasets archive. Reanalysis datasets can be summarized as follows.

Reanalysis datasets are created by assimilating ("inputting") climate observations using the same climate model throughout the entire

15

reanalysis period in order to reduce the effects of modeling changes on climate statistics. Observations are from many different sources including ships, satellites, ground stations, RAOBS, and radar. (From NOAA/ESRL/PSD, available online at the following websitehttp://www.esrl.noaa.gov/psd/data/gridded/reanalysis)

In particular, we accessed via the ESRL site the NCEP/NCAR reanalysis dataset (Kalnay et al. 1996; Kistler et al. 2001), which can be summarized as follows.

This reanalysis was the first of its kind for NOAA. NCEP used the same climate model that was initialized with a wide variety of weather observations: ships, planes, RAOBS, station data, satellite observations and many more. By using the same model, scientists can examine climate/weather statistics and dynamic processes without the complication that model changes can cause. The dataset is kept current using near real-time observations. (From NOAA/ESRL/PSD, available online at the following website http://www.esrl.noaa.gov/psd/data/gridded/reanalysis)

With the aid of the ESRL/PSD online tools, we were able to plot seasonal composites of variables (means, anomalies, and long-term means), seasonal linear correlations of gridded variables with time series of ducting parameters that we created, and seasonal mean time series for variables averaged over an entire selected area. We used radiosonde soundings themselves as a secondary source of meteorological data. Computing tools, based on EXCEL or MATLAB software, were used as an additional aid for statistical computations (e.g., linear correlations), plotting, and other calculations.

III.   ANALYSIS AND RESULTS

A.   MAIN CLIMATOLOGICAL FEATURES OF THE AREA OF INTEREST

1.   Climate Factors Affecting the Area

The two seasons that we analyzed, winter (DJF) and summer (JJA), exhibited distinct differences over the Aegean region, that are governed by large-scale climate factors.

a.   Winter

During winter, the Aegean area is subject to extratropical cyclones entering the area from the west, having formed either over the Atlantic Ocean and western Europe or over the Mediterranean Sea. The weather associated with the passage of these depressions is dominated by southwesterly flow at the lower levels of the atmosphere, bringing high amounts of moisture and significant rainfall over the Aegean region. A secondary source of significant weather in the area is the invasion of cold air masses spawned by the Azores High and/or Siberian High (Figure 9). This cold air enters the area from the north or northeast and flows over relatively the warm water of the Aegean and bringing instability and significant weather changes (Mentes et al. 2007; Aviation Meteorology 2012).

The main systems that regulate the circulation over the Aegean area of interest are the Azores High, the Icelandic Low and the Siberian High. Figure 9 shows these major systems, with typical location and magnitude values for January. The magnitude of these global systems and the location of them relative to each other define, more or less, the main characteristics of the prevailing weather over the area of interest. Even slight variations of these systems can cause significant variations in meteorological conditions. For example, a strengthening and northward shift of the Azores High can block extratropical cyclones from entering the Aegean region, while opposite shifts can

allow extratropical cyclones to more frequently enter the Aegean region. As another example, the Siberian High can extend a ridge over eastern Europe that leads to northeasterly flow over the Aegean region.
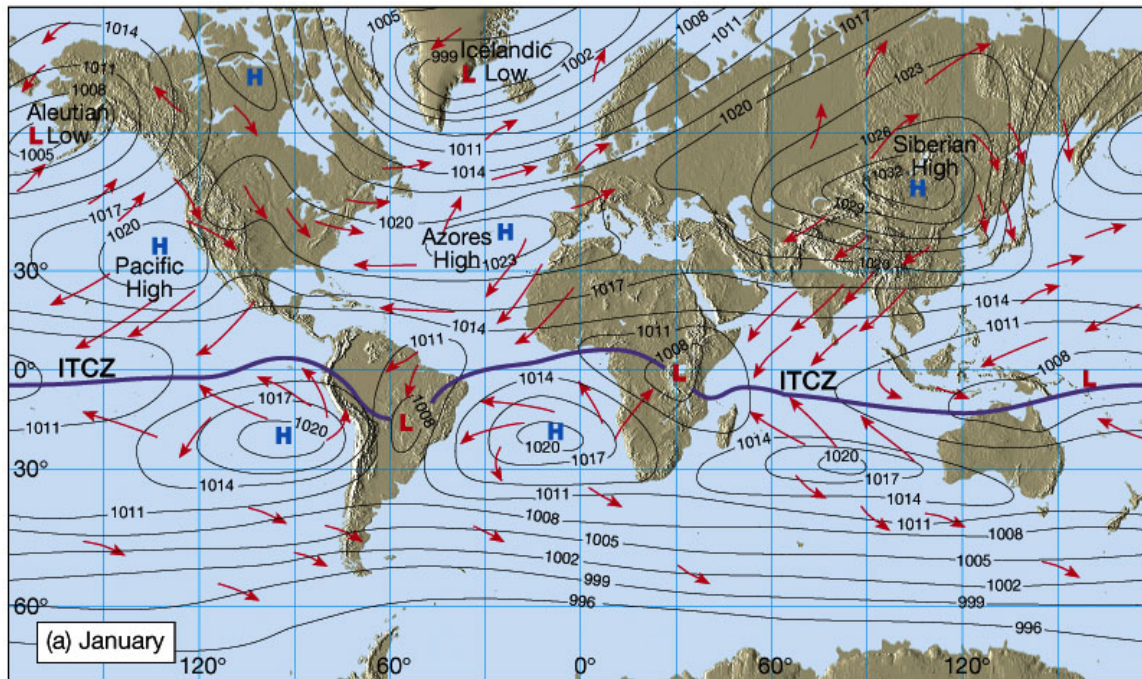
Figure 9.　　The Azores High, Icelandic Low, and Siberian High affect weather and climate in the Aegean region. Changes in the strength, position, and orientation of these large scale circulation features can cause significant changes in Aegean conditions. (From: Eastern Illinois University, Department of Geology/Geography website, available online at http://www.ux1.eiu.edu/~cfjps/1400/circulation.html, accessed January 2012)

A map of the long-term mean (climatological mean) of specific humidity, Q, at the 1000 hPa level shows relatively humid air over the main body of Mediterranean Sea compared to the surrounding land (Figure 10; cf. Romanou et al. 2010; Robinson et al. 2001). Southwesterly flow advects large amounts of moisture into the study area. On the other hand, the levels of humidity decrease when northeasterly flow sets in and brings dry, cold air from the Eurasia continental land.

NCEP/NCAR Reanalysis
1000mb Specific Humidity (g/kg) Climatology 1981–2010 climo

Dec to Feb: 1981 to 2010
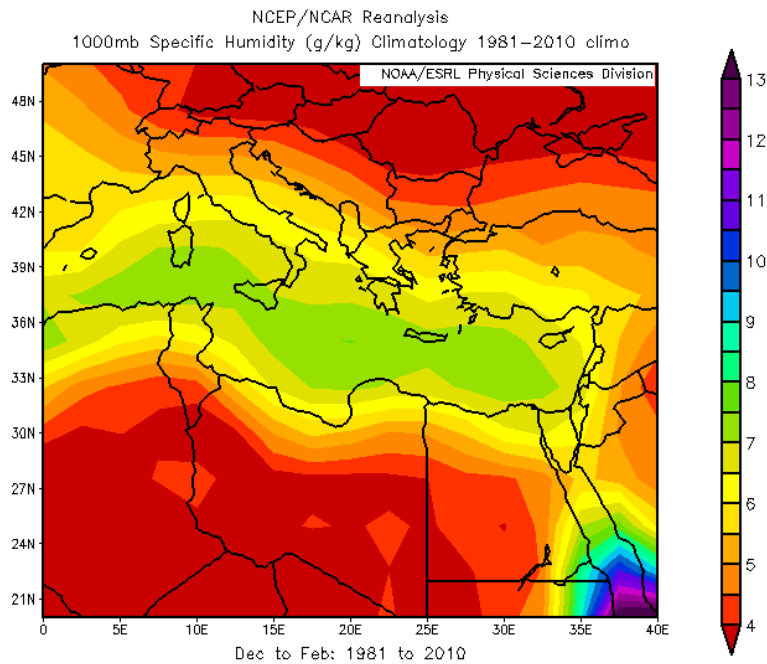
Figure 10. Long-term mean of specific humidity Q at 1000 hPa for winter. The relatively moist air over the Mediterranean can be a source of moisture for the Aegean region, while the surrounding land regions can be a source of dry air. Note the strong humidity gradient in the south-north direction over the Aegean Sea. Figure created at: NOAA/ESRL Physical Sciences Division website, available online at http://www.esrl.noaa.gov/psd/ , accessed January 2012.

b. *Summer*

During summer, the weather conditions in the Aegean region are mostly governed by the combination of the Azores High and the thermal low developing over much of southwest Asia and south-central Asia, from western India to the Red Sea. Figure 11 shows these major circulation features, with typical locations and magnitudes for July. The Azores High often extends eastward to the Balkans and causes medium and upper level subsidence over southeastern Europe and northerly or northeasterly flow over the Aegean. Northwestward extensions of the thermal low can also lead to northeasterly flow over the Aegean region (Aviation Meteorology 2012). This flow is known as the Etesian winds, which brings relatively dry air over the Aegean and the adjacent lands (Theocharis et al. 1998). Whenever the combination of these previously mentioned

systems weakens, a different circulation is set up, leaving room for westerly/southwesterly flow and, in very rare occasions, to mid-latitude disturbances propagating from Europe and the western Mediterranean. The last circulation causes winds to blow over the relatively warm eastern Mediterranean, resulting in high moisture fluxes into the atmosphere and high amounts of atmospheric moisture advection into the Aegean region.
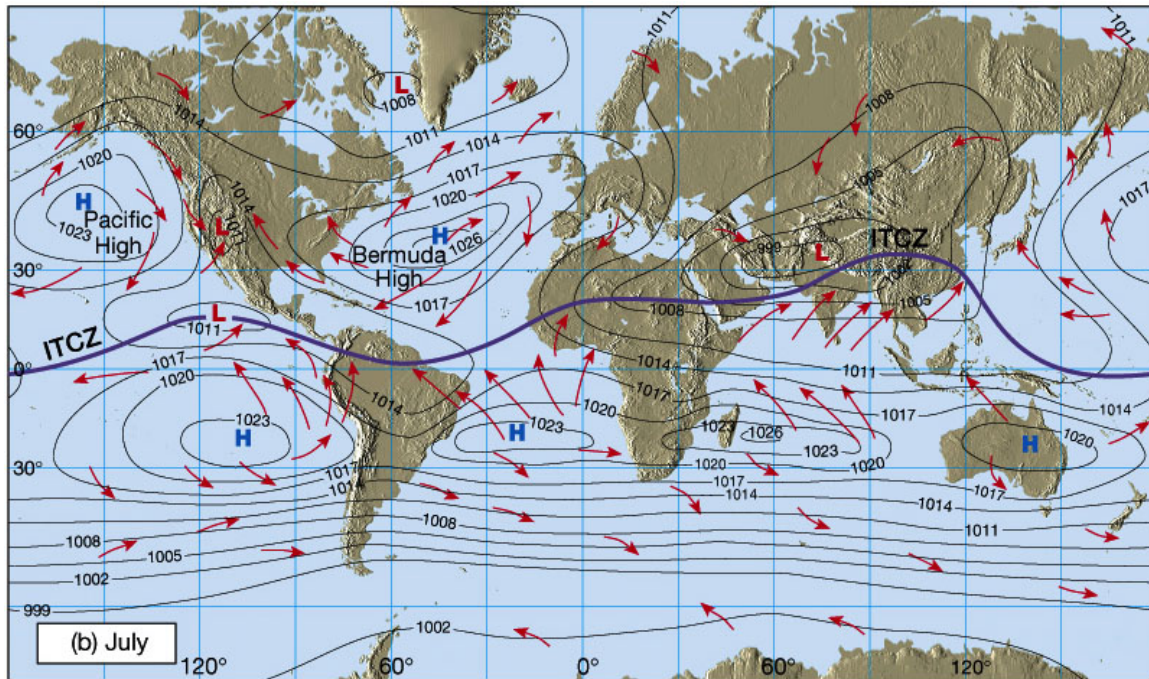
Figure 11.   The Azores or Bermuda High and southwest and south-central Asia thermal low tend to produce a northerly or northeasterly low-level flow over the Aegean region during summer. (From: Eastern Illinois University, Department of Geology/Geography website, available online at http://www.ux1.eiu.edu/~cfjps/1400/circulation.html, accessed January 2012)

Figure 12 shows the long-term mean of specific humidity, Q, at the 1000 hPa level for summer. The air over Mediterranean waters is relatively moist due to warm waters and high moisture fluxes to the atmosphere. The Aegean region is relatively dry due to its relatively cool waters and its being surrounded on three sides by land with relatively dry air (Skliris et al. 2011). Note that the summer values of Q are approximately double those in winter (Figure 10).
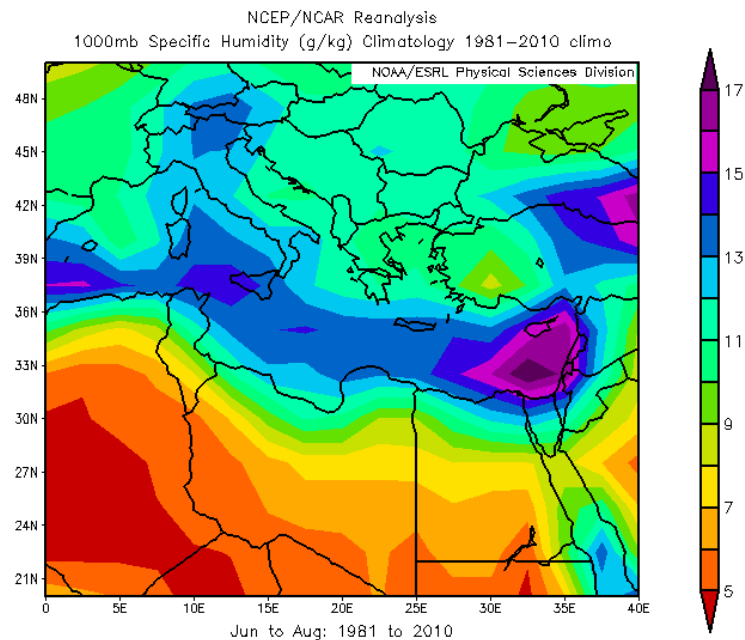
Figure 12.　　　Long-term mean of specific humidity Q at 1000 hPa for summer. The relatively moist air over the Mediterranean can be a source of moisture for the Aegean region. Figure created at: NOAA/ESRL Physical Sciences Division website, available online at http://www.esrl.noaa.gov/psd/ , accessed January 2012.

2.　　　Teleconnections

Well-established teleconnections have been discovered, which link the climate variations in the eastern Mediterranean region with variations in remote regions of the globe. The most robust of these are the Arctic Oscillation (AO) and North Atlantic Oscillation (NAO) during winter (Jacobeit et al. 2007; Zervakis et al. 2004). Both of these atmospheric oscillations, during their positive phases, create patterns that block the propagation of depressions and frontal activity from the Atlantic Ocean towards the eastern Mediterranean. The opposite happens during their negative phases. As a result, the Aegean region tends to experience anomalously dry and cool conditions during the positive phases, and anomalously wet and warm conditions during the negative phases of these two modes. The AO can be summarized as follows.

The AO is an intraseasonal and interseasonal oscillation in the strength of the northern polar vortex. In the positive AO phase (+AO), the polar vortex is anomalously strong and well defined, while in the negative AO phase (-AO), the polar vortex is anomalously weak and diffuse. +AO: Strong polar vortex leads to strong westerlies in midlatitudes, and confinement of midlatitude storm tracks to anomalously high latitudes, where precipitation and temperature anomalies are positive. Lower latitudes in midlatitudes have negative precipitation and temperature anomalies. –AO: Weak polar vortex leads to weak westerlies in midlatitudes, and southward shift of midlatitude storm tracks to anomalously low latitudes, where precipitation and temperature anomalies are positive. Higher latitudes in midlatitudes have negative precipitation and temperature anomalies. (Murphree 2011)

Figure 13 illustrates the AO phases and their associated impacts on Europe.
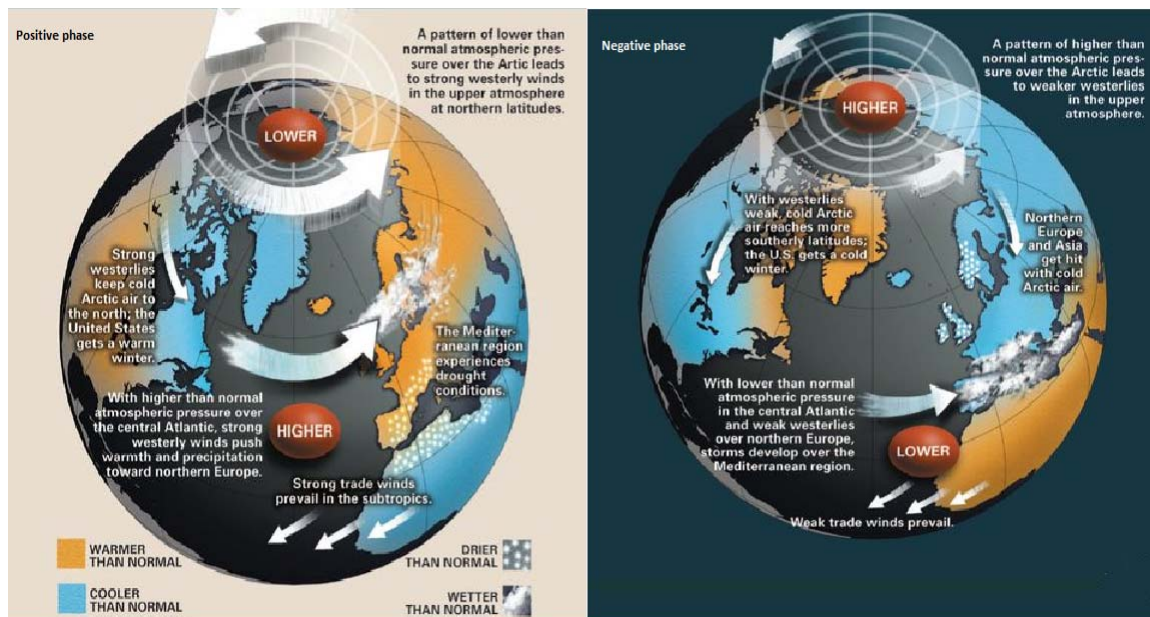
Figure 13.   Schematic illustration of the AO positive phase (left panel) and negative phase (right panel). (After: http://jisao.washington.edu/wallace/natgeo/ArcticSubart.pdf, accessed January 2012)

The NAO is closely related to the AO and can be summarized as follows.

The NAO consists of a north-south dipole of anomalies, with one center located over Greenland and the other center of opposite sign spanning the central latitudes of the North Atlantic between 35°N and 40°N. The positive phase of the NAO reflects below-normal heights and pressure

across the high latitudes of the North Atlantic and above-normal heights and pressure over the central North Atlantic, the eastern United States and Western Europe. The negative phase reflects an opposite pattern of height and pressure anomalies over these regions. Both phases of the NAO are associated with basin-wide changes in the intensity and location of the North Atlantic jet stream and storm track. Strong positive phases of the NAO tend to be associated with above-average temperatures in the eastern United States and across northern Europe and below-average temperatures in Greenland and oftentimes across southern Europe and the Middle East. They are also associated with above-average precipitation over northern Europe and Scandinavia in winter, and below-average precipitation over southern and central Europe. Opposite patterns of temperature and precipitation anomalies are typically observed during strong negative phases of the NAO. (Climate Prediction Center, 2012)

Figure 14 illustrates the NAO phases and their associated impacts in Europe.
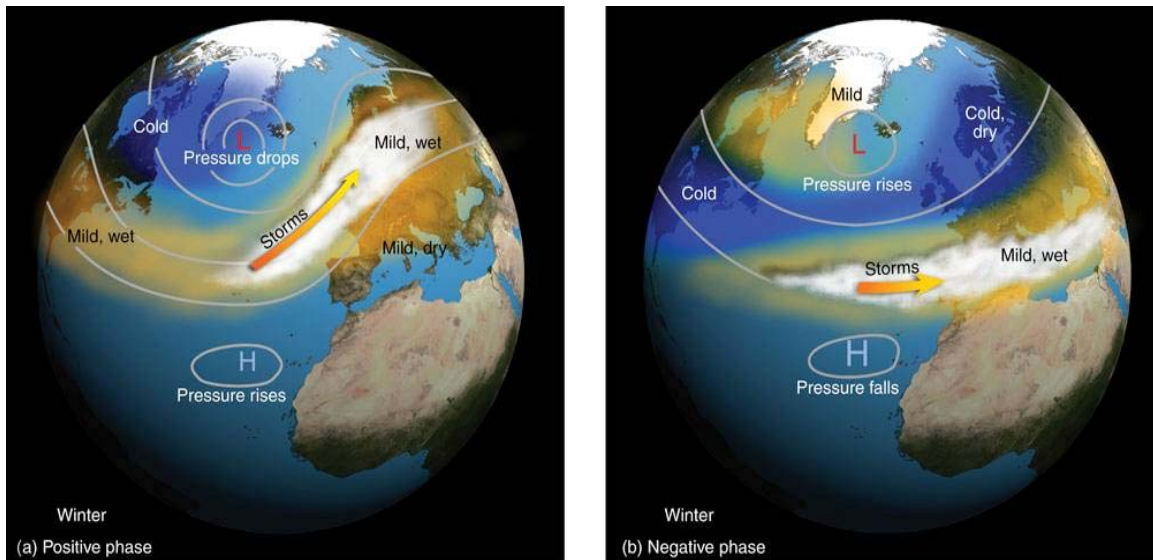
Figure 14.   Schematic illustration of the NAO positive phase (left panel) and negative phase (right panel). (After: http://www.ldeo.columbia.edu/NAO/ , accessed January 2012)

Figures 15-18 are maps of linear correlations between selected meteorological variables and the AO and NAO indices. From these maps, it becomes obvious that the AO tends to have a larger impact on the Aegean region than the NAO (Unal et al. 2010).
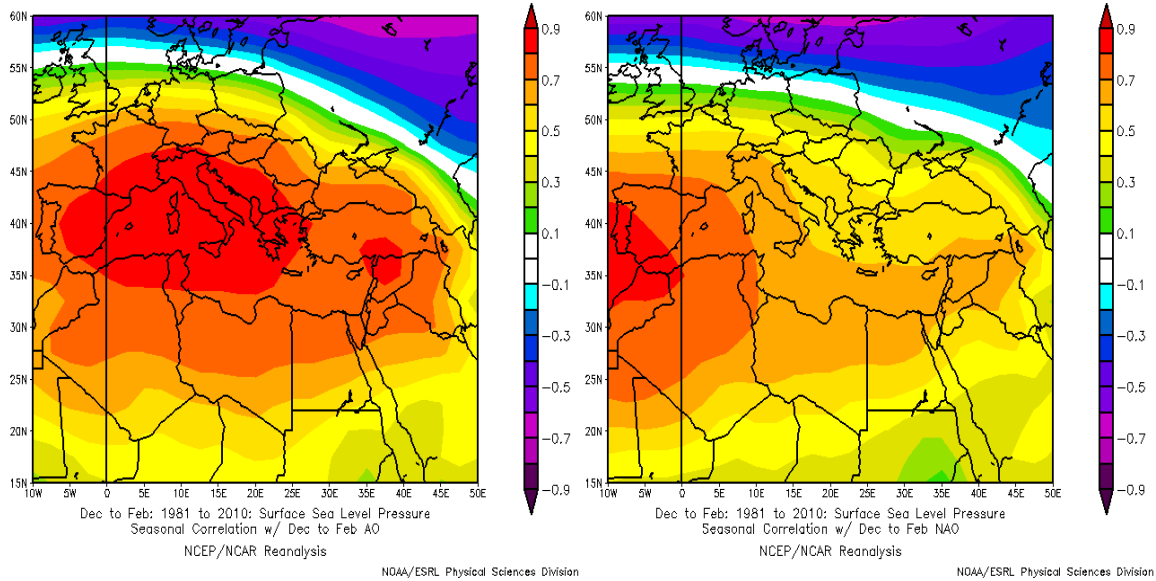
Figure 15.   Linear correlations in winter between sea level pressure (SLP) and the: (a) AO index (left panel); and (b) NAO index (right panel), based on 1981-2010 NCEP reanalysis dataset. Correlation magnitudes ≥ 0.30 and greater indicate significance at the 95% level or greater. Figures created at: NOAA/ESRL Physical Sciences Division website, available online at http://www.esrl.noaa.gov/psd/, accessed January 2012.
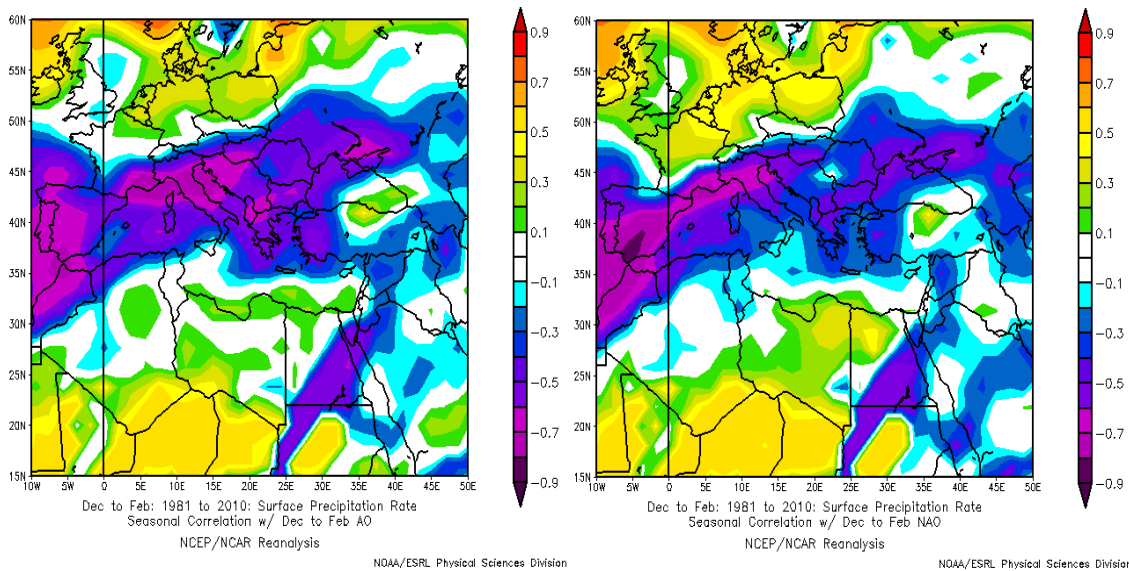
Figure 16.   Linear correlations in winter between precipitation rate (PR) and the: (a) AO index (left panel); and (b) NAO index (right panel), based on 1981–2010 NCEP reanalysis dataset. Correlation magnitudes ≥ 0.30 and greater indicate significance at the 95% level or greater. Figure created at: NOOA/ESRL Physical Sciences Division website, available online at http://www.esrl.noaa.gov/psd/, accessed January 2012.

24
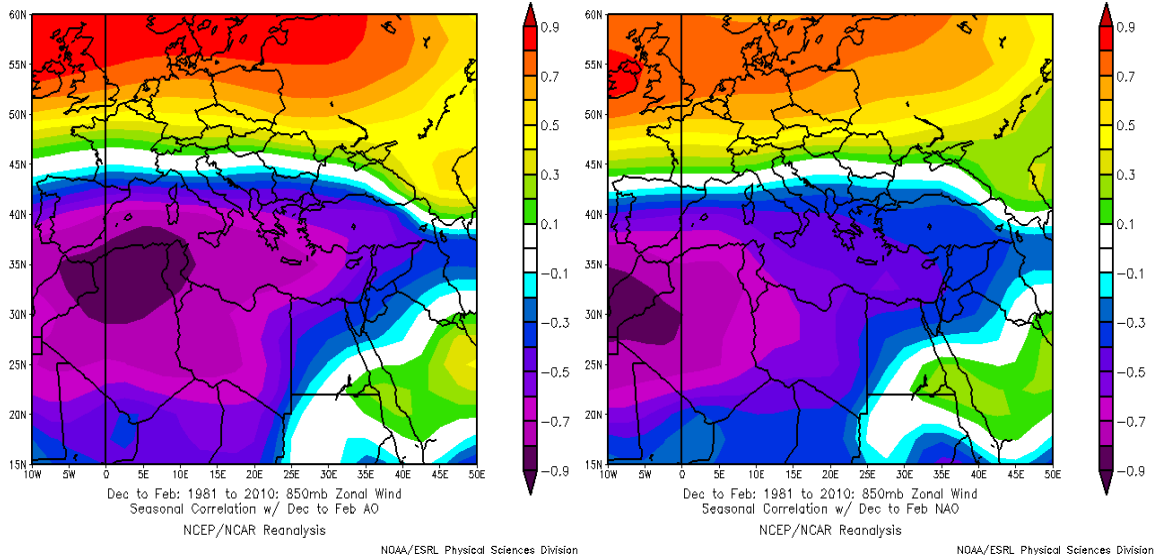
Figure 17.   Linear correlations in winter between zonal wind at 850 hPa (ZW) and the: (a) AO index (left panel); and (b) NAO index (right panel), based on 1981–2010 NCEP reanalysis dataset. Correlation magnitudes ≥ 0.30 and greater indicate significance at the 95% level or greater. Figures created at: NOAA/ESRL Physical Sciences Division website, available online at http://www.esrl.noaa.gov/psd/ , accessed January 2012)
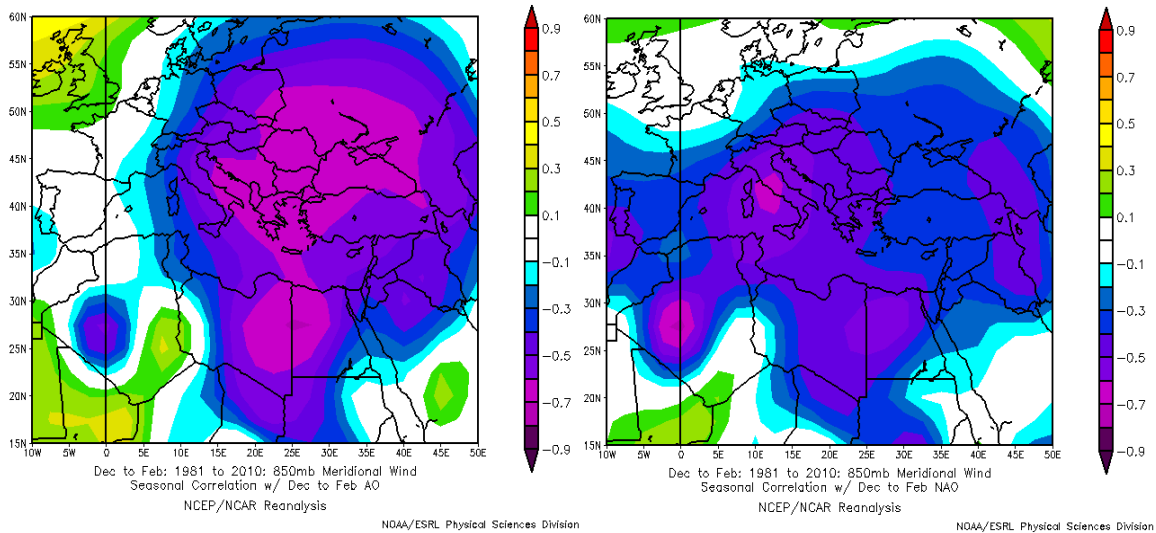
Figure 18.   Linear correlations in winter between meridional wind at 850 hPa (MW) and the: (a) AO index (left panel); and (b) NAO index (right panel), based on 1981–2010 NCEP reanalysis dataset. Correlation magnitudes ≥ 0.30 and greater indicate significance at the 95% level or greater. Figures created at: NOAA/ESRL Physical Sciences Division website, available online at http://www.esrl.noaa.gov/psd/ , accessed January 2012.

These correlations are consistent with what one would expect from the effects of the AO and NAO on the area of study. For example, the AO and NAO are positively correlated with Aegean SLP, and negatively correlated with Aegean precipitation rate, zonal wind, and meridional wind. This indicates that during the positive phases of the AO, the Aegean region experiences anomalously high pressures, low precipitation, and northeasterly winds, all due to changes in large scale circulations and a northward shift in extratropical storm tracks. The opposite anomalies tend to occur during the negative phases, so that the Aegean region experiences anomalously low SLP, high precipitation, and southwesterly winds, and more frequent mid-latitude depressions.

## B.	ANALYSIS OF DUCTING CONDITIONS OVER ATHENS STATION

### 1.	Derived Statistics

Initially, we examined the variation of the ducting parameters over an entire year. Figure 19 shows the yearly distribution of these parameters. Summer has the highest Frequency, highest Height, and highest Strength gradient, suggesting that favorable conditions for ducting formation prevail during summer months. In contrast, winter exhibits the lowest values of Frequency and Height. Strength gradient has relatively low values during winter, with the lowest ones during the February-March-April (FMA) period.

The variability of these parameters is quantified by the standard deviation. Comparing the two seasons, one can see in Figure 19 that the summer months display much lower variability, relative to mean values, for Frequency, a slightly higher variability for Height, and the same variability for Strength gradient. This indicates that summer generates robust ducting conditions, but with relatively low variability due to relatively stable conditions during summer compared to winter during which relatively high variability is imposed by the synoptic scale circulations.
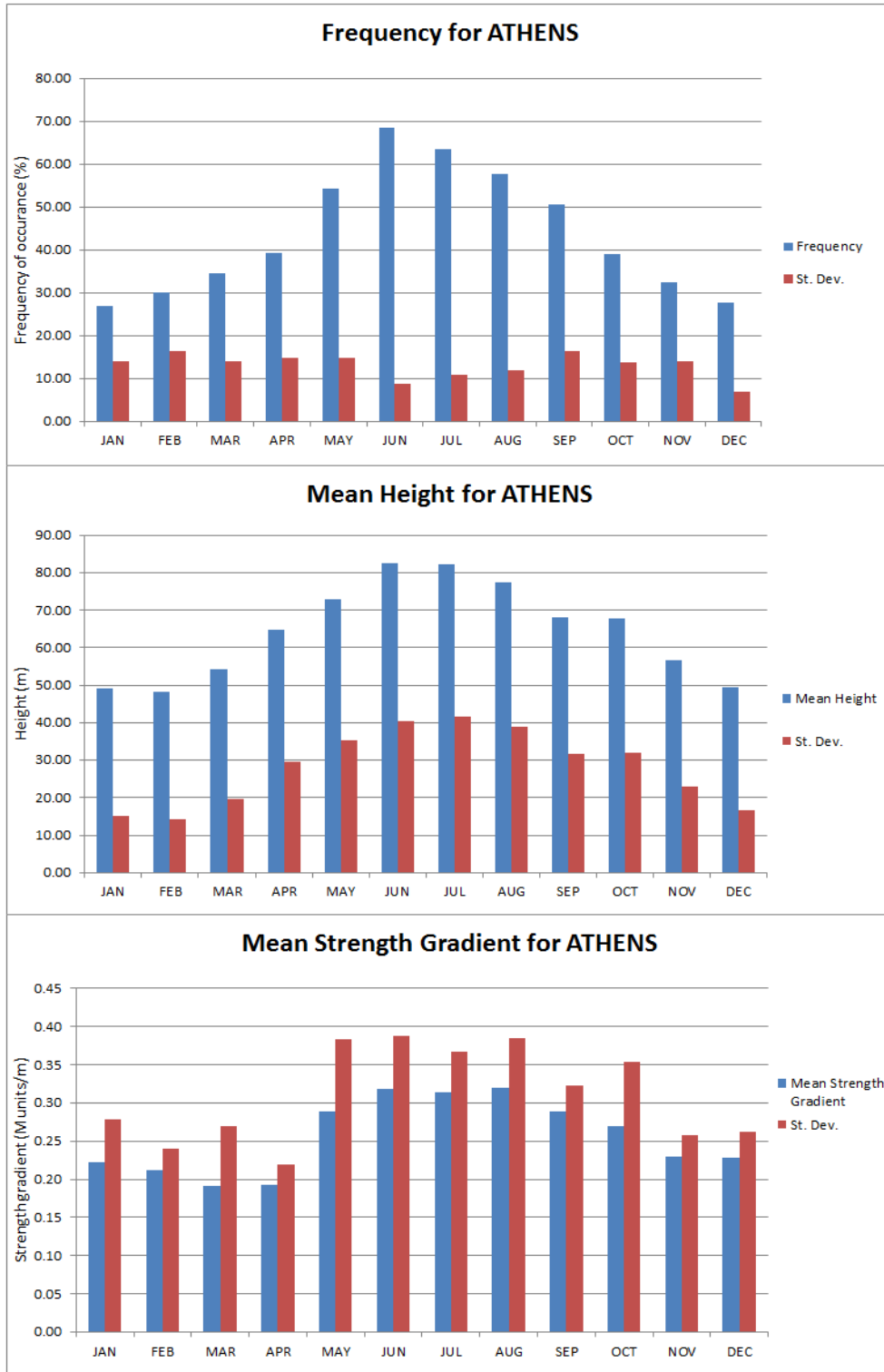
Figure 19. Distribution plots of ducting parameters for Athens station. The values used for this plot have been derived by averaging the monthly means over the 1991-2010 period.

Next, we examined the interannual variability of ducting parameters. By taking the seasonal mean for each year, we constructed time series separately for each parameter and season. In Figure 20, the resultant plots for the winter are presented with linear trend lines to show long term vairations.
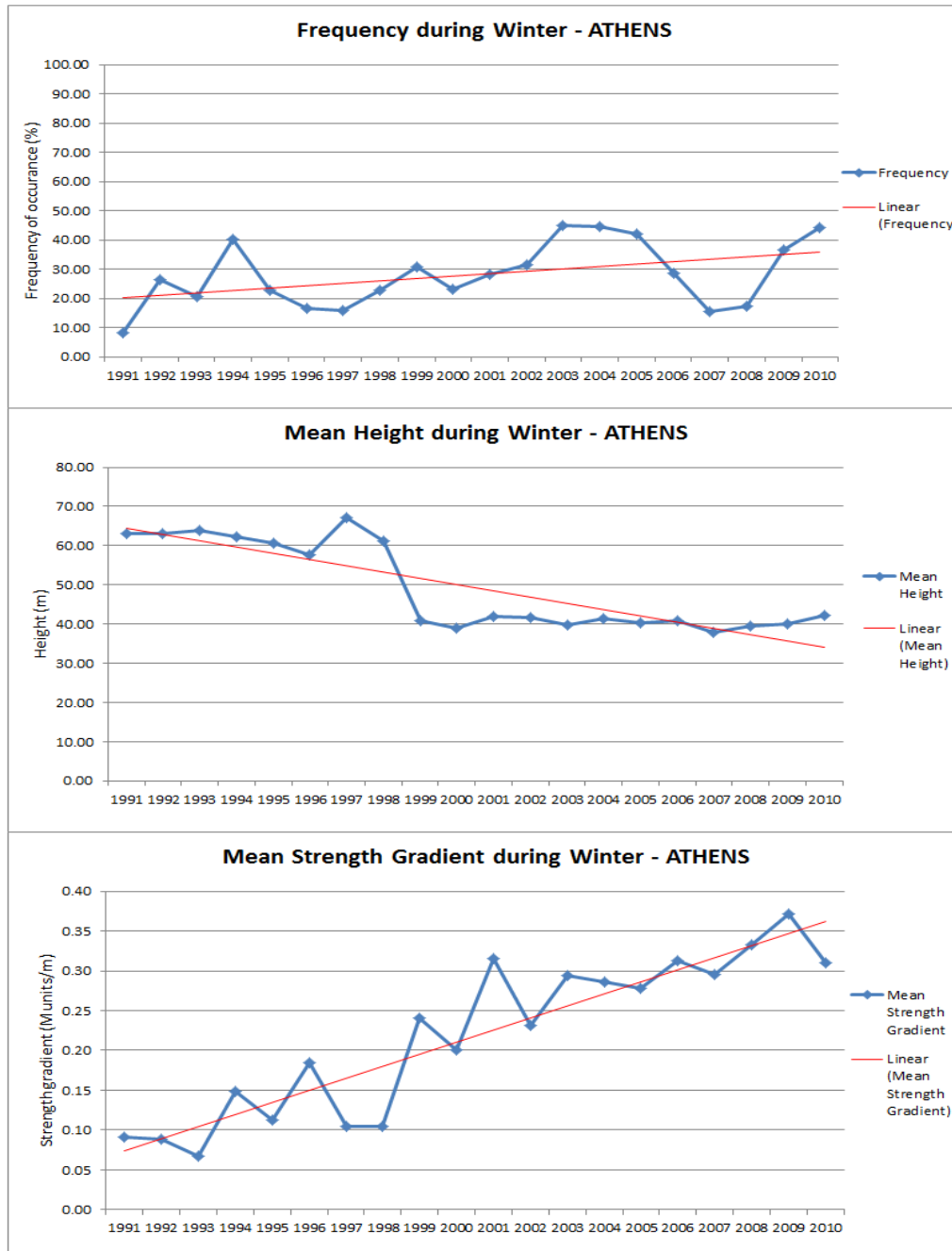
Figure 20.   Time series of ducting parameters during winter for Athens. The blue (crooked) line connects the seasonal means of the respective ducting parameter for each year. The red (straight) line depicts the linear trend of the series.

The trend lines uncovered significant but unexpected trends for all three parameters. Such trends signify the existence of more frequent and strong ducts with the progression of the years, implying that something has changed during the period of study — either with the meteorological conditions described by the data or with the measurement and data recording processes used during the collection of those data.

The interannual variation in the ducting parameters for Athens is pictured in Figure 21. The summer trends are similar to those for winter but lower in magnitude (Figure 20).
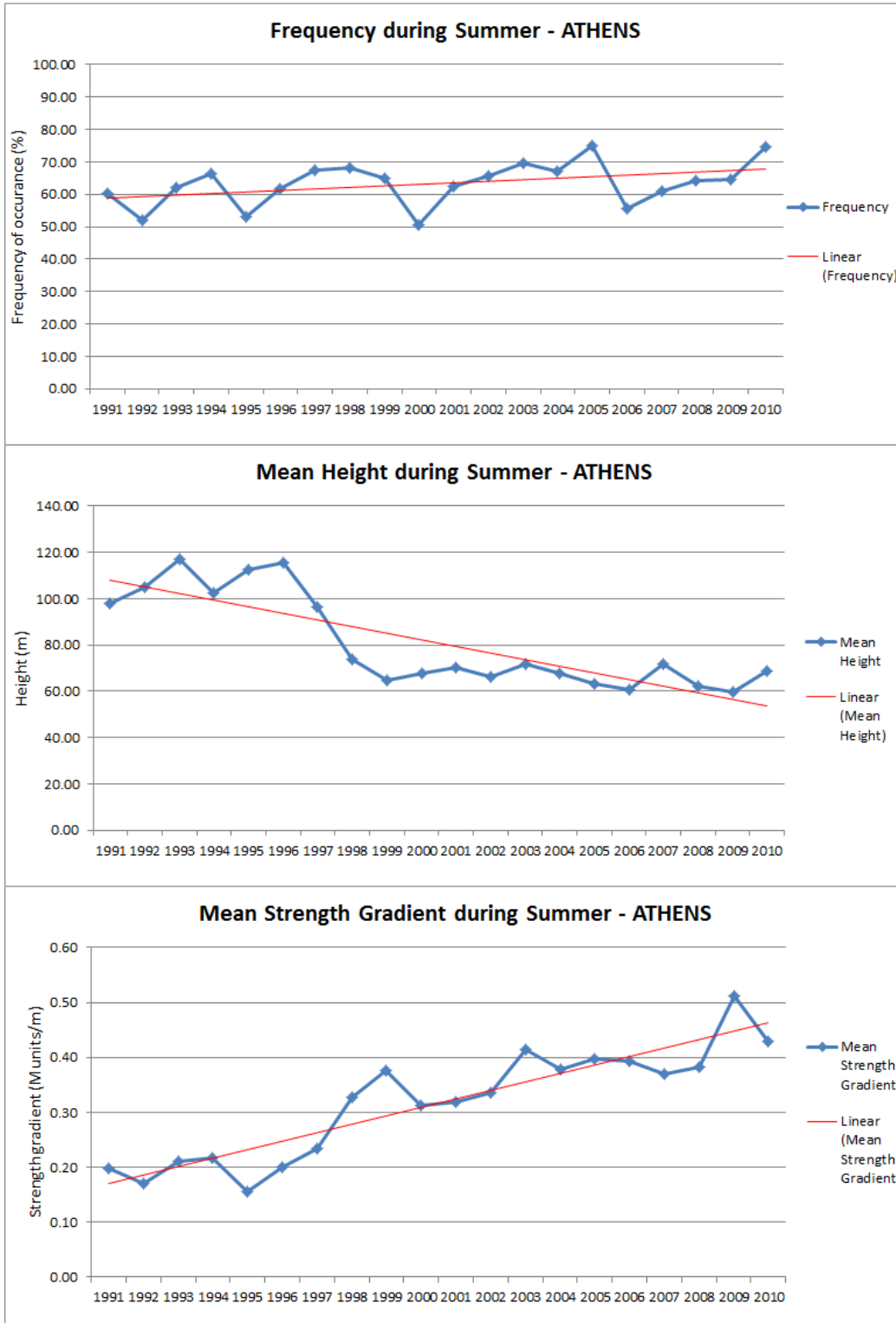
Figure 21.   Time series of ducting parameters during summer for Athens. The blue (crooked) line connects the seasonal means of the respective ducting parameter for each year. The red (straight) line depicts the linear trend of the series.

A careful examination of both the winter and summer plots (Figures 20-21) shows that, between 1997 and 1999, marked shifts occurred in the Height and Strength gradient values, with the Height shifts being more distinct. No corresponding marked shifts occurred in the Frequency values.

To understand these changes during 1997-1999 and the long term trends, we examined the climate variations that occurred in the Aegean and nearby regions during the entire study period and found no obvious explanation for the changes. For this reason, we turned our attention to the data processing procedures throughout the study period, to identify potential processing changes that could account for this peculiar ducting variability. By carefully inspecting the raw data, we realized that there were notable differences in the number of vertical levels contained in the radiosonde datasets. This meant that the processing of the radiosonde measurements was generating data distributed at different vertical levels for different observation periods, with the vertical distances between significant levels being different for different periods. In particular, we observed that the vertical resolution of the recorded data was much finer after 1998, with many more vertical levels being included in the sounding data files. We also noticed that the increase in vertical resolution in 1998 coincided with the previously mentioned shifts in Height and Strength gradients (Figures 20 and 21).

Variations in the vertical resolution of radiosonde data due to data processing and recording differences have been identified and documented in prior studies (Craig et al. 1995; COST Action 255 2002). Many reasons account for this situation. The variability of the atmospheric conditions, which cause the radiosonde to ascend with varying speeds and sample at varying significant levels, or the utilization of different equipment, are some possible reasons. In this research, we have not covered in depth the topic of data resolution but we have dealt with the implications that this issue has for our study.

Surface ducts occur in the lower part of the atmospheric boundary layer (ABL). To determine how well the radiosonde data resolved that part of the atmosphere, we used the following technique. We calculated the mean height of surface ducts by averaging the seasonal mean heights over the 1999–2010 period, during which the resolution was finer. Next, we calculated with the same method the mean height of the upper quartile of duct

heights (i.e., the uppermost 25% of the ducts). For the winter, we found that the mean height of surface ducts was 40.38 m, with a mean upper quartile height of 51.03 m. For the summer, the numbers were 66.80 m and 85.95 m, respectively. Then, we rounded up to the nearest 10 meters the upper quartile values and we treated the resultant numbers as critical levels, based on the assumption that 75% of surface ducts should occur below these levels. The critical level for the winter was determined to be 60 m, and the critical level for the summer was determined to be 90 m. Based on these numbers, we calculated the vertical resolution as the percentage of the sounding times for which data was collected at one or more levels below the relevant critical level. We assumed that if a surface duct was present below a critical level, it would have been captured by the radiosonde only at those times (i.e., when at least one level below the critical level was recorded). Applying this method to all our sounding data, we came up with some quite interesting results, and even more interesting correlations between the resolution and the ducting parameters.

Figure 22 shows the same information as in Figure 20, for the winter, along with a curve representing the yearly variation of seasonal mean vertical resolution. Comparison of the ducting parameters time series with their corresponding resolution time series indicates that the resolution variations is well correlated with the ducting parameters. The linear correlations for the entire 20-year period are summarized in Table 2.
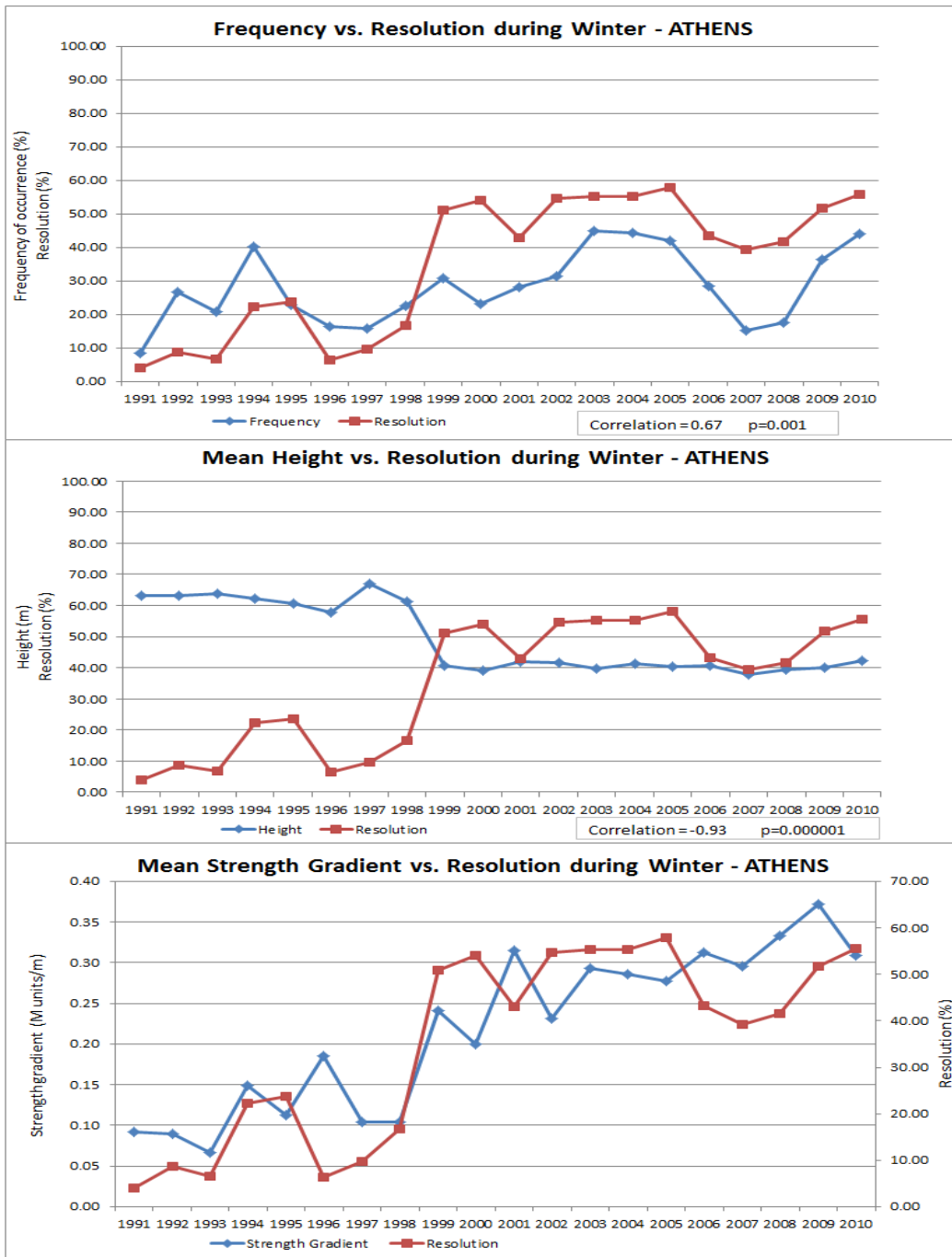
Figure 22.   Time series during winter for Athens. The blue line (rhombus markers) connects the seasonal means of ducting parameters for each year. The red line (square markers) connects the seasonal means of resolution, expressed in %.

Table 2.   Linear correlations coefficients (r) and significance levels (p) between ducting parameters and sounding data vertical resolution during winter.

WINTER	Frequency	Height	Strength Gradient
Resolution	r = 0.67	r = -0.93	r = 0.83
	p > 99%	p = 100%	p ≈ 100%

The correlations are particularly strong for the Height and the Strength gradient. The plots in Figure 22 and the correlation coefficients in Table 2 suggest that whenever coarse resolution takes place (i.e., there is no recorded data below the critical level defined by the average upper quartile of the mean height), then the statistically derived Frequency is lower, the statistically derived Height is higher and the statistically derived Strength gradient is higher. The opposite effect occurs with finer resolved vertical profiles. In summary, coarser vertical resolution: (1) fails to capture real ducts that develop in lower layers and, simultaneously; and (2) captures only the deep ducts, thus artificially making the Frequency too low, the Height too high, and the Strength gradient too low.

The same connection between resolution and ducting parameters statistics holds during summer. Figure 23 illustrates the respective plots and Table 3 summarizes the relevant correlation coefficients for the summer. The main difference now is that the correlation between Frequency and Resolution is much weaker, remaining positive, however. This less strong correlation during summer is explained by the fact that the data resolution takes on double values compared to the winter, having reached almost its upper limit (100%) after 1998. As a consequence, the majority of surface ducts are captured by the soundings, and only a few "elude," thus causing the Frequency variability often become "disconnected" from the resolution variability. On the other hand, the Height and Strength gradient correlation coefficients are even higher during summer, because the almost permanent existence of ducts causes these statistically derived parameters to fluctuate in accordance with the resolution fluctuations.
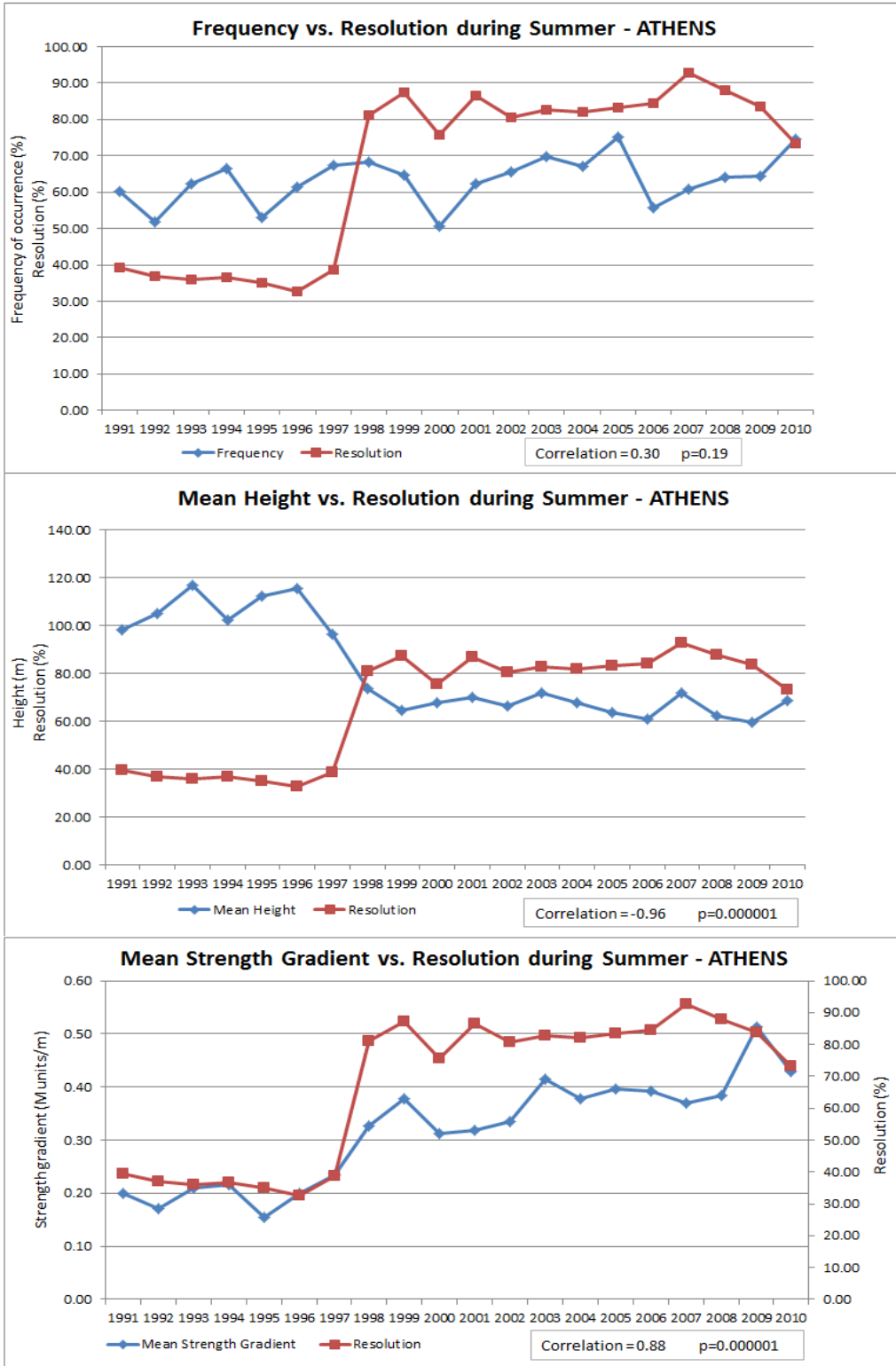
Figure 23.   Time series during summer for Athens. The blue line (rhombus markers) connects the seasonal averages of ducting parameters for each year. The red line (square markers) connects the seasonal means of resolution, expressed in %.

Table 3.   Linear Correlation Coefficients (r) and Significance Levels (p) between ducting parameters and sounding data vertical resolution during summer.

SUMMER	Frequency	Height	Strength Gradient
Resolution	r = 0.30	r = -0.96	r = 0.88
	p = 81%	p = 100%	p ≈ 100%

Considering both seasons together, we have concluded that long-term variations in vertical resolution are responsible for the trends and shifts in the ducting parameters time series shown in Figures 20 and 21. The large shift in resolution in 1998 is the major factor that led to, for example, the large changes in ducting conditions after this year. The Hellenic National Meteorological Service reported to us that improvements in the software used to analyze radiosonde data were applied during the spring of 1998. This software change appears to be the major factor that led to improved vertical resolution in the Athens data during 1998.

In Table 4, a synopsis of the average values for the periods before and after 1998 is given. Note the large differences between the periods, for both winter and summer, in the Frequency, Height, and Strength gradient, and that these differences are consistent with the differences in vertical resolution. Thus, the raw radiosonde data is biased in the earlier period by the lower resolution during that period.

Table 4.   Average values of ducting parameters for the low-resolution period before 1998 and the high-resolution period after 1998.

	WINTER		SUMMER	
	1991–1998	1999–2010	1991–1997	1998–2010
Frequency (%)	21.71	32.21	60.40	64.85
Height (m)	62.37	40.38	106.73	66.80
Strength gradient (M units/m)	0.11	0.29	0.20	0.38
Resolution (%)	12.25	50.25	36.48	83.18

2. Interseasonal Ducting Variability

Initially, we examined the striking difference in ducting conditions between winter and summer (Figure 19, Table 4). There is a two-fold explanation for those enhanced conditions during summer. First, a major ducting mechanism is established along the coastline; intense evaporation, due to warm conditions prevailing over the eastern Mediterranean, feeds the lower levels of the atmosphere with very large amounts of moisture. As a result, a strong negative water vapor pressure gradient forms in the vertical, generating ducting conditions. Additionally, any process creating relative humidity gradients is going to have a magnified effect on specific humidity gradients when the temperature is warmer, as discussed in Chapter I (subsection B1). High amounts of moisture remaining over an area render the ducting mechanisms more effective for this specific area. In Chapter I, we referred to equation (1.3) and the exponential growth of water vapor pressure e as a function of temperature, in order to justify this claim. We can reach the same conclusion if we express modified refractivity M directly as a function of temperature T and relative humidity RH.

For illustrative purposes, we produced Figure 24, where several graphs of M are plotted for several values of RH. The resulting graphs are based on equation (2.1) where e has been replaced and expressed with its components, according to the equations (2.2) and (2.3). An altitude of $z = 15\,m$ (Athens' altitude) and a typical pressure of $p = 1014\,hPa$ have been chosen for our calculations. These plots indicate that M changes more at higher temperatures and relative humidity. This is the main difference between winter and summer ducting conditions. During summer, M lies at the right part of the depicted curves and, therefore, is much more sensitive to temperature and relative humidity variations than it is during winter. This means that the same changes in temperature or relative humidity cause considerably larger changes to M in summer than in winter. As a consequence, the ducting mechanisms become more effective during summer, thus improving in general the ducting conditions. In other words, the atmosphere is more sensitive to the processes that create ducts during summer, and so even the minor differential changes in relative humidity or temperature profiles tend to generate ducting conditions.
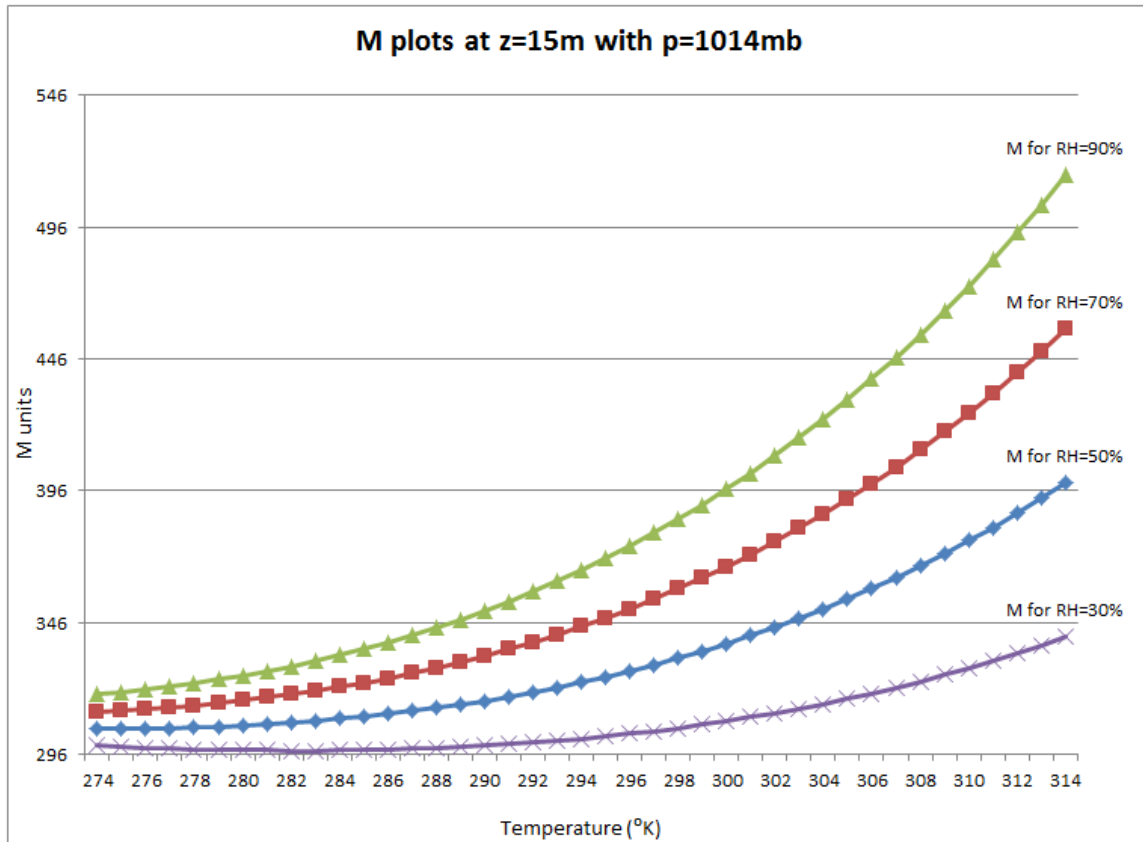
Figure 24.　　Modified refractivity M graphs as a function of temperature T in K. Four different graphs are plotted corresponding to four different amounts of relative humidity. An altitude of z=15 m and of pressure p=1014 hpa have been used for the M computations.

To better understand the impact of the overall moisture amount on the ducting mechanisms, we set up a conceptual simulation of ducting conditions under different moisture regimes. The simulation and its results are presented in Table 5.

Table 5. Summary of a simulation of ducting conditions under different moisture regimes. Top section of table: meteorological values at the two boundaries of a surface duct. M values and the corresponding differences between the two levels are also included. The values specified in the upper part of the table are real data based on real surface ducting conditions that have occurred at the Athens station. Middle sections of table: Simulation results based on changing only temperature. Bottom sections of table: Simulation results based on changing only relative humidity.

5 June 2002 00Z ATHENS

UPPER LEVEL	P=1009.0mb	h=31m	T=21.0 C	RH=60%	MU=335.45
			1.8C lower	23.4% higher	-7.20
LOWER LEVEL	P=1011.0mb	h=15m	T=19.2 C	RH=74%	ML=342.65

CONFIGURATION I

We changed only the temperature values and keep the other variables unchanged. The temperature values have been set up in such a way so that always the UL temerature is by 1.8 °C higher than the LL temperature

UPPER LEVEL	P=1009.0mb	h=31m	T=11.0 C	RH=60%	MU=316.85
			1.8C lower	23.4% higher	-3.71
LOWER LEVEL	P=1011.0mb	h=15m	T=9.2 C	RH=74%	ML=320.56

UPPER LEVEL	P=1009.0mb	h=31m	T=31.0 C	RH=60%	MU=371.10
			1.8C lower	23.4% higher	-13.21
LOWER LEVEL	P=1011.0mb	h=15m	T=29.2 C	RH=74%	ML=384.31

CONFIGURATION II

We changed only the RH values and keep the other variables unchanged. The RH values have been set up in such a way so that always the LL RH is by 23.4% higher than the UL RH

UPPER LEVEL	P=1009.0mb	h=31m	T=21.0 C	RH=78%	MU=354.78
			1.8C lower	23.4% higher	-9.56
LOWER LEVEL	P=1011.0mb	h=15m	T=19.2 C	RH=96.3%	ML=364.34

UPPER LEVEL	P=1009.0mb	h=31m	T=21.0 C	RH=42%	MU=316.13
			1.8C lower	23.4% higher	-4.94
LOWER LEVEL	P=1011.0mb	h=15m	T=19.2 C	RH=51.8%	ML=321.07

The upper part of the table provides a sample of real ducting conditions that occurred in Athens on June 5, 2002, 00Z. With a temperature inversion of $1.8^{o}C$ and a relative humidity at the surface (at 15 m) higher by 23.4% than the relative humidity at the 31 m level, a duct formed between the upper and the lower vertical levels with an M deficit of -7.20 units.

In the middle part of the table (configuration I), we simulated similar atmospheric conditions, keeping all the meteorological values the same except temperature. To simulate the differences between winter and summer conditions, we modified the observed temperature values by 10 degrees, but kept the temperature difference between the two levels the same. By leaving the relative humidity values unchanged, we generated moist conditions during summer and dry conditions during winter. The resultant M values are shown on the right part of the table. During the simulated summer conditions, when the moisture levels were much higher, the M deficits were larger, and improved ducting conditions occurred. The opposite occurred in the winter simulation, as one can tell from the same table (configuration I).

In the lower part of the table (configuration II), we applied the same technique, but this time we portrayed the different moisture regimes by modifying equally for both levels the relative humidity values and keeping the temperature the same. In this case, too, we ended up with analogous results. Under moist conditions, the M difference between upper and lower level were higher, than under dryer conditions.

The mechanisms discussed above hold for intraseasonal and interannual variations of moisture amounts, but are significantly less effective in the winter, since the refractivity conditions are represented by the left, lower part of the M curves (Figure 24). Whenever the moisture levels increase, the atmospheric conditions become more favorable for ducting formation. The effect of moisture on interannual variations of ducting conditions is analyzed in the next subsection.

Regarding the winter, the mechanisms that generate surface ducts operate under a regime of lower moisture amounts and, therefore, their ability to create ducting

conditions is substantially reduced, as previously explained. Furthermore, the evaporation is much less because of much lower temperatures.

On the other hand, the passage of frontal systems can favor duct development, and this process is much more common in the winter than in the summer. In Figure 25, an example of ducting associated with fronts is given. The cross sections of cold and warm fronts are sketched along with the associated M distributions. One can notice that the regions where surface ducts form are just ahead of a cold front and behind a warm front, and they are related to the RH vertical gradients over these particular regions. Many other cases of different M distributions can occur, depending on the structure and the dynamics of the front.
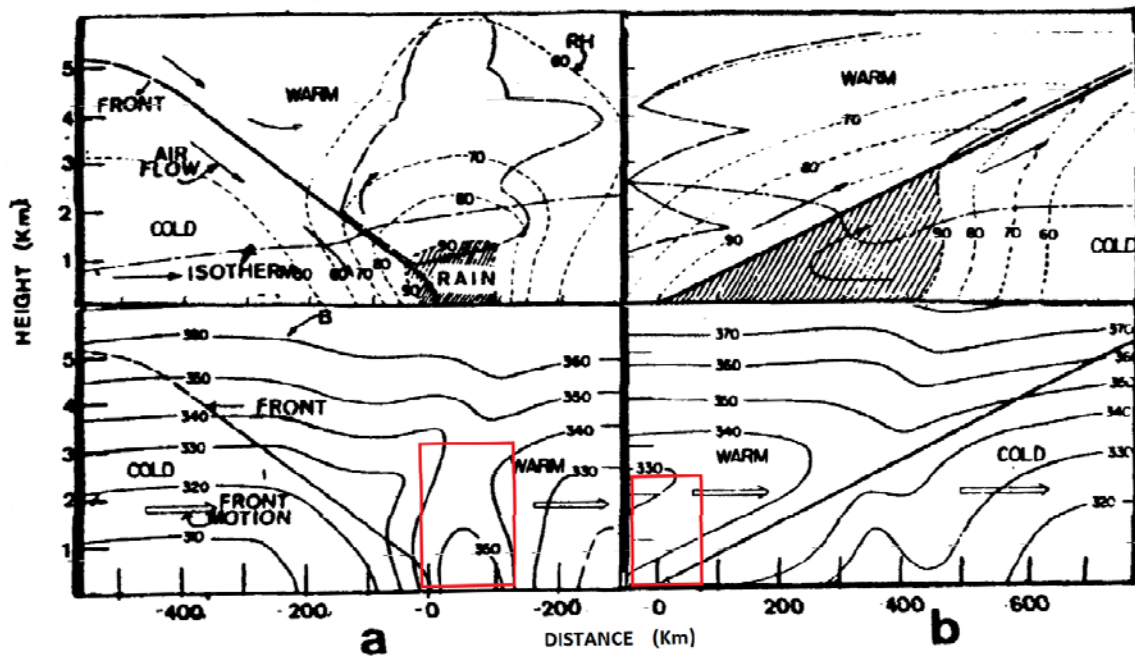
Figure 25. Vertical cross sections of cold front (left panels) and warm front (right panels), with the corresponding M distributions (bottom panes). The dotted lines at the top panes represent relative humidity isopleths. The red rectangles define the regions where M decreases with height and therefore surface ducts form (After: Davidson 2003).

3. Interannual Ducting Variability

We analyzed correlations between the time series of the ducting parameters and the time series of relevant climate system variables. Our goal was to identify the

relationships between ducting and regional and remote variables, and the physical processes that determine those relationships, so that improved prediction of ducting can ensue. Due to the resolution issue that emerged, we decided to work only with data from the second period (after 1998). By doing so, we removed the long-term bias caused by the resolution issue, and more realistic statistics can be derived. We are aware of the fact that biases attributed to the short-term resolution variations still remain. However, those variations tend to be relatively small. Thus, we concluded that we could use the post-1998 data to investigate how interannual variations in ducting in the Aegean region are related to regional and remote climate variations.

Before proceeding with that investigation, we needed to determine the extent to which moisture variations in the lower troposphere explain interannual variations in surface ducting, as they explain interseasonal (summer - winter) variations in surface ducting. We used mixing ratio, a variable that is directly available from the radiosonde data, as the parameter to represent the amount of moisture in the air and as a surrogate for water vapor pressure in Equation 2.1. Thus, changes in the mixing ratio are directly linked directly to changes in M, via Equation 2.1, and thus to changes in surface ducting. Figure 26 shows time series of ducting frequency and mixing ratios for the two lower levels of the recorded vertical levels. Both winter and summer parameters are shown.
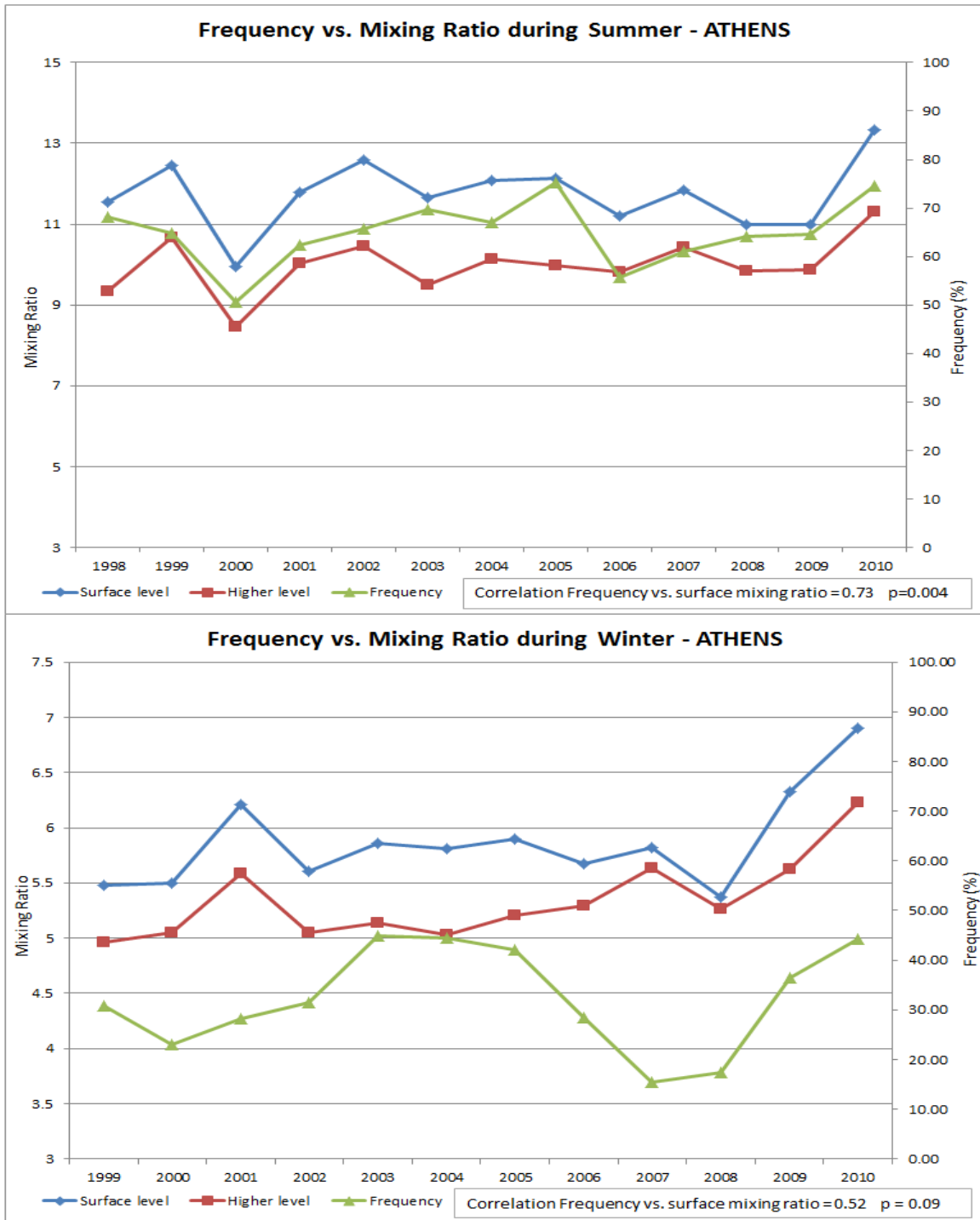
Figure 26.   Time series for Athens in summer (upper panel) and winter (lower panel) of
Frequency (green lines with triangle markers), moisture mixing ratio at the
surface level (blue lines with rhombus markers) and moisture mixing ratio at the
next higher level recorded by the radiosonde sounding (red lines with square
markers). The correlation between the Frequency and surface mixing ratio is
shown in the lower right of each panel.

A visual inspection of these plots indicates that, in general, interannual variations in Frequency tend to follow the interannual variations in the surface mixing ratio, with a higher correlation during summer. By correlating the Frequency with the mixing ratio at the surface, we received noteworthy correlation values, especially during summer, which reveal the important role of interannual variations in moisture in determining interannual variations in Frequency. For the summer, $r = 0.73$ and significance level $p > 99\%$. The values for the winter are $r = 0.52$ with $p = 91\%$. The lower correlation during the winter is expected, since M lies at the left part of the exponential curves (Figure 24).

Having these relationships as a guide, and based on the methods and the tools described in Chapter II, we produced maps of the correlations between Frequency at Athens and selected climate system variables. Only the more statistically significant and dynamically relevant correlations are shown. The dynamically relevant correlations are those that indicate clear and physical plausible dynamical relationships between the Frequency and the climate system variables.

a.   *Winter*

Figure 27 shows the correlation between Athens Frequency and SLP for winter 1999-2010. Note the large region of negative correlation centered on the Mediterranean. The black box indicates a region in the eastern Mediterranean, over and close to the Aegean focus region, for which the area-average correlation is especially strong, with $r = -0.84$ and a corresponding significance level, $p > 99\%$.

44
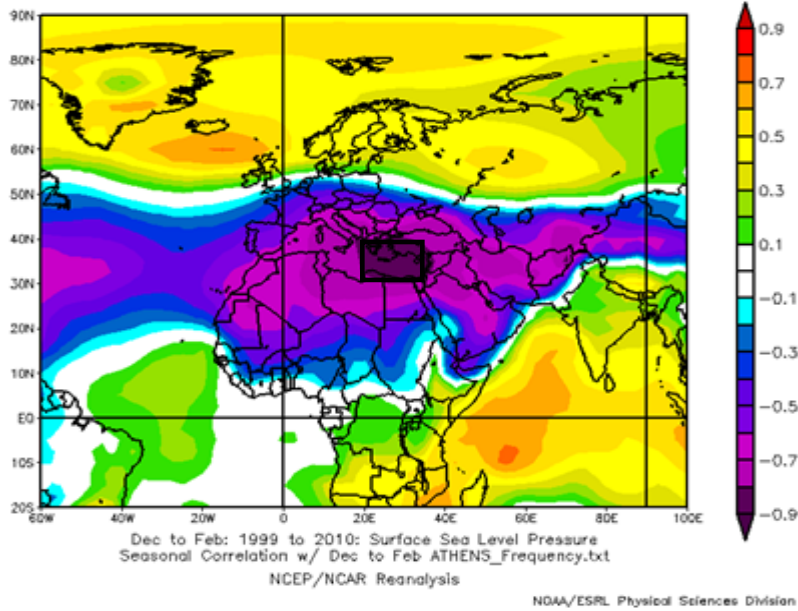
Figure 27.   Linear correlations in winter between SLP and Frequency at Athens for the period 1999-2010, based on 1981–2010 NCEP reanalysis dataset. The black rectangle in the eastern Mediterranean region indicates an area of strong negative correlation that is over and near the Aegean focus region of our study. Correlation magnitudes ≥ 0.30 and greater indicate significance at the 95% level or greater. Figure created at: NOAA/ESRL Physical Sciences Division website, available online at http://www.esrl.noaa.gov/psd/, accessed January 2012.

Other prominent features in this map are the north-south dipole of negative and positive correlation over the mid-latitude and sub-polar North Atlantic Ocean, which is consistent with the NAO and AO. We computed the corresponding correlation coefficients between Frequency and these indices with the following results: $r = -0.49$ with significance level $p = 89\%$ for the NAO, and $r = -0.62$ with significance level $p = 97\%$ for the AO. Additionally for the AO index, large correlation exists between it and the Height with values $r = -0.70$ and $p = 99\%$.

Figure 28 illustrates the correlation maps for PR, and for RH at *700 hPa*. There are significant positive correlations over the Aegean Sea and the surrounding area (see black boxes in Figure 28), with the PR correlation taking on the very high value of $r = 0.9$ and $p \approx 100\%$. Note also the consistency between the results in Figures 27-28

45

over much of the region surrounding the Aegean. For example, in the general eastern Mediterranean region, the negative correlation with SLP is consistent with the positive correlation with PR and RH at *700 hPa*.
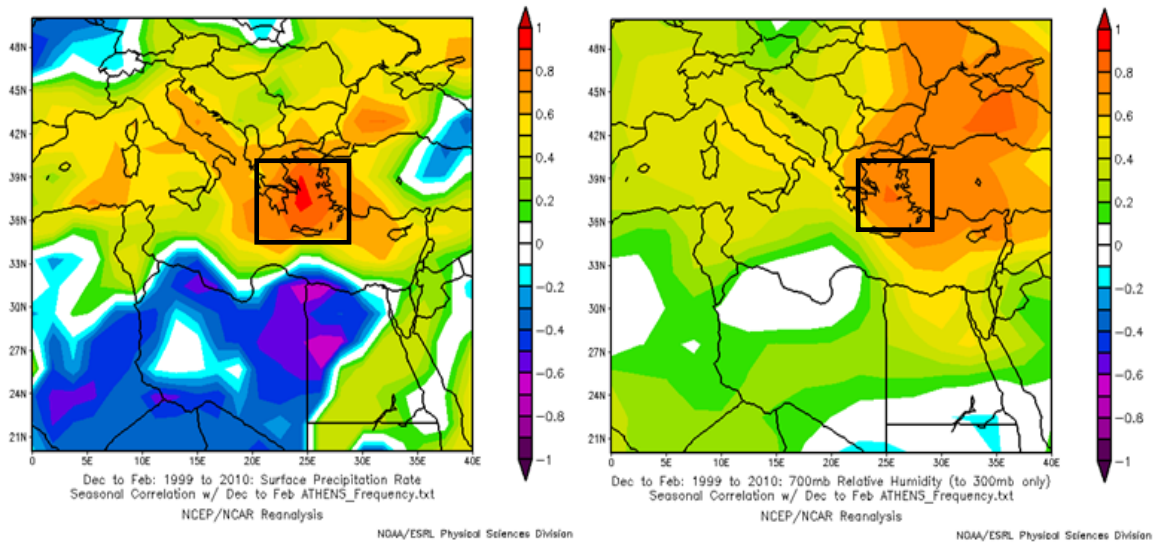
Figure 28.　　Linear correlations in winter between Frequency at Athens and the: (a) PR (left panel); and (b) RH at 700 hPa (right panel) for the period 1999-2010, based on 1981–2010 NCEP reanalysis dataset. The black rectangles in the eastern Mediterranean region indicate areas of strong positive correlation that are over and near the Aegean focus region of our study. Correlation magnitudes ≥ 0.30 and greater indicate significance at the 95% level or greater. Figures created at: NOAA/ESRL Physical Sciences Division website, available online at http://www.esrl.noaa.gov/psd/ , accessed January 2012.

In Figure 29, the correlation maps for ZW and MW at *850 hPa* are depicted. Highly significant positive correlations occur for both zonal and meridional winds over the eastern Mediterranean. The values for the black boxes shown in Figure 29 are $r = 0.78$ with $p > 99\%$ for the ZW, and $r = 0.79$ with $p > 99\%$ for the MW. Note also the consistency between the correlations shown in Figures 27-29. For example, all these figures are consistent in indicating that high Frequency at Athens tends to be associated with the passage of extratropical cyclones through the eastern Mediterranean region, and corresponding low SLP, high PR, high RH, and southwesterly winds.

Figure 29. Linear correlations in winter between Frequency at Athens and the: (a) ZW at 850 hPa (left panel); and (b) MW at 850 hPa (right panel) for the period 1999-2010, based on 1981–2010 NCEP reanalysis dataset. The black rectangles in the eastern Mediterranean region indicate areas of strong positive correlation that are over and near the Aegean focus region of our study. Correlation magnitudes ≥ 0.30 and greater indicate significance at the 95% level or greater. Figures created at: NOAA/ESRL Physical Sciences Division website, available online at http://www.esrl.noaa.gov/psd/ , accessed January 2012.

Figure 30 shows correlation maps for SST. Both concurrent and lagging correlations were plotted (Frequency lagging SST by one month). We focused on the concurrent positive correlation in the Aegean region (black box in Figure 30, left panel), with $r = 0.61$, $p = 96\%$, and the lagging negative correlation in the North Atlantic with $r = -0.67$, $p = 98\%$. Note that the correlation pattern in the North Atlantic has a quadripole structure consistent with the SST anomalies associated with the NAO and AO (Murphree 2011).
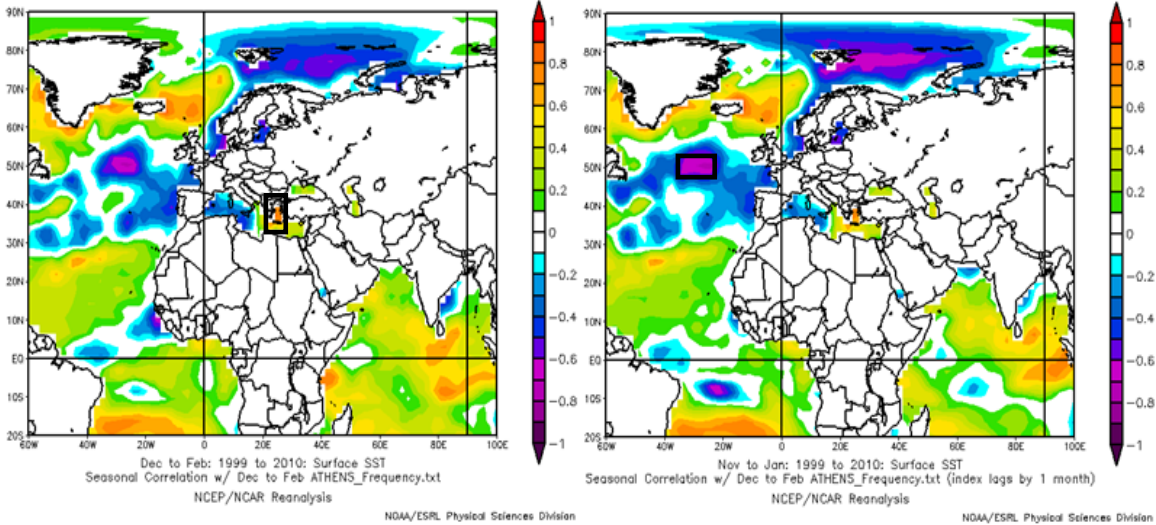
Figure 30.   Linear correlations in winter between Frequency at Athens and the: (a) SST (left panel); and (b) SST leading by one month (right panel) for the period 1999-2010, based on 1981–2010 NCEP reanalysis dataset. The black rectangles indicate areas of strong correlation. Correlation magnitudes ≥ 0.30 and greater indicate significance at the 95% level or greater. Figures created at: NOAA/ESRL Physical Sciences Division website, available online at http://www.esrl.noaa.gov/psd/ , accessed January 2012.

Table 6 is a summary of all the correlations between ducting parameters and meteorological variables for winter 1999-2010. Correlations with the NAO and AO indices are also included. Significance levels have been calculated only for correlations larger than 0.5 . Among them, the correlations with SLP, PR, and RH at *700 hPa* level are especially significant, with values up to 0.9 for the PR over the Aegean Sea (Figure 28). Equally important is that all three ducting parameters (Frequency, Height, and Strength gradient) tend to have the same correlation sign, as indicated by the red and green arrows in Table 6. This indicates that the correlations represent real dynamical relationships. In the next section, the physical processes that explain the correlations are described in detail.

48

Table 6. The winter mean values of the ducting parameters for Athens (top four rows) and the correlations between those parameters and corresponding area-average environmental variables for selected regions. Only significance levels greater than or equal to 90% are shown. The correlations with significance levels greater than or equal to 95% are highlighted in yellow. Correlations with NAO and AO indices are also included. The sign of the correlation is indicated by the colored arrows: red indicates negative and green indicates positive.

DEC - JAN - FEB	1999	2000	2001	2002	2003	2004	2005	2006	2007	2008	2009	2010
Frequency	30.78	23.07	28.16	31.40	44.87	44.42	42.09	28.40	15.35	17.43	36.39	44.17
Strength gradient	0.24	0.20	0.32	0.23	0.29	0.29	0.28	0.31	0.30	0.33	0.37	0.31
Height	40.73	39.00	41.85	41.58	39.63	41.38	40.31	40.75	37.74	39.54	39.93	42.10
SLP at Europe	1018.5	1020.2	1019.1	1020.1	1017.5	1017.2	1018.4	1018.0	1020.7	1021.8	1017.4	1014.7
(31N-39N, 21E-40E)					Frequency r= -0.84		p>99%					
					Strength r= -0.25							
					Height r= -0.55		p=94%					
RH700 at E. Mediterranean	48.5	45.1	40.7	44.8	51.1	47.9	47.3	44.5	38.7	42.9	47.3	50.5
(35N-40N, 23E-30E)					Frequency r= 0.85		p>99%					
					Strength r= -0.07							
					Height r= 0.37							
PR at E. Mediterranean	2.75	2.31	1.94	2.51	3.35	2.88	2.58	2.18	1.24	1.76	2.81	3.05
(34N-40N, 22E-28E)					Frequency r= 0.90		p>99%					
					Strength r= -0.07							
					Height r= 0.46							
ZW850 at E. Mediterranean	5.2	4.4	4.3	4.0	5.5	5.0	4.1	3.9	2.8	2.3	5.4	7.4
(32N-38N, 20E-30E)					Frequency r= 0.78		p>99%					
					Strength r= 0.03							
					Height r= 0.54		p=92%					
MW850 at E. Mediterranean	1.4	0.0	0.4	-0.1	1.0	1.0	1.4	1.2	-0.9	-1.5	2.2	2.7
(32N-39N, 23E-34E)					Frequency r= 0.79		p>99%					
					Strength r= 0.21		p=					
					Height r= 0.52		p=91%					
SST at N. Atlantic - 1 month lead	11.179	11.097	10.864	11.48	10.494	11.024	11.215	11.28	11.366	11.97	11.283	10.562
(48N-54N, 35W-22W)					Frequency r= -0.67		p=98%					
					Strength r= 0.06							
					Height r= -0.33							
SST at E. Mediterranean	15.867	15.793	16.26	15.657	15.905	15.731	16.069	15.592	15.522	15.403	16.186	16.524
(35N-39N, 23E-28E)					Frequency r= 0.61		p=96%					
					Strength r= 0.22							
					Height r= 0.52		p=92%					
NAO Index	0.33	1.02	-0.26	-0.02	-0.34	-0.32	0.59	-0.18	-0.03	0.38	-0.42	-2.12
					Frequency r= -0.49							
					Strength r= -0.47							
					Height r= -0.51		p=91%					
AO Index	0.65	1.13	-1.31	0.45	-0.65	-0.98	0.11	-0.81	1.00	0.86	0.26	-3.42
					Frequency r= -0.62		p=97%					
					Strength r= -0.32							
					Height r= -0.70		p=99%					

The observed correlation patterns (Figures 27–30) and the individual correlation values (Table 6) together indicate that surface ducting conditions in Athens are more likely in winter when mid-latitude depressions are occurring in the area. These depressions constitute a major source of humidity, especially by producing southwesterly moisture advection over the Aegean Sea from the relatively humid regions over the Mediterranean (see Figure 10). Additionally, they are accompanied by frontal activity, which also improves ducting conditions, as explained in the previous section. The very strong correlations with the PR and the RH (Table 6) over Aegean Sea support these arguments.

Moreover, the SST correlations in the Aegean Sea and the North Atlantic Ocean (Figure 30) are consistent with the same processes. The positive correlation at the Aegean Sea indicates that higher SST results in higher evaporation, leading to higher humidity levels, and thus leading to enhanced ducting conditions. The SST correlation patterns in the North Atlantic Ocean are linked with the NAO and AO, with the negative (positive) phase of each oscillation being associated with more (less) frequent extratropical cyclone activity in the Mediterranean, thus leading to more ducting over the Aegean.

Figures 31–35 illustrate composite anomaly maps of selected climate system variables for the two years that exhibited the highest Frequency during the 1999–2010 period and the two years that exhibited the lowest Frequency during the 1999–2010 period. These maps complement the correlation maps (Figures 27-30) by showing the anomalous conditions, including the spatial patterns and signs of the climate variations, associated with high and low Frequency.

The anomaly maps give results consistent with the correlation maps. The years of the highest Frequency are those with negative phases of the NAO and AO modes, as is evident from the SLP anomaly dipole over the North Atlantic (Figure 31). During those years, more mid-latitude storms were directed towards the eastern Mediterranean, as indicated by the negative SLP anomaly over the Aegean region, the positive precipitation rate anomaly (Figure 32), the positive RH anomaly (Figure 33), and the generally southwesterly flow anomaly indicated by the vector wind (VW) anomalies

(Figure 34). For the years of the lowest Frequency, we find exactly the opposite anomaly patterns. The SST anomalies in the Aegean Sea and the North Atlantic (Figure 35) are also in agreement with the corresponding correlation maps and the physical interpretations given earlier.
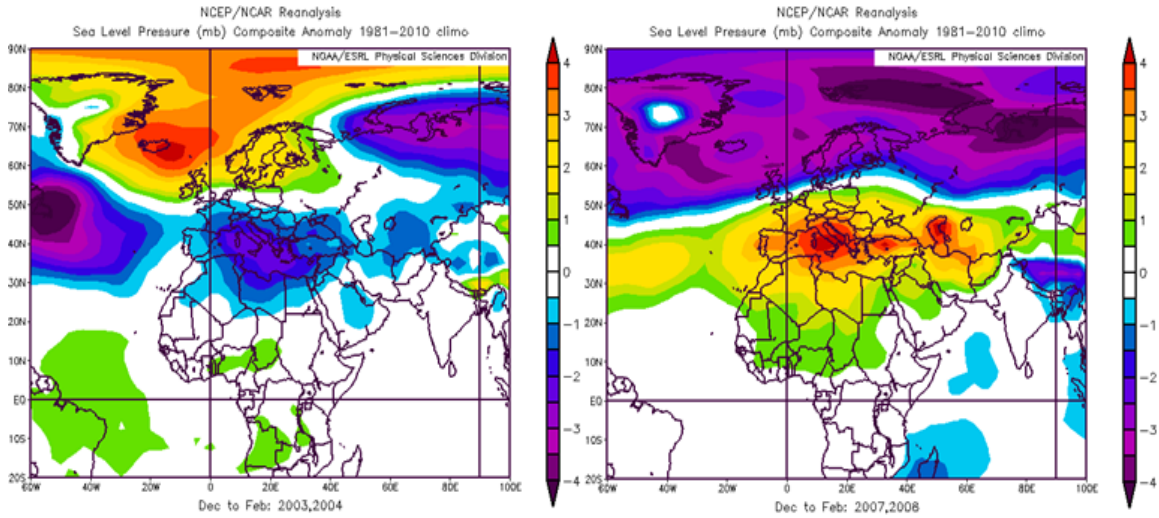
Figure 31.   SLP composite anomaly maps for the two winters with the highest Frequency at Athens (left panel) and the lowest Frequency at Athens (right panel). Figures created at: NOAA/ESRL Physical Sciences Division website, available online at http://www.esrl.noaa.gov/psd/, accessed February 2012.
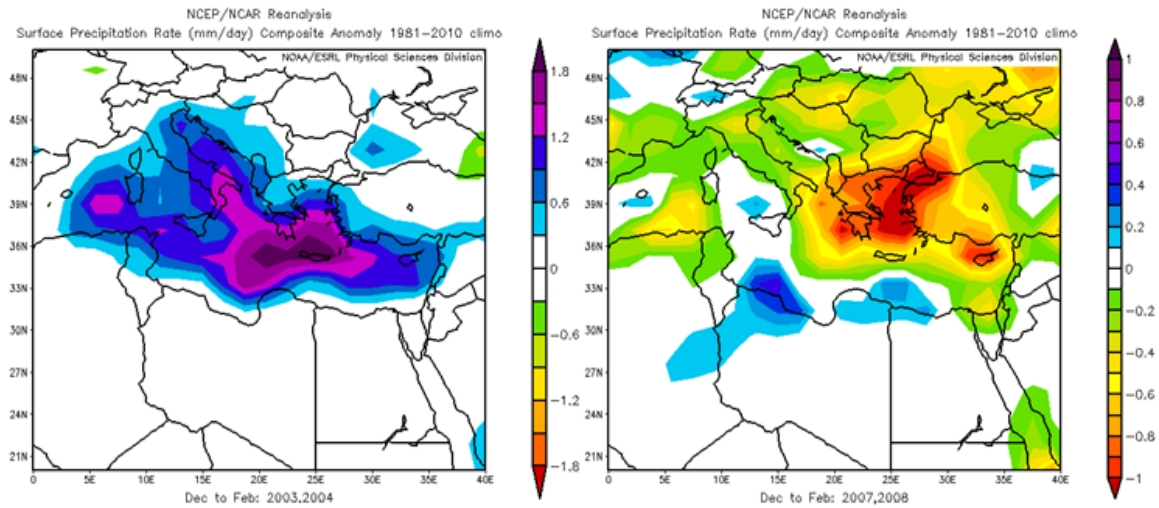
Figure 32.   PR composite anomaly maps for the two winters with the highest Frequency at Athens (left panel) and the lowest Frequency at Athens (right panel). Figures created at: NOAA/ESRL Physical Sciences Division website, available online at http://www.esrl.noaa.gov/psd/ , accessed February 2012.

51
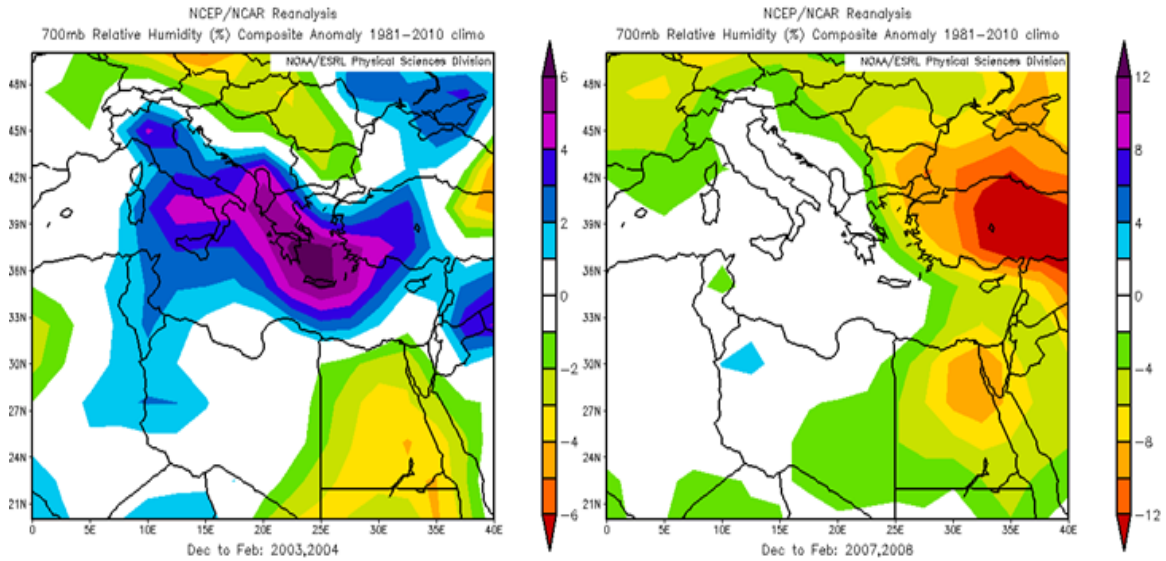
Figure 33.   RH at 700 hPa composite anomaly maps for the two winters with the highest Frequency at Athens (left panel) and the lowest Frequency at Athens (right panel). Figures created at: NOAA/ESRL Physical Sciences Division website, available online at http://www.esrl.noaa.gov/psd/ , accessed February 2012.
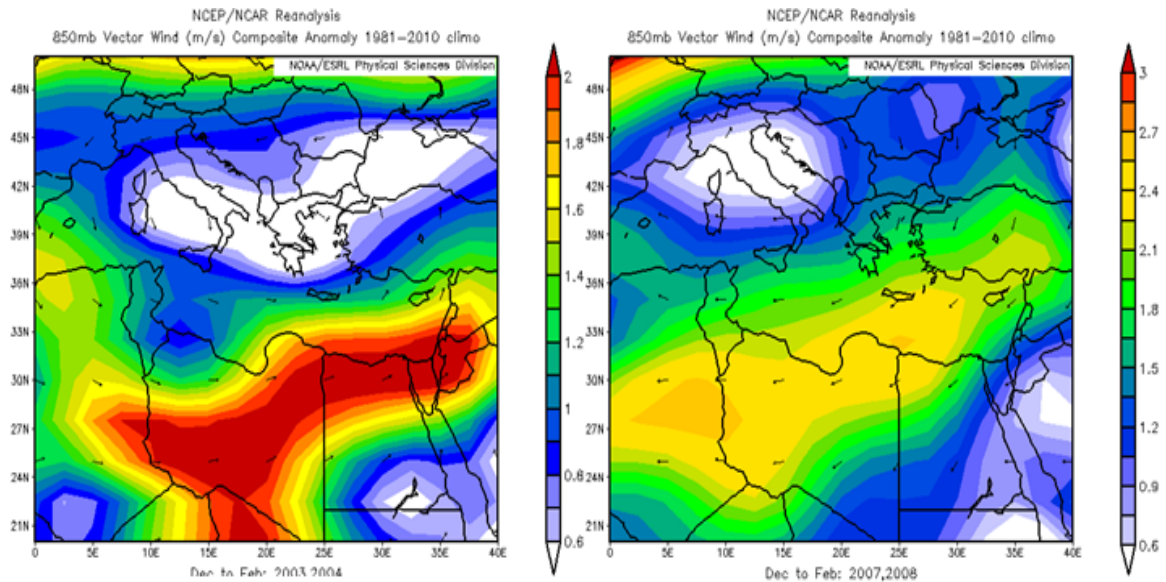
Figure 34.   VW at 850 hPa composite anomaly maps for the two winters with the highest Frequency at Athens (left panel) and the lowest Frequency at Athens (right panel). Figures created at: NOAA/ESRL Physical Sciences Division website, available online at http://www.esrl.noaa.gov/psd/ , accessed February 2012.
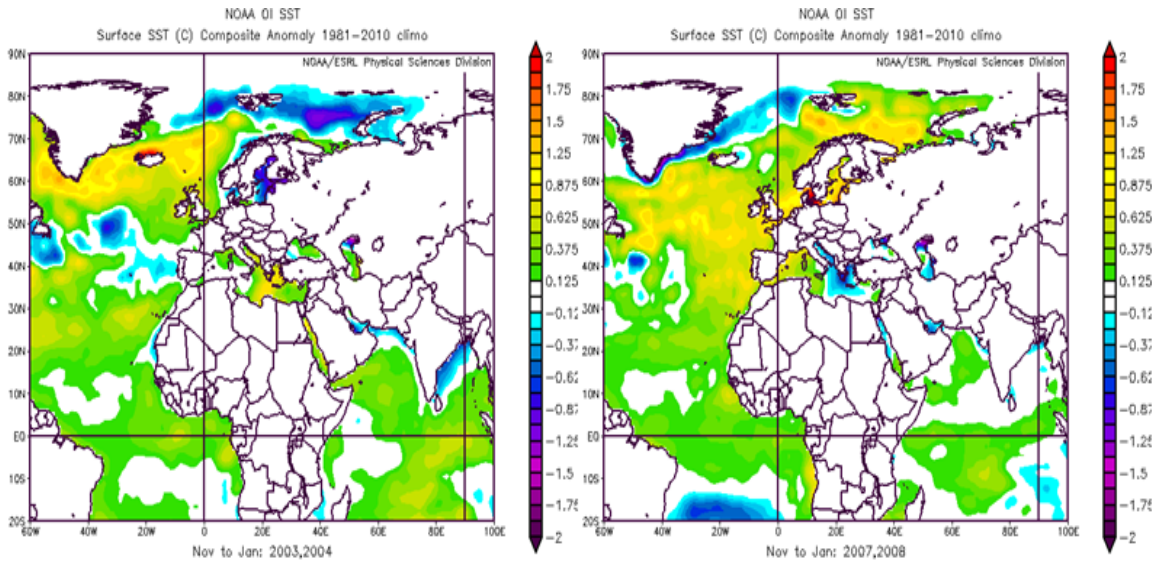
Figure 35.   SST composite anomaly maps for the two winters with the highest Frequency at Athens (left panel) and the lowest Frequency at Athens (right panel). SST leads by one month. Figures created at: NOAA/ESRL Physical Sciences Division website, available online at http://www.esrl.noaa.gov/psd/ , accessed February 2012.

b.   Summer

Figure 36 shows the correlation between Athens Frequency and SLP for summer 1998-2010. Note the regions within the black boxes of negative correlation over the N. Atlantic Ocean and positive correlation over the Indian subcontinent. The respective values are $r = -0.72$ with $p > 99\%$ for the N. Atlantic Ocean and $r = -0.70$ with $p > 99\%$ for the Indian subcontinent.
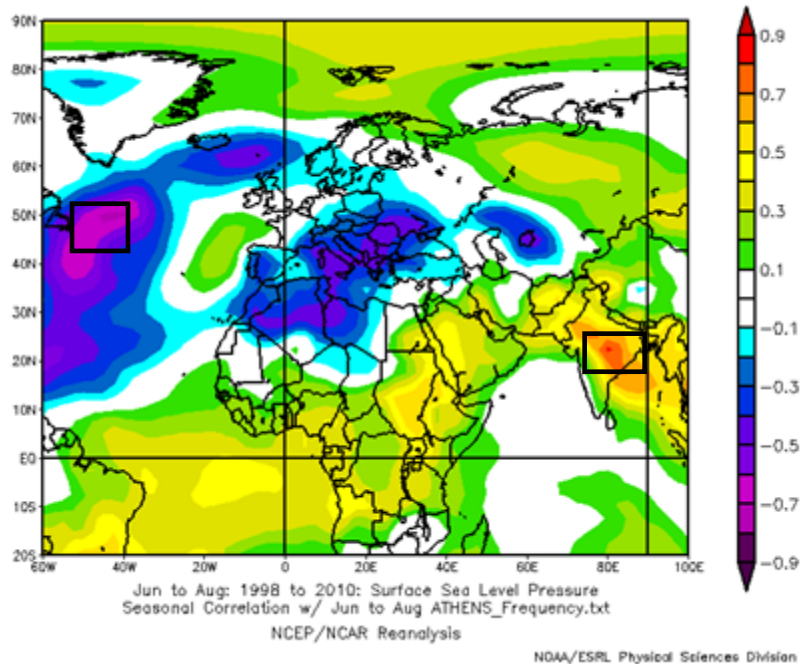
Figure 36.   Linear correlations in summer between SLP and Frequency at Athens for the period 1998-2010, based on 1981–2010 NCEP reanalysis dataset. The black rectangles indicate areas of strong correlation. Correlation magnitudes ≥ 0.30 and greater indicate significance at the 95% level or greater. Figure created at: NOAA/ESRL Physical Sciences Division website, available online at http://www.esrl.noaa.gov/psd/ , accessed January 2012.

A weaker negative correlation exists over almost the entire European continent. In contrast with the winter when the NAO and AO pattern are distinct (Figure 27), for the summer, no correlation exists between these two modes and the Frequency index. Noteworthy negative correlations, however, emerge between both the NAO and AO indices and the Strength gradient index. The corresponding values that they take on are $r = -0.56$ with $p = 95\%$ for the NAO, and $r = -0.55$ with $p = 95\%$ for the AO.

In Figure 37, the correlation maps for ZW and MW, at 850 hPa are depicted. Significant positive correlations occur for both zonal and meridional winds over Aegean Sea and the neighboring areas. The corresponding values that have been calculated are $r = 0.48$ with $p = 90\%$ for the ZW and $r = 0.55$ with $p = 95\%$ for the MW.
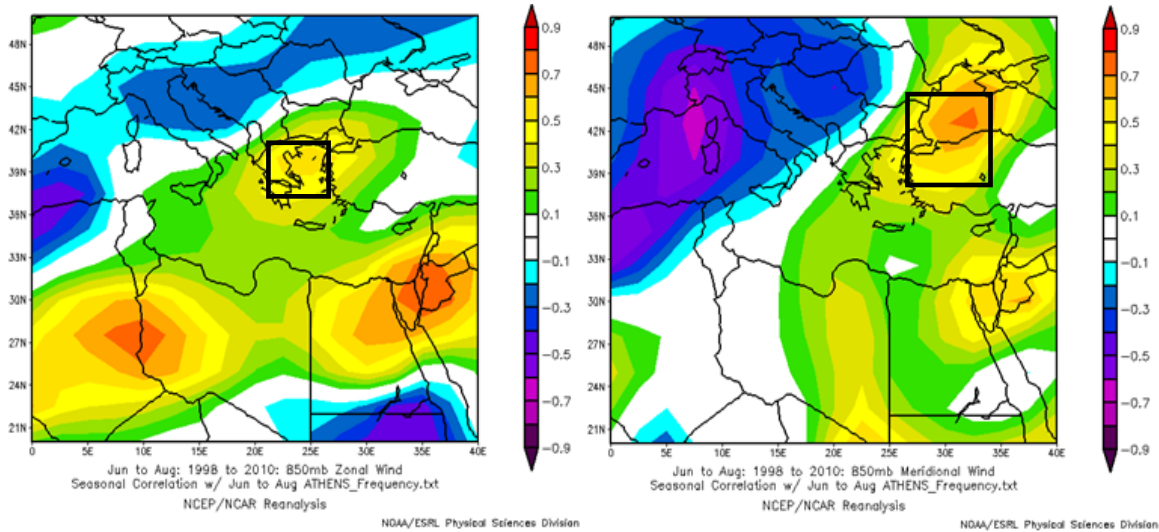
Figure 37.   Linear correlations in summer between Frequency at Athens and the: (a) ZW at 850 hPa (left panel); and (b) MW at 850 hPa (right panel) for the period 1998-2010, based on 1981–2010 NCEP reanalysis dataset. The black rectangles indicate areas of strong positive correlation that are over and near the Aegean focus region of our study. Correlation magnitudes ≥ 0.30 and greater indicate significance at the 95% level or greater. Figures created at: NOAA/ESRL Physical Sciences Division website, available online at http://www.esrl.noaa.gov/psd/ , accessed January 2012.

Figure 38 shows correlation maps for SST. Both concurrent and lagging correlations were plotted (Frequency lagging SST by one month). We focused on the lagging correlations in the Arabian Sea and in the North Atlantic (black boxes in Figure 38, right panel).. Positive correlation occurs at the Arabian Sea with values $r = 0.72$, $p > 99\%$ and negative correlation occurs at the N. Atlantic Ocean with values $r = -0.66$, $p = 99\%$. Additionally for the Arabian Sea, a positive correlation takes place between SST and the Strength gradient index lagging by one month with corresponding values $r = 0.64$ and $p = 98\%$.
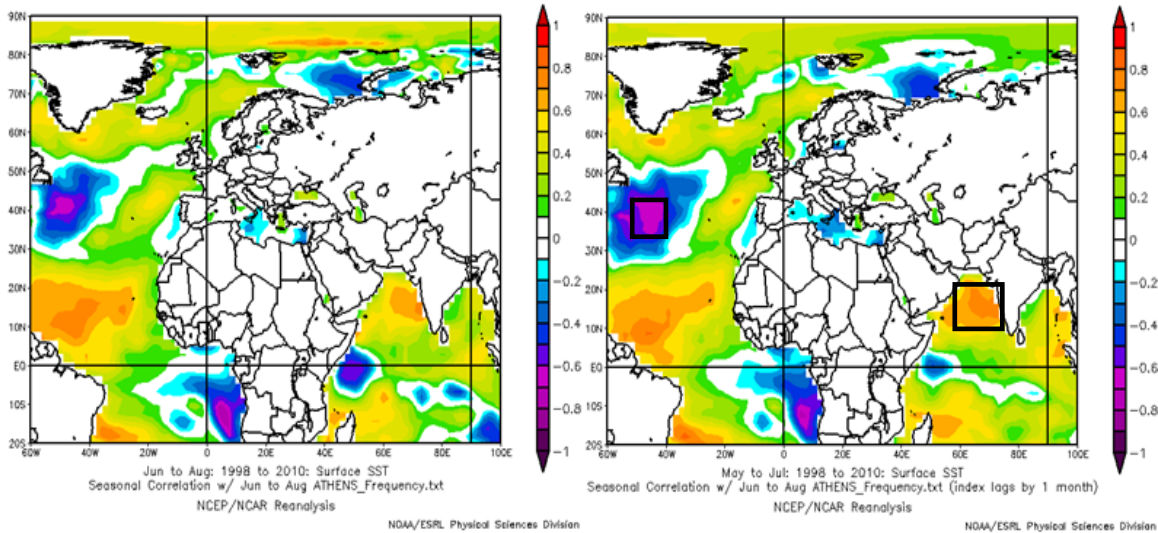
Figure 38.   Linear correlations in summer between Frequency at Athens and the: (a) SST hPa (left panel); and (b) SST leading by one month (right panel) for the period 1998-2010, based on 1981–2010 NCEP reanalysis dataset. The black rectangles indicate areas of strong correlation. Correlation magnitudes ≥ 0.30 and greater indicate significance at the 95% level or greater. Figures created at: NOAA/ESRL Physical Sciences Division website, available online at http://www.esrl.noaa.gov/psd/ , accessed February 2012.

Table 7 is a summary of all the correlations between ducting parameters and meteorological variables for summer 1998-2010. Correlations with the NAO and AO indices are also included. Significance levels have been calculated only for correlations larger than 0.5. Among them, the correlations with SLP in India and North Atlantic are especially significant. Noteworthy in this table is the fact that the Height correlations tend to be negative whenever the correlations with the other ducting parameters are positive. This tendency seems to be opposite from the one observed during winter, where the correlations with all the ducting parameters have the same sign.

Table 7.   The summer mean values of the ducting parameters for Athens (top four rows) and the correlations between those parameters and corresponding area-average environmental variables for selected regions. Only significance levels greater than or equal to 90% are shown. The correlations with significance levels greater than or equal to 95% are highlighted in yellow. Correlations with NAO and AO indices are also included. The sign of the correlation is indicated by the colored arrows: red indicates negative and green indicates positive.

JUN - JUL - AUG	1998	1999	2000	2001	2002	2003	2004	2005	2006	2007	2008	2009	2010
Frequency	70.19	64.82	50.48	62.42	65.63	69.71	66.97	75.15	55.68	60.95	64.06	64.50	74.53
Strength gradient	0.51	0.38	0.31	0.32	0.33	0.41	0.38	0.40	0.39	0.37	0.38	0.51	0.43
Height	33.67	64.65	67.72	70.05	66.19	71.89	67.70	63.48	60.89	71.70	62.31	59.66	68.53
SLP at India	1002.8	1002.0	1001.8	1001.8	1002.3	1002.4	1002.4	1002.1	1001.9	1001.7	1002.1	1002.1	1003.0
(17N-25N, 78E-90E)					↑	Frequency r= 0.70	p>99%						
					↑	Strength r= 0.53	p=95%						
					↓	Height r= -0.40							
SLP at N. Atlantic	1016.6	1015.6	1017.6	1015.9	1016.9	1015.2	1015.8	1016.0	1017.3	1016.2	1015.8	1016.3	1015.0
(42N-52N, 52W-38W)					↓	Frequency r= -0.72	p>99%						
					↓	Strength r= -0.23							
					↓	Height r= -0.28							
ZW850 at E. Mediterranean	-0.46	-0.15	-1.37	-0.16	0.39	-1.44	0.10	0.19	-0.66	-1.04	-1.19	-0.75	-0.13
(37N-41N, 22E-27E)					↑	Frequency r= 0.48	p=90%						
						Strength r= -0.07							
						Height r= -0.08							
MW850 at E. Mediterranean	-2.54	-2.97	-3.38	-2.46	-2.41	-3.37	-2.58	-2.28	-2.63	-2.86	-3.09	-2.77	-2.02
(38N-45N, 27E-34E)					↑	Frequency r= 0.55	p=95%						
					↑	Strength r= 0.18							
					↓	Height r= -0.17							
SST at N. Atlantic - 1 month lead	20.266	20.002	20.652	19.153	19.733	19.855	19.165	19.22	20.375	19.583	19.891	19.807	18.825
(34N-44N, 50W-38W)					↓	Frequency r= -0.66	p=99%						
						Strength r= 0.03							
					↓	Height r= -0.39							
SST at Arabian Sea - 1 month lead	29.329	28.376	28.25	28.359	28.852	29.279	28.489	29.145	28.711	28.923	28.55	28.88	29.45
(10N-20N, 60E-75E)					↑	Frequency r= 0.72	p>99%						
					↑	Strength r= 0.64	p=98%						
					↓	Height r= -0.30							
NAO Index	-1.01	0.32	-0.41	-0.11	0.57	0.06	-0.06	0.04	-0.09	-0.62	-1.32	-1.13	-0.87
						Frequency r= -0.03							
					↓	Strength r= -0.56	p=95%						
					↑	Height r= 0.40							
AO Index	-0.09	0.01	0.03	0.16	0.22	-0.10	-0.39	-0.13	0.30	-0.33	-0.22	-0.92	0.10
					↓	Frequency r= -0.13							
					↓	Strength r= -0.55	p=95%						
						Height r= 0.08							

By comparing Table 7 with Table 6 (winter correlations), a noteworthy difference is observed. During winter, there is the same correlation tendency for all the three ducting parameters. This suggests that the mid-latitude depressions and the incipient southwesterly flow serve as constructive mechanisms inclined to build ducting conditions; that is, more frequent, higher and stronger ducts. In contrast, during summer, the correlations attendant to Height appear to have opposite signs from the other parameters' correlations. This happens because the summer correlations are dictated by the prevailing northeasterly flow over the Aegean, which actually signifies a destructive for the ducting conditions process. This destructive mechanism tends to erode the ducts, and only the stronger and usually higher surface ducts survive. As a result, they drive the average Height up. This may explain why the summer correlations between Frequency, Strength gradient and Height appear with opposite signs.

In this part of the analysis, we try to provide reasonable and physical explanations for the patterns and the correlations observed between surface ducting and meteorological conditions during summer. As discussed in Section A, northeasterly flow prevails at lower levels over the Aegean Sea due to the relative position between the Azores High and the Indian Thermal Low. The cases of southwesterly flow due to synoptic scale effects are rare. Southerly and southwesterly winds are frequently observed, however, at the meteorological station of Athens, due to the sea breeze circulation that develops when the background northeasterly flow is not strong enough to suppress it.

For the 1998–2010 period we created a time series of the percentage of occurrence of southwesterly flow over Athens station during the summer. This was correlated with the ducting frequency time series to see the impact of sea breeze on ducting conditions for this specific area. The correlation coefficient that arose was $r = 0.03$. The other ducting parameters had equally low correlations. This means that sea breeze is not a factor that dictates the variation of ducting parameters, at least when it is averaged over a whole season period. A possible explanation accounting for this is that, in the case of the sea breeze, two moisture-related forces act against each other. The onshore flow brings moist air, creating favorable conditions for ducting. On the other

hand, however, the lower level flow is weaker from the higher one, mostly due to friction effects, resulting in the transport of lower amounts of moisture at the surface than at higher levels, therefore, creating unfavorable ducting conditions. The net outcome is neutral for the ducts.

We also correlated the ducting frequency with the percentage of occurrence of offshore flow, which technically, for the case of the Athens station, is the synoptic northeasterly flow itself. The resultant correlation was $r = -0.74$ with significance level $p > 99\%$. This significantly negative correlation is consistent with the correlation maps in Figure 37, which show the correlations with the wind components. Gathering all this evidence together, we infer that whenever the northeasterly flow is strong, the ducting frequency is low, and whenever the northeasterly flow relaxes, the ducting frequency increases. The reason for this is that the prevailing northeasterly flow over Athens advects less humid air from the relatively dry Aegean Sea region (Figure 12), therefore reducing the total moisture amounts over the station. Moreover, the advected air parcels before reaching the Athens station cross over the hot land and mix with dry air, reducing even more the amounts of moisture that they contain. On top of that, the persistent northeasterly winds cause mixing within the surface layer by means of mechanically generated turbulence, and therefore tend to destroy the humidity and temperature gradients.

Figure 39 is a map of the Athens station area and shows its disposition in relation to the prevailing winds. Before reaching the Athens station, the northeasterly winds have to flow over land and mix with dryer air.
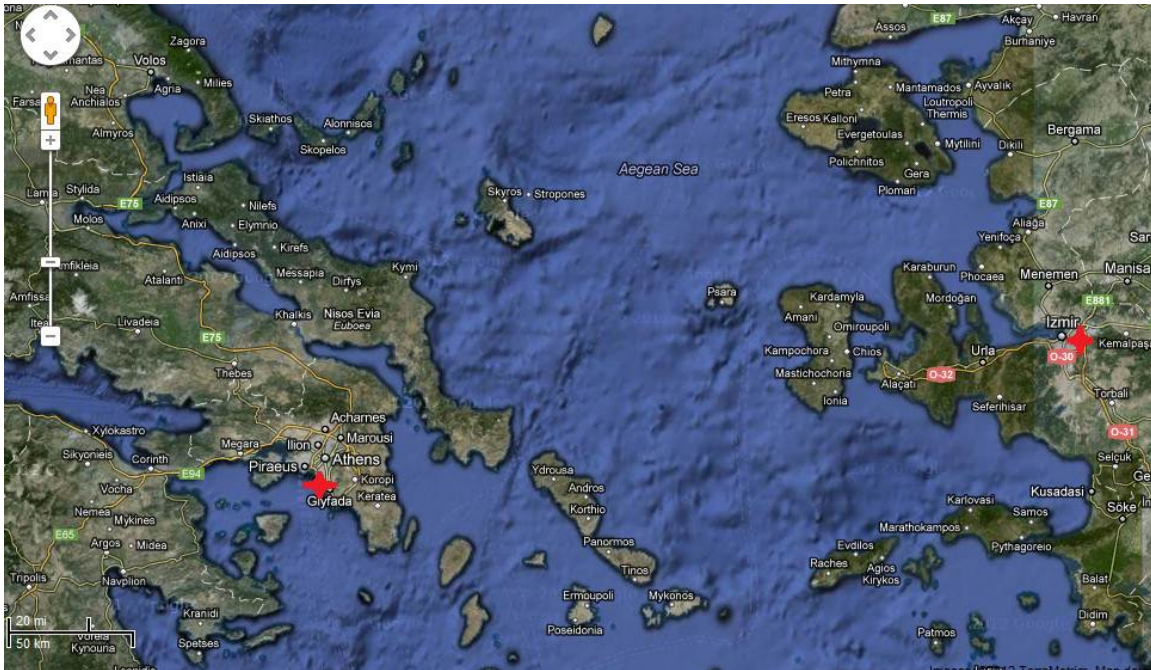
Figure 39.   Part of the Aegean Sea and the surrounding land masses are captured in this figure. The red stars denote the locations of Athens and Izmir. (After Google Maps)

Consistent with the wind correlations are the correlations associated with the SLP presented in Figure 36 and the correlations associated with the SST presented in Figure 38. The correlation map in Figure 36 implies that when the thermal low over Indian subcontinent amplifies, then the northeasterly flow over Aegean Sea gets stronger, depleting the moisture amount over Athens and causing more wind-generated mixing. The same effect takes place whenever the Azores High amplifies but without being able to displace the west flank of the Indian Low hovering over the Aegean Sea (Figure 11). In this situation, a strong pressure gradient develops, generating very strong and persistent northeasterly flow, with analogous implications. If the intensifying Azores High expands eastward, covering the Aegean Sea region with high pressure levels, with the thermal low retreating, then a different situation develops, but with the same negative effects on ducting conditions. Persistent fair weather and extensive insolation warms the ground, causing a thermally driven mix of the surface layer, eventually smoothing over the vertical profile gradients and destroying ducts.

60

Concerning SST correlation maps (Figure 38), the relevant correlations appearing over the N. Atlantic Ocean and Arabian Sea are consistently coupled with the respective SLP correlations. The negative correlation of SST at the N. Atlantic links with the negative correlation of SLP over the same region, due to air-sea interaction effects. The positive correlation of SST at the Arabian Sea links with the positive correlation of SLP over the Indian subcontinent. When the SLP is low, it implies an intensification of the dominant thermal low, and consequently stronger summer monsoons. This situation, in turns, involves more persistent cloudiness, heavier rain and increased river run off for the Arabian Sea. These last three factors contribute to lower SST for that region. The opposite effects take place when the SLP over the Indian subcontinent increases. Associates

Figures 40–42 illustrate composite anomaly maps of selected climate system variables for the two years that exhibited the highest Frequency during the 1998–2010 period and the two years that exhibited the lowest Frequency during the 1998–2010 period. These maps complement the correlation maps (Figures 36-38) by showing the anomalous conditions, including the spatial patterns and signs of the climate variations, associated with high and low Frequency.

The anomaly maps give results consistent with the correlation maps. The years of the highest Frequency (2005, 2010) are those with lower than normal SLP over Europe and higher than normal SLP over India, suggesting a weaker pressure gradient over the Aegean Sea (Figure 40). This results in an anomaly at 850mb VW with a southerly direction, bringing air rich in moisture over Athens (Figure 41). The opposite situation takes place during the lowest Frequency years (2000, 2006). Positive SLP anomaly over Europe and negative SLP anomaly over Saudi Arabia indicate a strong combination of Azores anticyclone with the thermal low amplifying over India and the Middle East. This results in an anomaly at 850mb VW with a northeasterly direction, bringing relatively dry air over Athens. SST anomalies at the N. Atlantic Ocean and Arabian Sea (Figure 42) are also in agreement with the corresponding correlation maps and the physical interpretations given earlier.

Figure 40.   SLP composite anomaly maps for the two summers with the highest Frequency at Athens (left panel) and the lowest Frequency at Athens (right panel). Figures created at: NOAA/ESRL Physical Sciences Division website, available online at http://www.esrl.noaa.gov/psd/ , accessed February 2012.

Figure 41.   VW at 850 hPa composite anomaly maps for the two summers with the highest Frequency at Athens (left panel) and the lowest Frequency at Athens (right panel). Figures created at: NOAA/ESRL Physical Sciences Division website, available online at http://www.esrl.noaa.gov/psd/ , accessed February 2012.

Figure 42.   SST composite anomaly maps for the two summers with the highest
Frequency at Athens (left panel) and the lowest Frequency at Athens (right panel).
The SST leads by one month. Figures created at: NOAA/ESRL Physical Sciences
Division website, available online at http://www.esrl.noaa.gov/psd/ , accessed
February 2012.

The SLP anomaly maps in Figure 40, and the SLP correlation maps in
Figure 36, show that the Frequency decreases when high pressure covers the wider region
around the Aegean Sea. We also explored the relation of the Frequency with the incipient
subsidence caused by high-pressure systems. We looked for correlations between the
Frequency and the vertical velocity ω at several vertical levels. We did not find any
vertical level where the correlation was positive. On the contrary, the correlations were
slightly negative throughout the vertical. In Figure 43, we provide a sample of the
correlation maps between Frequency and ω for two different levels. The resultant ω
negative correlations are consistent with the SLP negative correlations, and signify that
when stronger subsidence takes place, denoted by positive vertical motion, the Frequency
decreases. The Frequency is larger when the subsidence relaxes (less positive vertical
motion). After the previous results, we are inclined to believe that the subsidence, which
manifests itself mostly at the middle and higher atmosphere, does not penetrate the ABL
deep enough to be capable of affecting the surface ducting conditions. We consider that
the temperature inversions it produces are confined to higher altitudes and might rarely
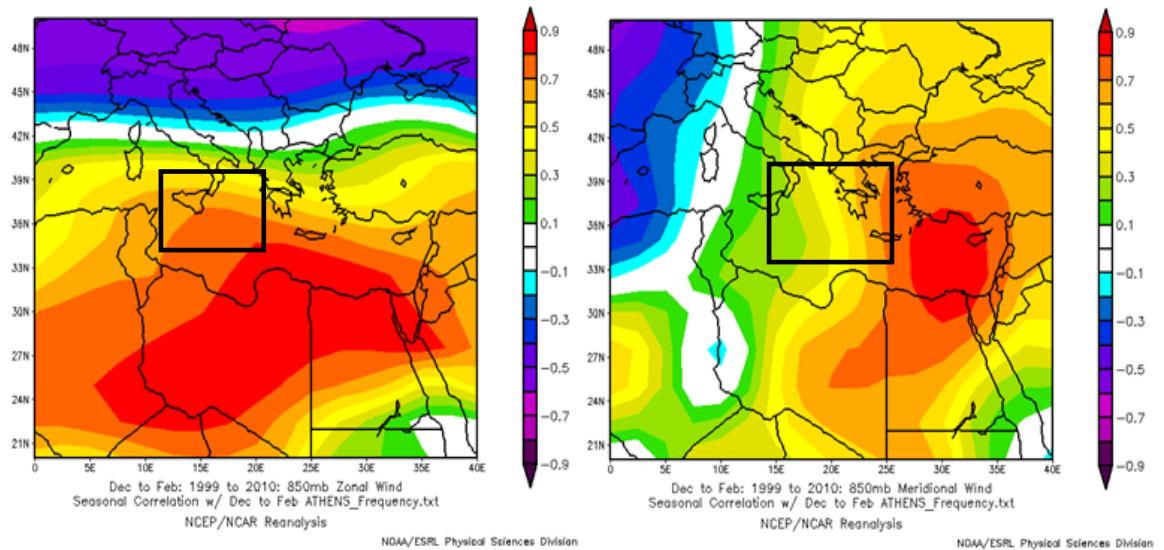reach the surface.

63
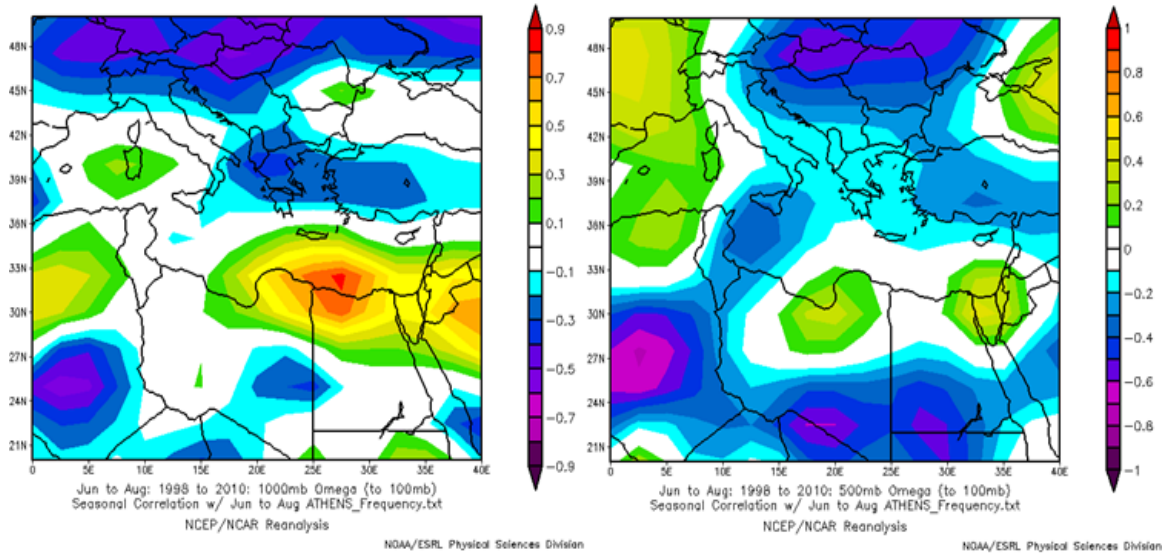
Figure 43.   Linear correlations in summer between Frequency at Athens and the: (a) ω at 1000 hPa (left panel); and (b) ω at 500 hPa (right panel) for the period 1998-2010, based on 1981–2010 NCEP reanalysis dataset. Correlation magnitudes ≥ 0.30 and greater indicate significance at the 95% level or greater. Figures created at: NOAA/ESRL Physical Sciences Division website, available online at http://www.esrl.noaa.gov/psd/ , accessed February 2012.

C.   ANALYSIS OF DUCTING CONDITIONS OVER IZMIR STATION

1.   Derived Statistics

Initially, we examined the variation of the ducting parameters over an entire year. Figure 44 shows the yearly distribution of these parameters. Summer has the highest Frequency and highest Strength gradient, as happens at the Athens station, suggesting that favorable conditions for ducting formation prevail during summer months. The Height distribution seems to follow a different pattern, demonstrating three local maxima: January, June and October. In contrast, winter exhibits the lowest values of Frequency and Height. Strength gradient has relatively low values during winter, with the lowest ones during the FMA period, similar to patterns observed in Athens.

The variability of these parameters is quantified by the standard deviation. As in Athens, one can see in Figure 44 that the winter months display higher variability, relative to mean values, for Frequency, implying that ducting conditions during winter follow the increased variability of atmosphere, imposed by the synoptic scale circulation. In contrast, summer's lower variability for Frequency can be attributed to the more stable weather during this season.
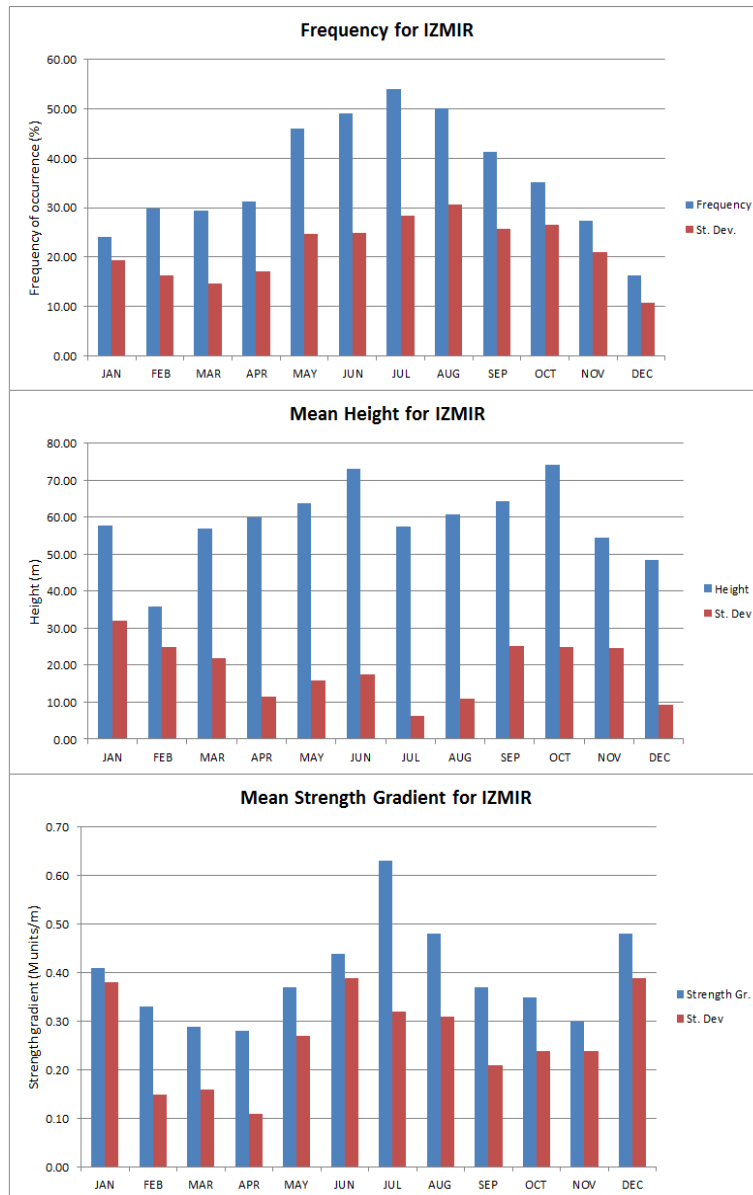
Figure 44.   Distribution plots of ducting parameters for IZMIR station. The values used for this plot have been derived by averaging the monthly means over the 1991–2010 period.

Next, we examined the interannual variability of ducting parameters. By taking the seasonal mean for each year, we constructed time series separately for each parameter and season. Aware of the resolution issue we confronted with the Athens station ducting statistics, we took the data vertical resolution for the Izmir station into consideration as well. By applying the same methodology as for Athens, we calculated the critical levels, below which the major volume of surface ducts are expected to be. For winter, we came up with a critical level of 70 m, and for summer, with a critical level of 80 m.

Figure 45 presents the resultant plots for the winter season, and linear trend lines for the ducting parameters were added to each plot. A situation similar to Athens is encountered here, with trends over the ducting parameters revealing statistical biases. The ducting conditions appear to be better during the second half of the 1991–2010 period. Significant positive correlation occurs between Frequency and vertical resolution with a coefficient of $r = 0.68$ and significance level $p > 99\%$. The correlations with the other two ducting parameters are not significant, but they still imply that a connection holds between them and the resolution.

Figure 45.   Time series during winter for Izmir. The blue line (rhombus markers) connects the seasonal means of ducting parameters for each year. The red line (square markers) connects the seasonal means of the resolution, represented in %. The red straight line depicts the linear trend of the ducting parameters series. For the years 1991 and 1995 there are no Height and Strength gradient values because the derived statistics show that no surface ducting occurred at those years (Frequency = 0%)

67

Regarding the correlation coefficients along with the relevant plots, we infer that the observed biases are due to the long-term variation of the vertical resolution. As one can readily see, the resolution graph displays two distinct modes, one at the first and one at the second decade, with an outstanding spike between them. The first decade is characterized by exceptionally low resolution and subsequently by exceptionally low ducting frequency. We have no relevant information at our disposal to account for this peculiar behavior, but we assume that it has to do with the utilization of different data processing software between these two major periods, as the case was for Athens. There is no recorded proof of an atmospheric change to explain this huge change in the resolution between these two periods.

The additional characteristic here on resolution graph is that, even within the same major periods, the resolution presents large fluctuations. Obviously short-term atmospheric variability can account for these interannual fluctuations, since their magnitude is much less than the interdecadal one. For the Athens station, this fluctuation was not so large, something that compels us to believe that the more complex topography around Izmir station explains those larger fluctuations because it is apt to produce more significant pressure levels in the vertical, recorded by the radiosonde.

It is important to stress here that the short-term resolution variability is related with short-term atmospheric variability and connected with the concept of the significant pressure levels. Significant pressure levels are calculated according to WMO criteria based on significant meteorological events occurring in the vertical. However, a significant level, from a meteorological perspective, does not necessitate that the same level is significant from a ducting perspective, or vice-versa. The M reversals in the profile can occur even without significant atmospheric variations, since the proper synergy of the meteorological variables involved in equation (2.1) is sufficient to produce those reversals. Consequently, we believe that the frequency variations, as a statistical product, are dictated to an important degree by the resolution fluctuations. On the contrary, we argue that the variations of the real ducting frequency are not connected with the variations of the resolution, even though both of them are influenced by the same meteorological variables, but with different manners.

Figure 46 shows the respective plots for summer. Note that the same connection between resolution and ducting statistics holds during summer. The main difference now is that the correlation between Frequency and resolution is much weaker, although remaining positive. The same explanation as for Athens applies here. The weaker correlation during summer is explained by the fact that the resolution is twice the winter values. Consequently, the greater part of surface ducts is detected by the radiosondes, and only a few evade, thus the Frequency variability tends to disengage from the resolution variability. On the other hand, the Height and Strength gradient correlation coefficients are much higher during summer, because the almost permanent existence of surface ducts makes these statistically derived parameters fluctuate in accordance with the resolution fluctuations.

The two distinct periods are still evident, as well as the spike between them, but with less magnitude applying for both of these features. One more notable characteristic on the summer plots is the large fluctuation of resolution during the first decade.

Figure 46.   Time series during winter for Izmir. The blue line (rhombus markers) connects the seasonal means of ducting parameters for each year. The red line (square markers) connects the seasonal means of the resolution, represented in %. The red straight line depicts the linear trend of the ducting parameters series.

On the grounds of the existing link between resolution and ducting parameters variation, and in order to study the yearly variation of the ducting conditions in connection with the weather variations, we are compelled, as happened in Athens case, to examine only those periods that present relatively low resolution fluctuation. In this way, we eliminate, to a significant degree, the biases imposed by the resolution issue, and we allow for the ducting variations to be dictated mainly by the meteorological variations.

2. Analysis and Discussion Around Ducting Variability

In this section, we analyze the interseasonal and interannual surface ducting variations, try to interpret them and give sensible explanations based on physical rules and fundamental meteorological principles.

a. *Interseasonal Variability*

The striking difference, which holds in ducting conditions, between winter and summer (Figure 44) stems from the same causes as those described and analyzed for Athens. The main cause for the interseasonal dissimilarity has to do with the amounts of moisture present in the lower levels of atmosphere. The intense evaporation during summer produces strong water vapor pressure gradients at the vertical, generating surface ducts and, at the same time, renders the potential ducting mechanisms more effective, as has already been analyzed.

On the other hand, during winter, the mechanisms that generate surface ducts operate under a regime of lower moisture amounts and, therefore, their ability to create ducting conditions is substantially reduced. Furthermore, the evaporation is much less, due to much lower temperatures.

b. *Interannual Variability*

Following the same reasoning we applied for Athens, in this section we try to verify that the moisture amounts present in the lower atmosphere account, to a great degree, for the yearly variations observed in surface ducting conditions. Again, we have used mixing ratio as a surrogate of the water vapor pressure.

71

Figure 47 shows time series of ducting frequency and mixing ratios for the two lower levels of the recorded levels. Both winter and summer parameters are shown. By correlating the Frequency with the mixing ratio at the surface, we obtained a very high correlation coefficient for summer and no correlation for winter. The lower correlation for winter should have been expected, since M lies at the left part of the exponential curves (Figure 24), but we did not expect to receive no correlation at all. The respective numbers are $r = 0.84$ with $p > 99\%$ for the summer, and $r = 0.02$ for the winter.
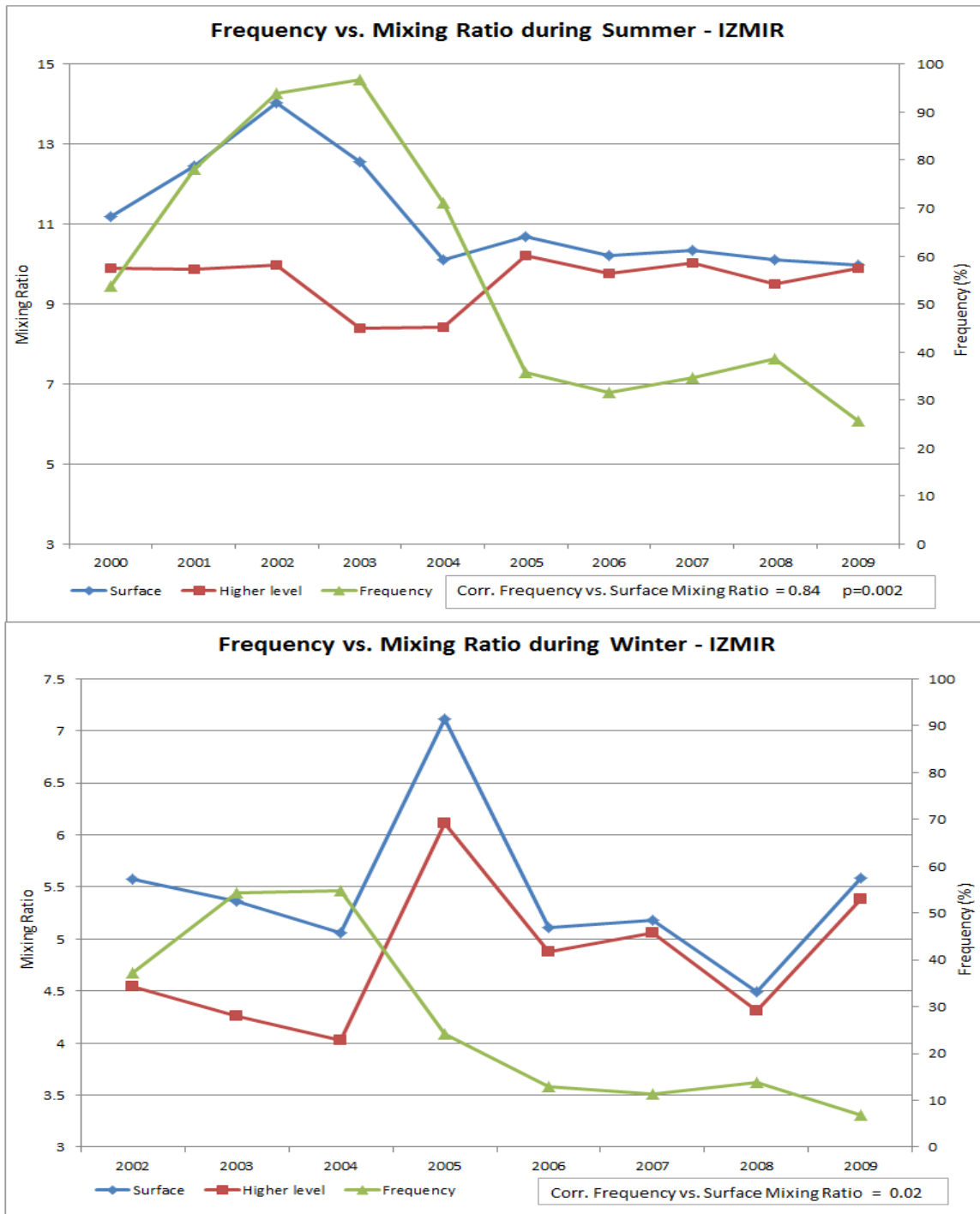
Figure 47.   Time series for Izmir in summer (upper panel) and winter (lower panel) of Frequency (green lines with triangle markers), moisture mixing ratio at the surface level (blue lines with rhombus markers) and moisture mixing ratio at the next higher level recorded by the radiosonde sounding (red lines with square markers). The correlation between the Frequency and surface mixing ratio is shown in the lower right of each panel

By correlating the Frequency with the mixing ratio at the surface, we received the following correlation coefficients: $r = 0.73$ with significance level $p > 99\%$ for the summer, and $r = 0.02$ for the winter. We expected that the winter correlation values would be lower than the summer ones, but we did not expect to receive almost zero correlation. A reasonable explanation for that could be that the more complex topography of the area surrounding Izmir allows mesoscale and local effects to manifest themselves, and eventually to affect surface ducting conditions by modulating the climatic large-scale influence upon the last ones

Based on the methods and the tools described in Chapter II and following the same routine as we did for Athens, we demonstrate only the more significant correlations, for which an adequate physical interpretation applies. A train of figures follows with correlation maps between Frequency at Izmir and selected climate system variables. As for Athens, we expect to see correlations dictated by the relationship between surface ducting conditions and the existing amounts of moisture.

Due to the results of the previous section with regard to the resolution, we decided to isolate and work with the period 2002–2009 for the winter and 2000–2009 for the summer. These periods do not display large resolution variability and we consider that trying to correlate ducting parameters with meteorological variables for these specific time intervals will give us realistic results, free from resolution-induced biases.

(1) Winter. Figure 48 shows the correlation between Izmir Frequency and SLP for winter 2002-2009. Negative correlation is observed over the E. Mediterranean and Minor Asia, but the resultant correlation coefficient is not as strong as in Athens. More significant correlations occur over the N. Atlantic and Arctic Oceans, being related with the NAO and AO modes. Even though the correlations of the ducting frequency with the NAO and AO indices proper are not strong enough, it turns out that they are significant with the associated SLP patterns. We calculated correlation coefficient for the N. Atlantic SLP $r = -0.78$ with significance level $p = 98\%$ and for the Arctic SLP $p = 0.76$ with $p = 97\%$. Equally important are the correlations that were computed between the ducting height and the SLP over these two regions. All the

74

calculated correlation coefficients with their corresponding significance levels are summarized in Table 8, after the correlation maps.
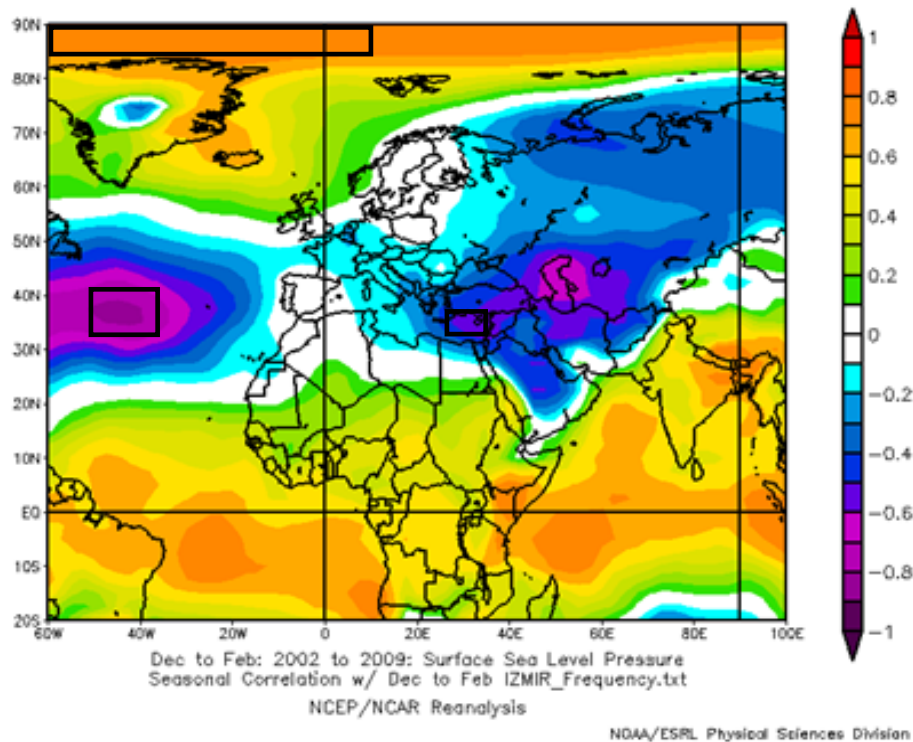
Figure 48.   Linear correlations in winter between SLP and Frequency at Izmir for the period 2002-2009, based on 1981–2010 NCEP reanalysis dataset. The black rectangles indicate areas of strong correlations. Correlation magnitudes ≥ 0.30 and greater indicate significance at the 95% level or greater. Figure created at: NOAA/ESRL Physical Sciences Division website, available online at http://www.esrl.noaa.gov/psd/ , accessed January 2012.

Figure 49 illustrates the correlation maps for PR, and RH at 700mb level. As in Athens, the correlations with these two meteorological variables seem to be the most resilient ones. All the three ducting parameters are considerably correlated with them (Table 8), with the Frequency correlations being the highest. The correlation with RH takes on the values of $r = 0.86$ and $p > 99\%$, and the correlation with PR assumes values of $r = 0.76$ and $p = 97\%$.
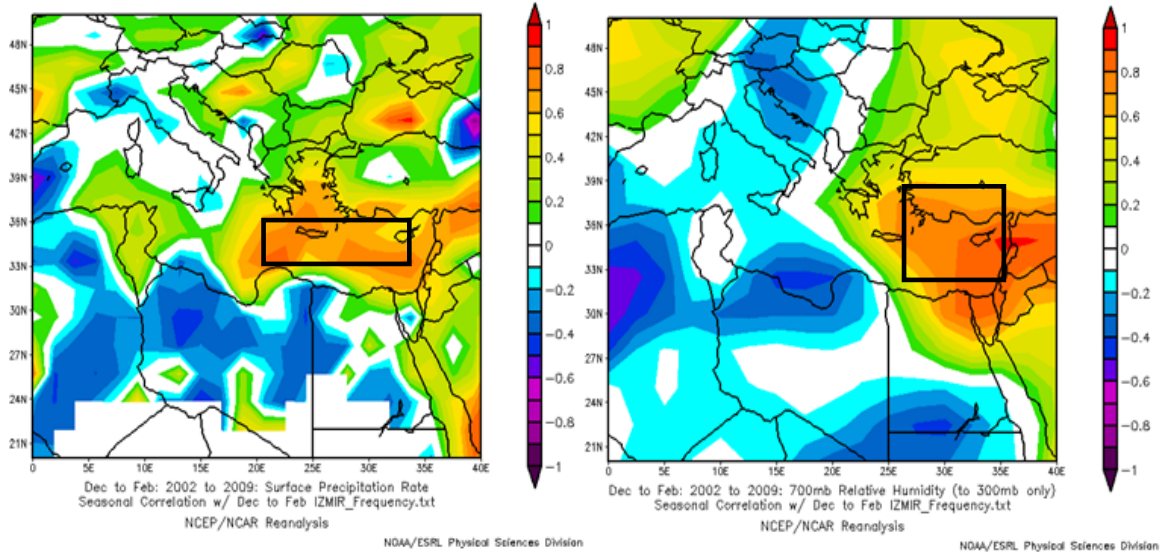
Figure 49.   Linear correlations in winter between Frequency at Izmir and the: (a) PR (left panel); and (b) RH at 700 hPa (right panel) for the period 2002-2009, based on 1981–2010 NCEP reanalysis dataset. The black rectangles in the eastern Mediterranean region indicate areas of strong positive correlation that are over and near the Aegean focus region of our study. Correlation magnitudes ≥ 0.30 and greater indicate significance at the 95% level or greater. Figures created at: NOAA/ESRL Physical Sciences Division website, available online at http://www.esrl.noaa.gov/psd/ , accessed January 2012.

Figure 50 depicts the correlation maps for ZW and MW at 850 hPa. The positive correlations, which have also been observed for Athens, make their presence here too, however with less intensity, and being shifted to the southeast.
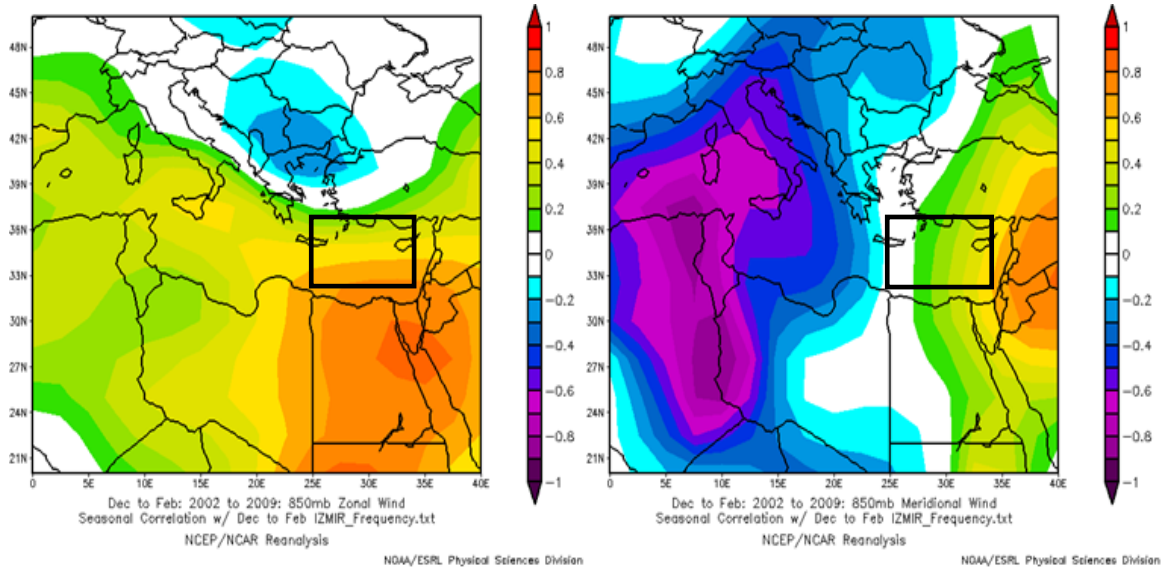
Figure 50.   Linear correlations in winter between Frequency at Izmir and the: (a) ZW at 850 hPa (left panel); and (b) MW at 850 hPa (right panel) for the period 2002-2009, based on 1981–2010 NCEP reanalysis dataset. The black rectangles in the eastern Mediterranean region indicate areas of strong positive correlation that are over and near the Aegean focus region of our study. Correlation magnitudes ≥ 0.30 and greater indicate significance at the 95% level or greater. Figures created at: NOAA/ESRL Physical Sciences Division website, available online at http://www.esrl.noaa.gov/psd/ , accessed January 2012.

Figure 51 shows correlation maps for SST. Both concurrent and lagging correlations have been plotted. As we did for Athens, we have focused on the positive correlation occurring at the Aegean Sea and the negative correlation occurring at the N. Atlantic Ocean between SST and the Frequency index lagging by one month. The respective values are presented on Table 8.
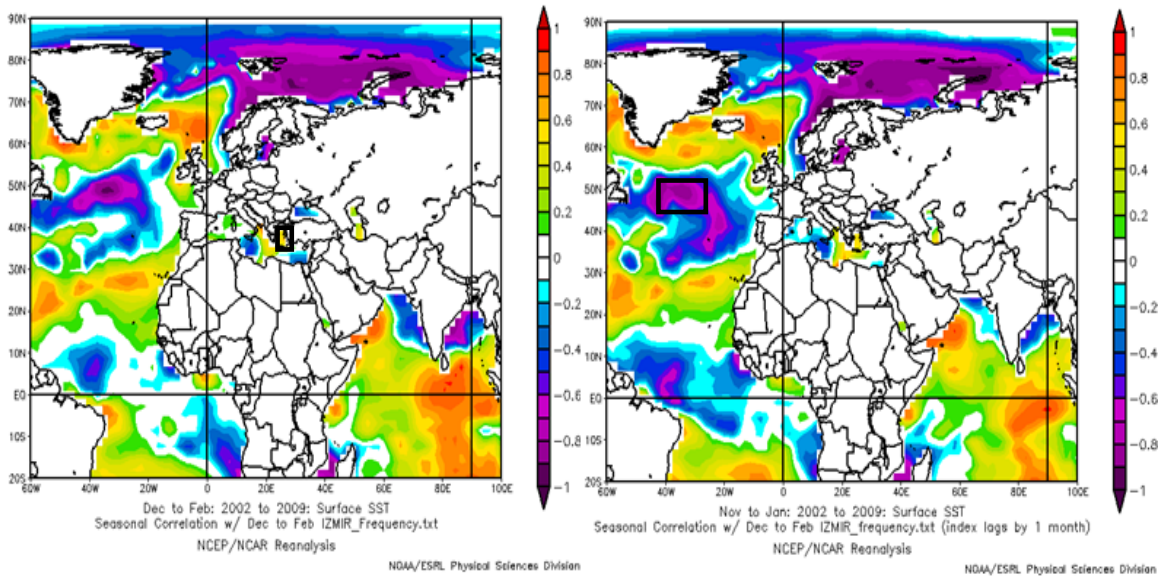
Figure 51.   Linear correlations in winter between Frequency at Izmir and the: (a) SST (left panel); and (b) SST leading by one month (right panel) for the period 2002-2009, based on 1981–2010 NCEP reanalysis dataset. The black rectangles indicate areas of strong correlations. Correlation magnitudes ≥ 0.30 and greater indicate significance at the 95% level or greater. Figures created at: NOAA/ESRL Physical Sciences Division website, available online at http://www.esrl.noaa.gov/psd/ , accessed January 2012.

Table 8 is a summary of all the correlations between ducting parameters and meteorological variables for winter 2002-2009 at the Izmir station. Correlations with the NAO and AO indices are also included. Among them, the correlations with SLP over the N. Atlantic and Arctic Ocean, PR and RH at the 700 hPa level over the E. Mediterranean distinguish. As with the correlations in Athens, all three ducting parameters (Frequency, Height and Strength gradient) exhibit the same trends; that is, all are correlated with the respective meteorological values with the same sign. A comparison between Table 8 and Table 6 for Athens confirms the consistency of correlation patterns between the two stations.

Table 8.   The winter mean values of the ducting parameters for Izmir (top four rows) and the correlations between those parameters and corresponding area-average environmental variables for selected regions. Only significance levels greater than or equal to 90% are shown. The correlations with significance levels greater than or equal to 95% are highlighted in yellow. Correlations with NAO and AO indices are also included. The sign of the correlation is indicated by the colored arrows: red indicates negative and green indicates positive.

DEC - JAN - FEB	2002	2003	2004	2005	2006	2007	2008	2009
Frequency	37.14	54.22	54.78	24.26	12.91	11.39	13.72	6.83
Strength gradient	0.30	0.29	0.45	0.40	0.12	0.13	0.15	0.41
Height	64.06	64.07	57.78	50.75	48.89	43.20	43.53	46.47
RH700 at E. Mediterranean (32N-38N, 27E-37E)	37.86	44.77	43.26	39.56	36.44	34.25	35.59	38.57
			↑	Frequency r= 0.86		p>99%		
			↑	Strength r= 0.68		p=94%		
			↑	Height r= 0.74		p=96%		
PR at E. Mediterranean (33N-36N, 21E-35E)	2.83	3.81	3.65	2.56	1.97	1.85	2.62	3.15
			↑	Frequency r= 0.76		p=97%		
			↑	Strength r= 0.70		p=95%		
			↑	Height r= 0.66		p=93%		
ZW850 at E. Mediterranean (32N-37N, 25E-36E)	2.96	4.42	3.99	2.64	3.06	1.88	1.77	4.14
			↑	Frequency r= 0.56				
			↑	Strength r= 0.63		p=91%		
			↑	Height r= 0.60				
MW850 at E. Mediterranean (32N-37N, 25E-36E)	0.70	1.35	1.88	1.41	1.36	-0.67	-1.09	2.17
			↑	Frequency r= 0.34				
			↑	Strength r= 0.73		p=95%		
			↑	Height r= 0.43				
SLP at E. Mediterranean (35N-32N, 27E-37E)	1018.7	1016.4	1016.3	1017.6	1017.1	1019.3	1019.9	1017.0
			↓	Frequency r= -0.52				
			↓	Strength r= -0.59				
			↓	Height r= -0.48				
SLP at N. Atlantic (42N-33N, 50W-30W)	1016.3	1017.6	1014.4	1020.6	1018.5	1018.7	1021.2	1020.6
			↓	Frequency r= -0.78		p=98%		
			↓	Strength r= -0.28				
			↓	Height r= -0.71		p=95%		
SLP at Arctic Ocean (90N-85N, 60W-20E)	1012.6	1011.8	1016.4	1007.3	1010.3	1008.4	1008.3	1009.9
			↑	Frequency r= 0.76		p=97%		
			↑	Strength r= 0.44				
			↑	Height r= 0.68		p=94%		
SST at N. Atlantic - 1 month lead (45N-52N, 42W-25W)	13.255	12.223	12.777	13.204	13.03	13.05	13.679	13.583
			↓	Frequency r= -0.75		p=97%		
			↓	Strength r= -0.10				
			↓	Height r= -0.64		p=91%		
SST at E. Mediterranean (35N-39N, 23E-28E)	15.657	15.905	15.731	16.069	15.592	15.522	15.403	16.186
				Frequency r= 0.09				
			↑	Strength r= 0.76		p=97%		
			↑	Height r= 0.20				
NAO Index	-0.02	-0.34	-0.32	0.59	-0.18	-0.03	0.38	-0.42
			↓	Frequency r= -0.28				
			↓	Strength r= -0.16				
			↓	Height r= -0.32				
AO Index	0.45	-0.65	-0.98	0.11	-0.81	1.00	0.86	0.26
			↓	Frequency r= -0.59				
			↓	Strength r= -0.35				
			↓	Height r= -0.51				

79

The observed correlation patterns (Figure 48–51) and the individual correlation values (Table 8) together indicate that surface ducting conditions in Izmir are very consistent with the respective ones for Athens, even if the correlations tend to be little lower. As discussed before, a possible reason may be the more active role of the local effects. So, the correlation patterns indicate that surface ducting conditions are more likely in winter when mid-latitude depressions are occurring in the area. These depressions constitute a major source of humidity, especially by producing southwesterly moisture advection over the Aegean Sea from the relatively humid regions over the Mediterranean (see Figure 10). Additionally, they are accompanied by frontal activity, which also improves ducting conditions, as explained in the previous section. The very strong correlations with the PR and the RH (Table 8) over the E. Mediterranean support these arguments.

Additionally, the SST correlations in the Aegean Sea and the North Atlantic Ocean (Figure 51) are consistent with the same processes. The negative correlation at N. Atlantic Ocean is linked with the negative correlation of SLP over the same area (Figure 48), and by extension with the NAO mode. The negative correlation with the NAO index confirms this reasoning. Another noteworthy feature is the same correlation tendency for all the three ducting parameters (Table 8), a tendency that has also been recorded for Athens.

Figures 52–56 illustrate composite anomaly maps of selected climate system variables for the two years that exhibited the highest Frequency during the 2002-2009 period and the two years that exhibited the lowest Frequency during the 2002–2009 period.

The anomaly maps give coherent results with the correlation maps. The years of the highest Frequency are those ones with negative phases of the NAO and AO modes, as it is evident from the SLP anomaly dipole over the N. Atlantic Ocean (Figure 52). During those years, more mid-latitude storms were directed towards the E. Mediterranean, as indicated by the negative SLP anomaly over the Aegean region, the positive precipitation rate anomaly (Figure 53), the positive RH anomaly (Figure 54) and the generally southwesterly flow anomaly indicated by the VW anomalies (Figure 55).

80

The SST anomalies at the Aegean Sea and the North Atlantic are also in agreement with the corresponding correlation maps and the physical interpretations given earlier (Figure 56).
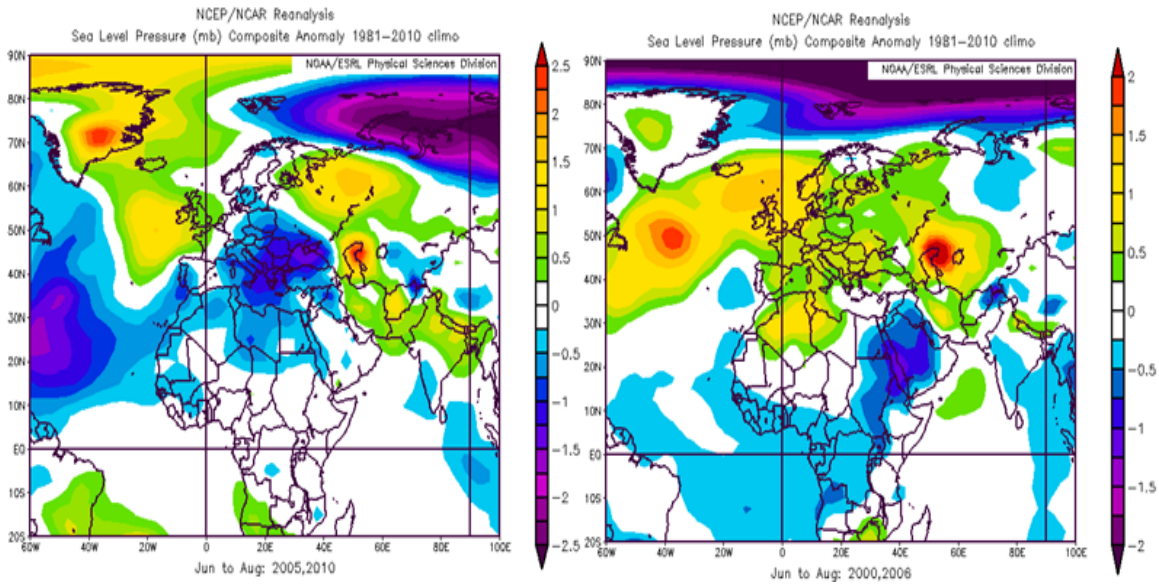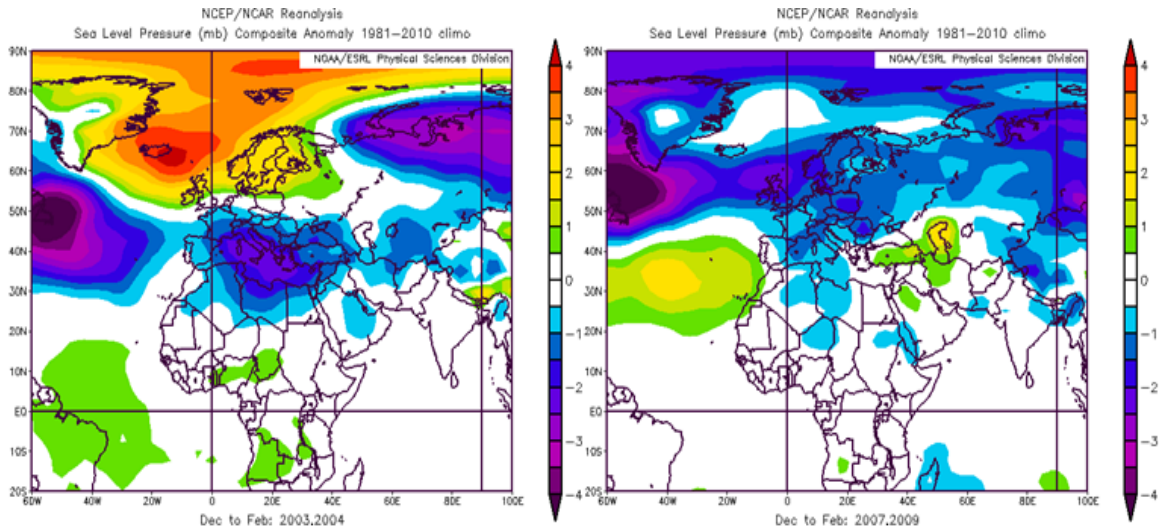

Figure 52.   SLP composite anomaly maps for the two winters with the highest Frequency at Izmir (left panel) and the lowest Frequency at Izmir (right panel).   Figures created at: NOAA/ESRL Physical Sciences Division website, available online at http://www.esrl.noaa.gov/psd/ , accessed February 2012.
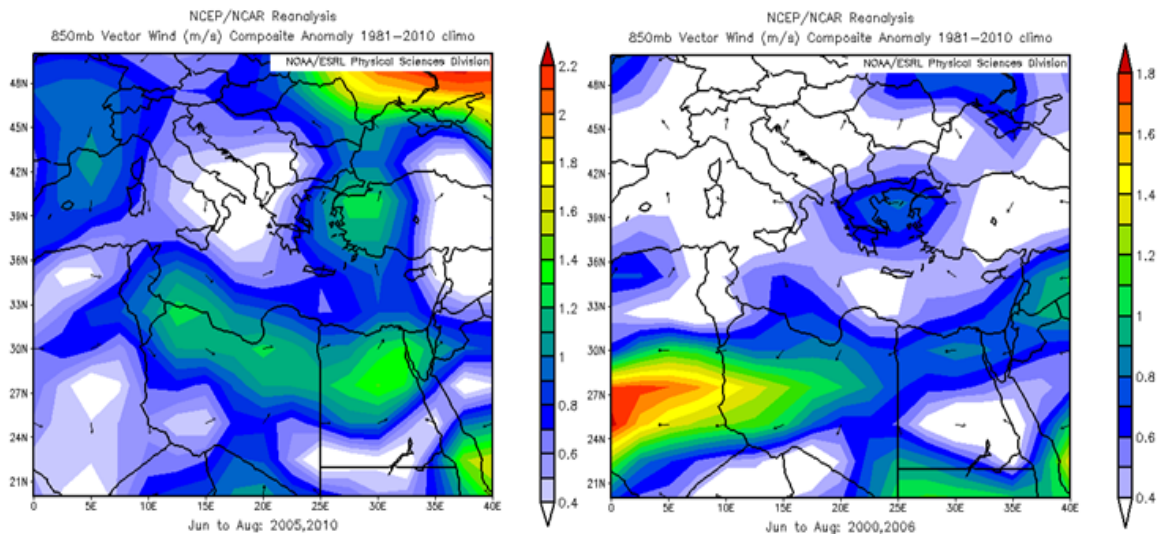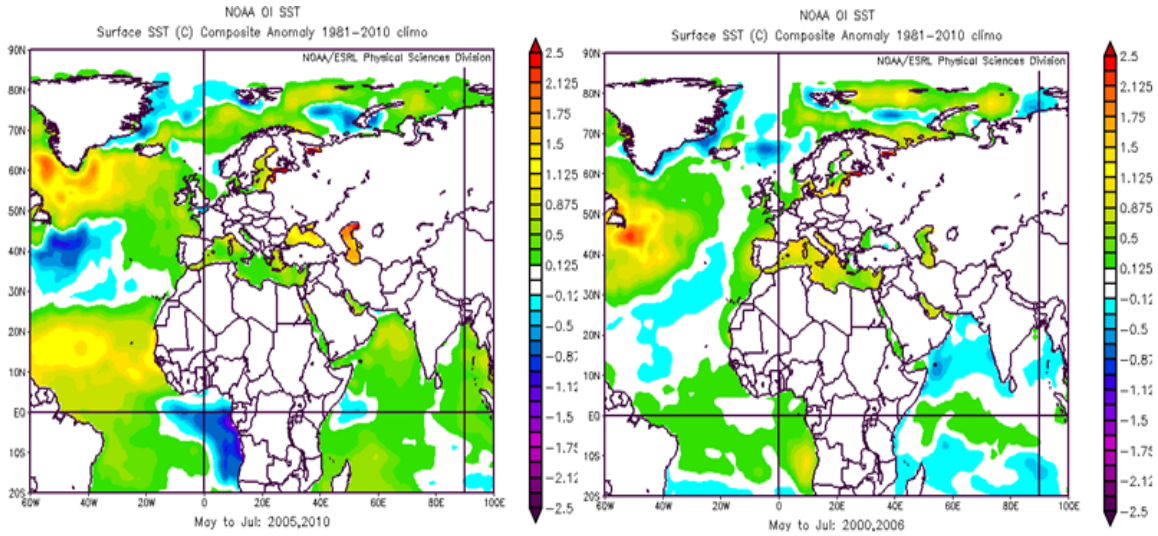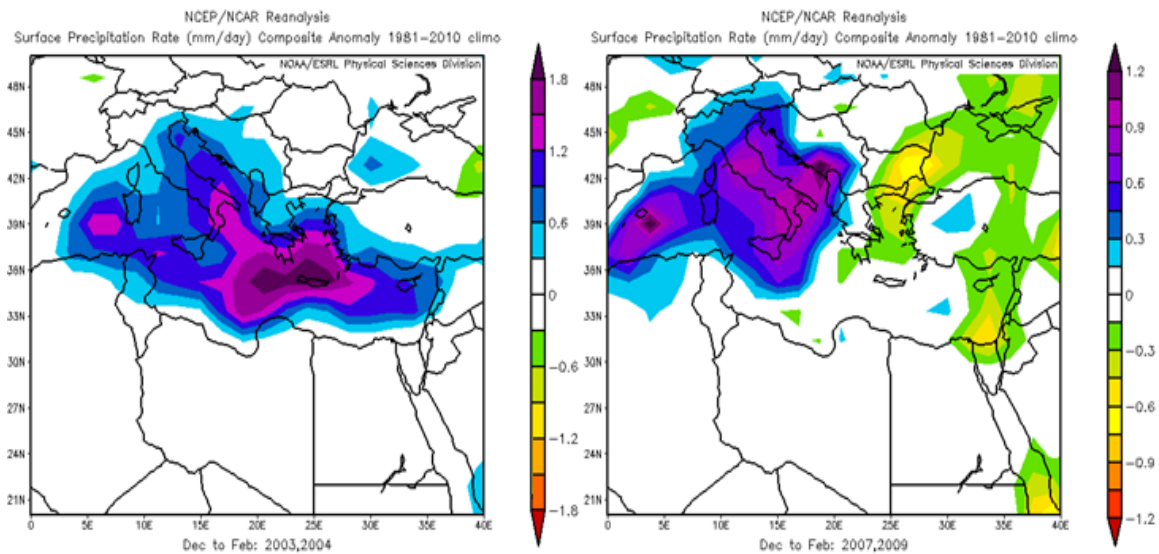

Figure 53.   PR composite anomaly maps for the two winters with the highest Frequency at Izmir (left panel) and the lowest Frequency at Izmir (right panel). Figures created at: NOAA/ESRL Physical Sciences Division website, available online at http://www.esrl.noaa.gov/psd/ , accessed February 2012.
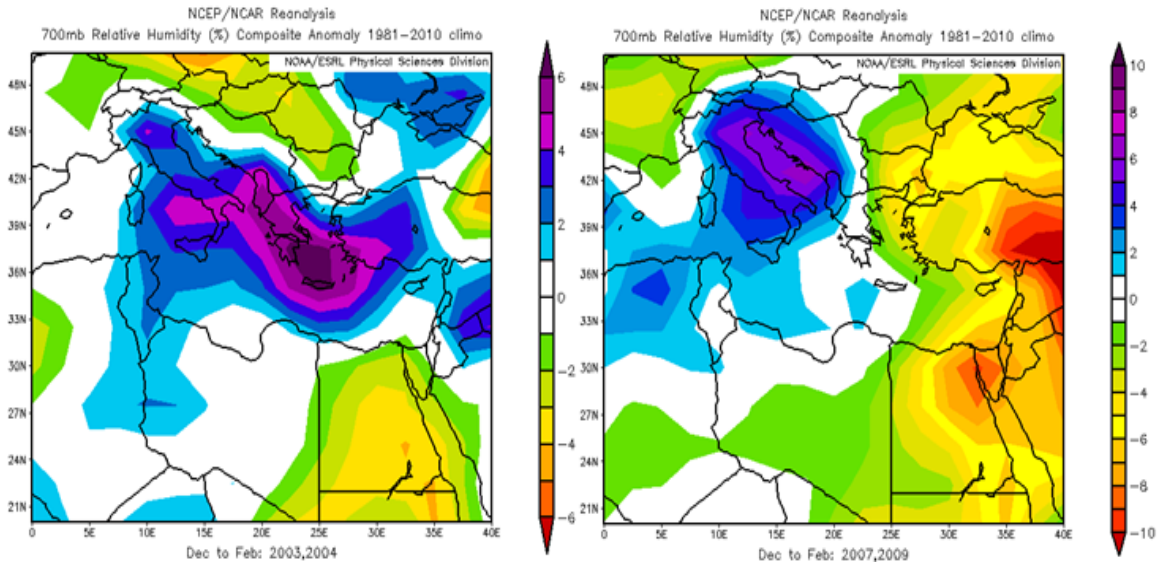
Figure 54.   RH at 700 hPa composite anomaly maps for the two winters with the highest Frequency at Izmir (left panel) and the lowest Frequency at Izmir (right panel). Figures created at: NOAA/ESRL Physical Sciences Division website, available online at http://www.esrl.noaa.gov/psd/ , accessed February 2012.
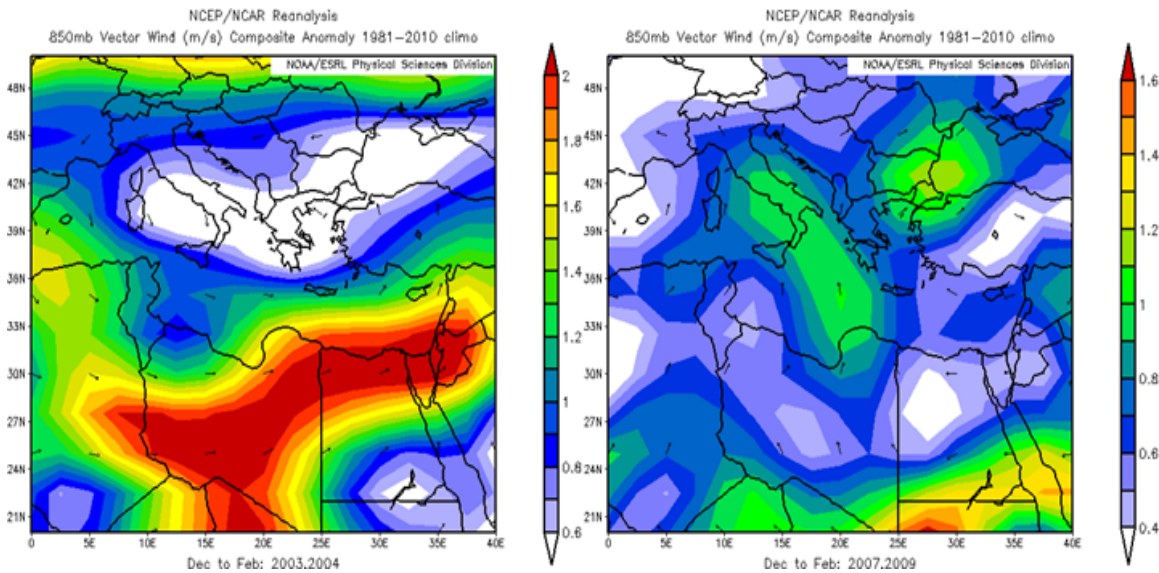
Figure 55.   VW at 850 hPa composite anomaly maps for the two winters with the highest Frequency at Izmir (left panel) and the lowest Frequency at Izmir (right panel). Figures created at: NOAA/ESRL Physical Sciences Division website, available online at http://www.esrl.noaa.gov/psd/ , accessed February 2012.
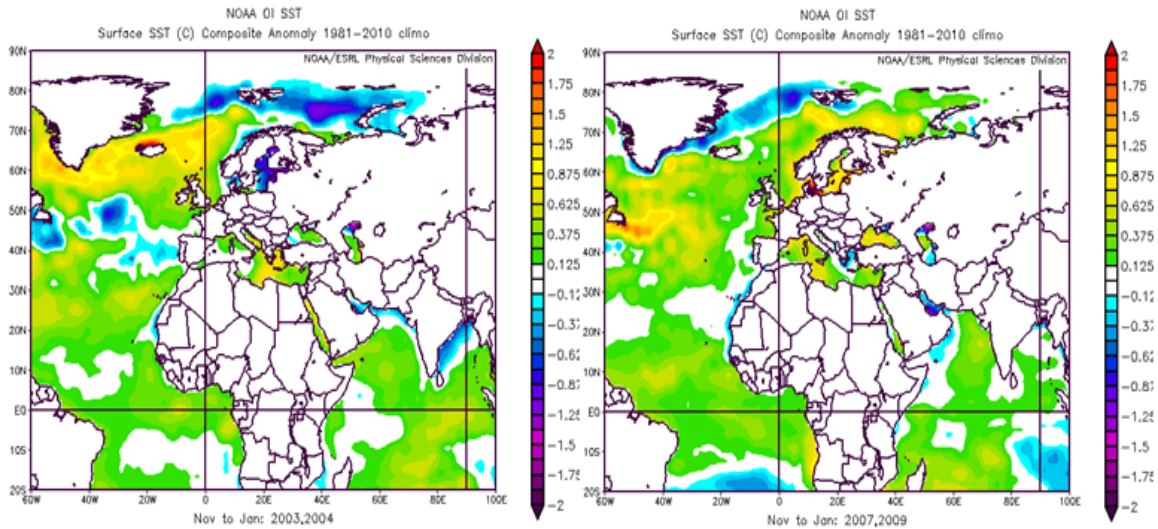
Figure 56.   SST composite anomaly maps for the two winters with the highest Frequency at Izmir (left panel) and the lowest Frequency at Izmir (right panel). SST leads by one month. Figures created at: NOAA/ESRL Physical Sciences Division website, available online at http://www.esrl.noaa.gov/psd/ , accessed February 2012.

For the years of the lowest Frequency, we see the opposite patterns, even though the opposite anomalies look weaker. Interestingly, during the low Frequency years, a southerly flow exists over the Aegean (Figure 55), something that contradicts the rest anomalies. Even more interesting is the fact that while the high Frequency years are common for both Athens and Izmir, for the low Frequency years, a discrepancy emerges; 2009 appears as a low year for Izmir but not for Athens. On the contrary, 2009 is a year of relatively high Frequency for Athens.

In order to understand what lies behind this discrepancy, Figure 57 shows the Frequency and resolution plots for both stations. By inspecting the 2007–2009 period we can see that 2007 is a low Frequency year for both stations, then a small increase is recorded at 2008 for both stations, but later on, 2009 appears to present opposite tendency. Focusing on the resolution graph from 2008 to 2009, we note an important difference between the two stations. While the resolution for Athens increases from 2008 to 2009 by approximately one-fourth (from 42% to 52%), the resolution for Izmir decreases during the same period by approximately one-fourth (from 46% to 36%). The implication of this opposite movement is that the recorded Frequency for Athens

83

converges to the real ducting conditions and appears higher than the previous year; whereas the recorded Frequency for Izmir diverges from the real ducting conditions and appears lower from the previous year.
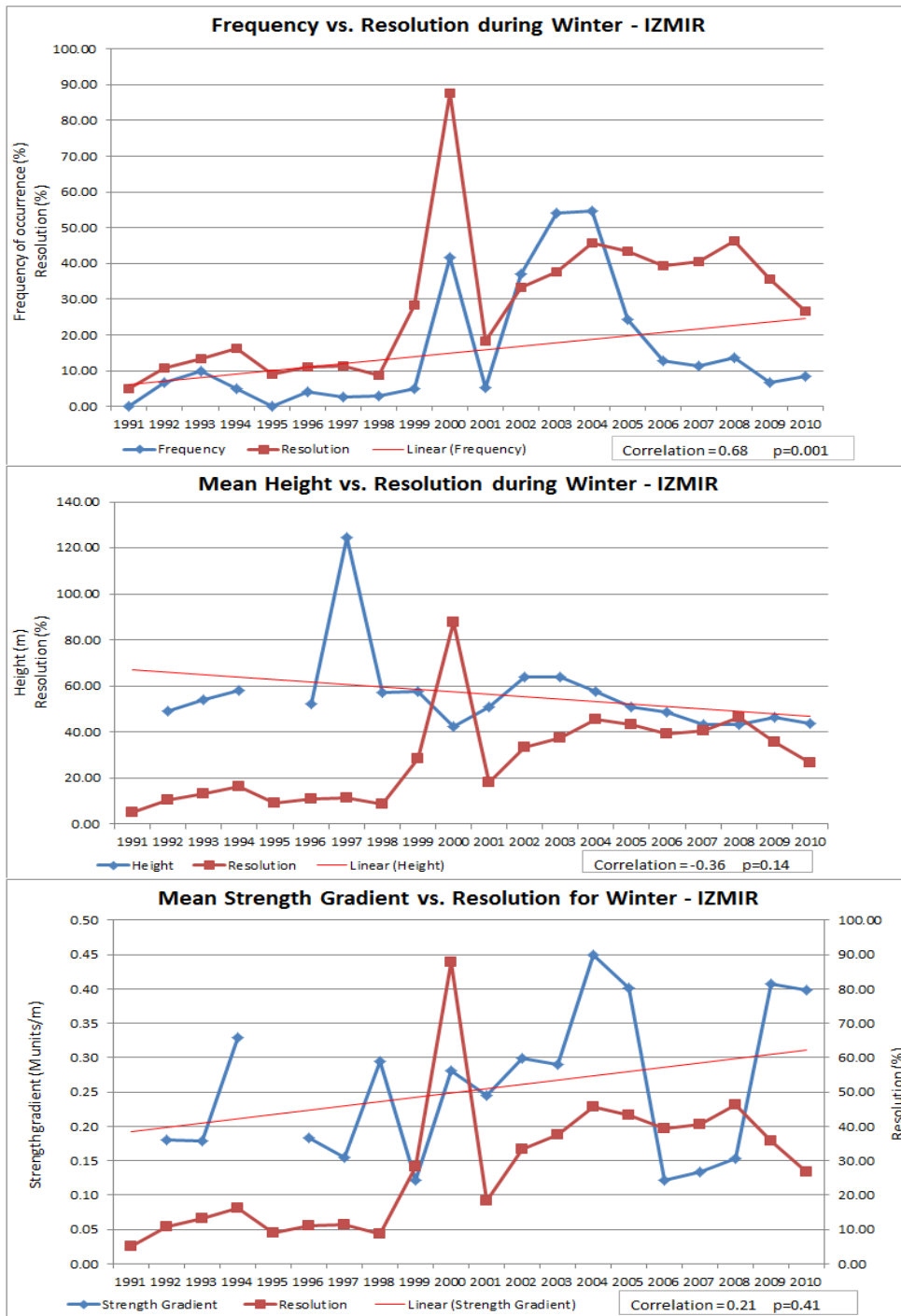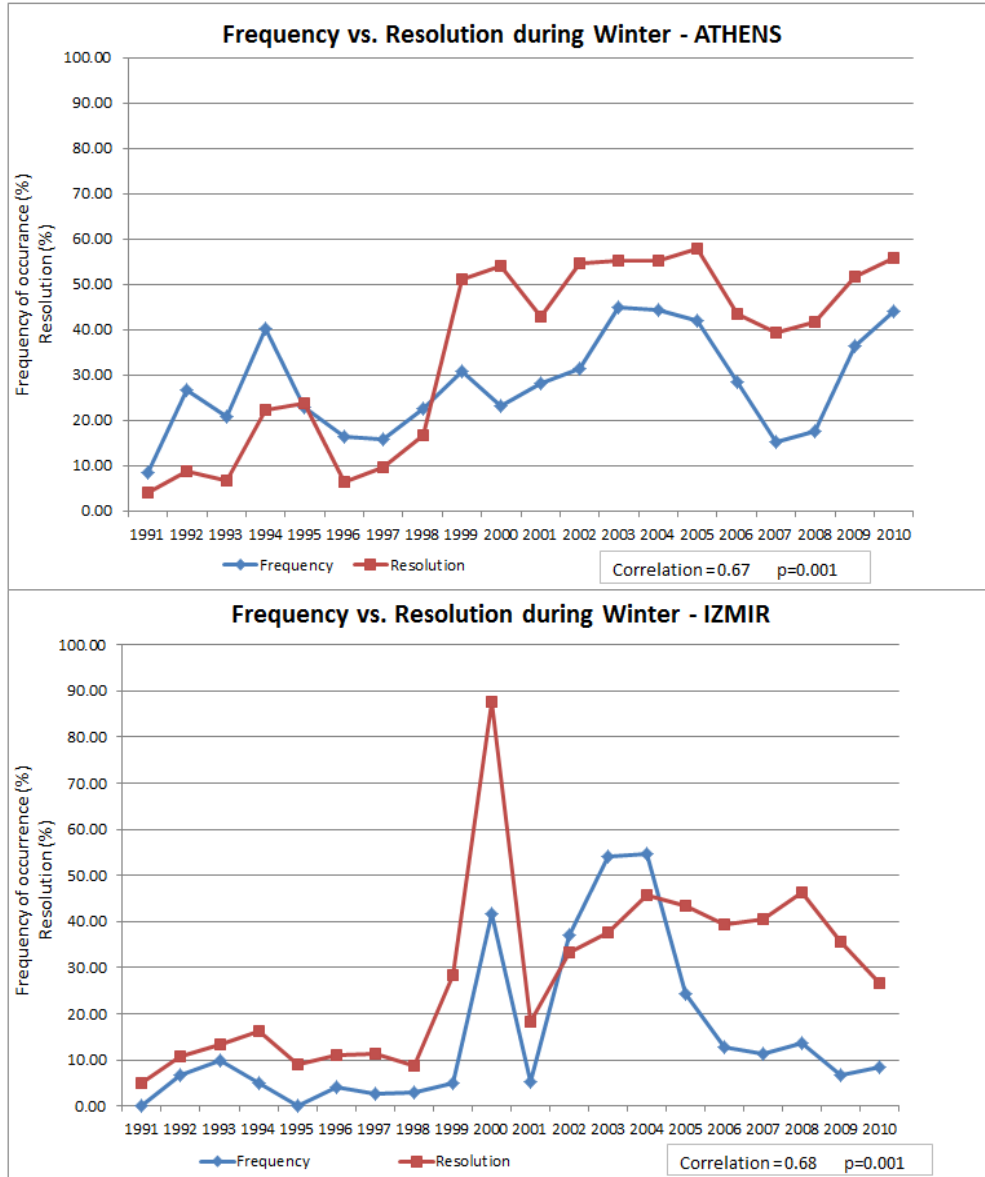

Figure 57.   Time series during winter. The blue line (rhombus markers) connects the seasonal means of ducting parameters for each year. The red line (square markers) connects the seasonal means of the resolution, represented in %.

In order to verify that the ducting conditions for the 2009 were actually improved, Figure 58 depicts the anomalies of the variables under study for that

year. Everything seems to be consistent with the interpretations that we have already given. Lower than usual SLP, related with anomalously southerly flow, leads to higher than normal PR and increased mid-altitude RH. Indeed, all the necessary ingredients for a high-frequency year are in place. In conclusion, we can definitely claim that the manifestation of 2009 as a year of low Frequency for Izmir is a superficial event, provoked by the resolution issue.
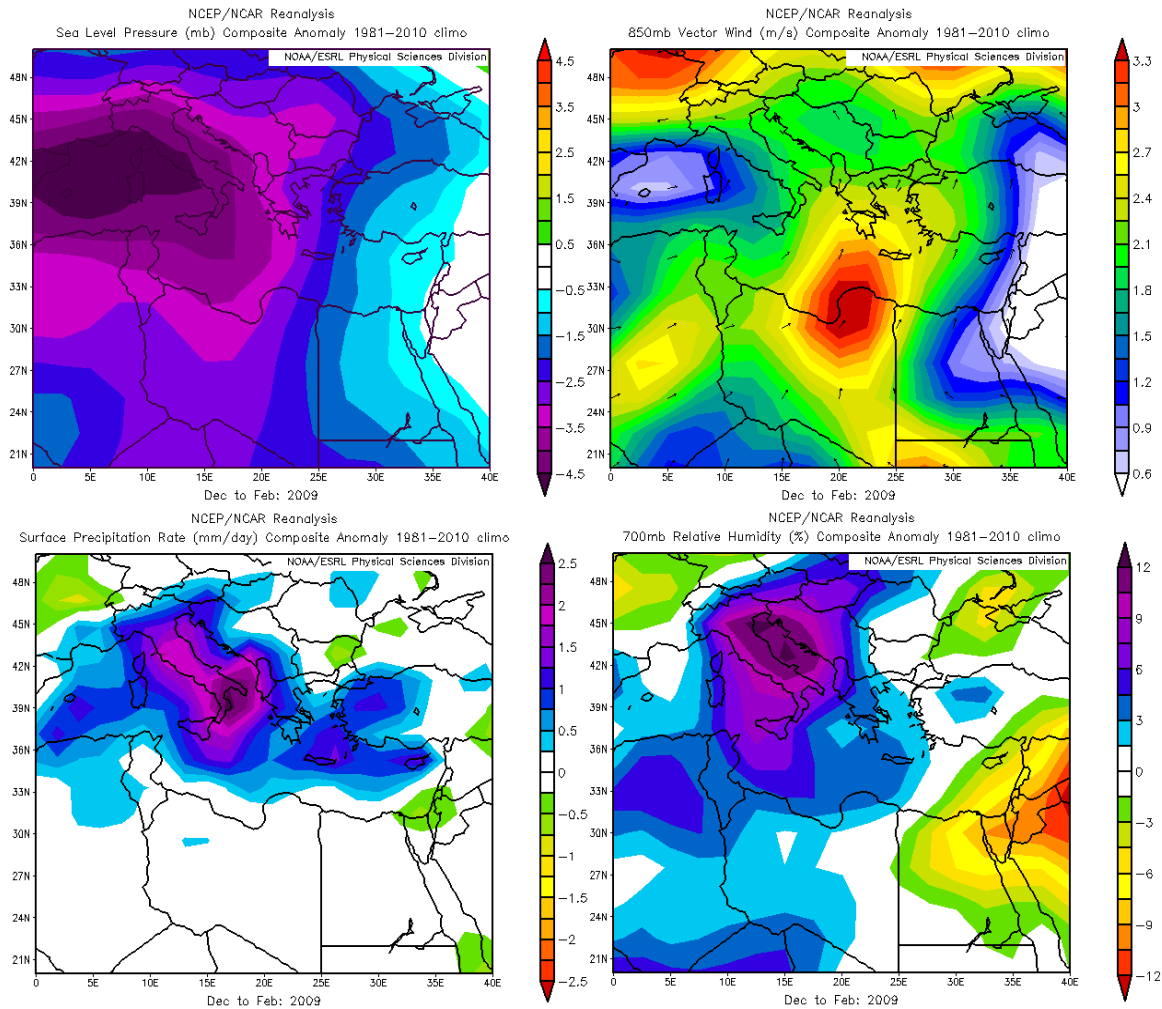
Figure 58. Winter anomaly maps for the year 2009. The top panes show the SLP composite anomaly (left map) and VW at 850mb composite anomaly (right map). The bottom panes show the PR composite anomaly (left map) and the RH at 700 hPa composite anomaly (right map). Figures created at: NOAA/ESRL Physical Sciences Division website, available online at http://www.esrl.noaa.gov/psd/ , accessed February 2012.

85

One more case with anomalous behavior is the year 2000. It does not belong in the 2002–2009 period that we have isolated for further investigation, but it seems associated with the odd, spike-like structure of the resolution graph. We think that it is worth further observation. The year 2000 appears as one with an excessively high Frequency. The other two ducting parameters also exhibit peaks at 2000 (Figure 45), signifying an altogether favorable year for the surface ducts.

Having looked at the atmospheric conditions for this specific year, we composed Figure 59 where anomaly maps of the meteorological variables of interest are assembled together. The interpretation of these maps indicates 2000 was a year of positive NAO, with relatively poor rainy conditions for the Aegean, relatively low RH and with a general northerly flow prevailing. All these parameters refer to weak ducting conditions. In spite of that, the winter of 2000 appears as a year of enhanced ducting conditions. Once more, we hold the resolution responsible for this situation that, for reason unknown to us, performed tremendously that year and drove the Frequency up, accordingly.
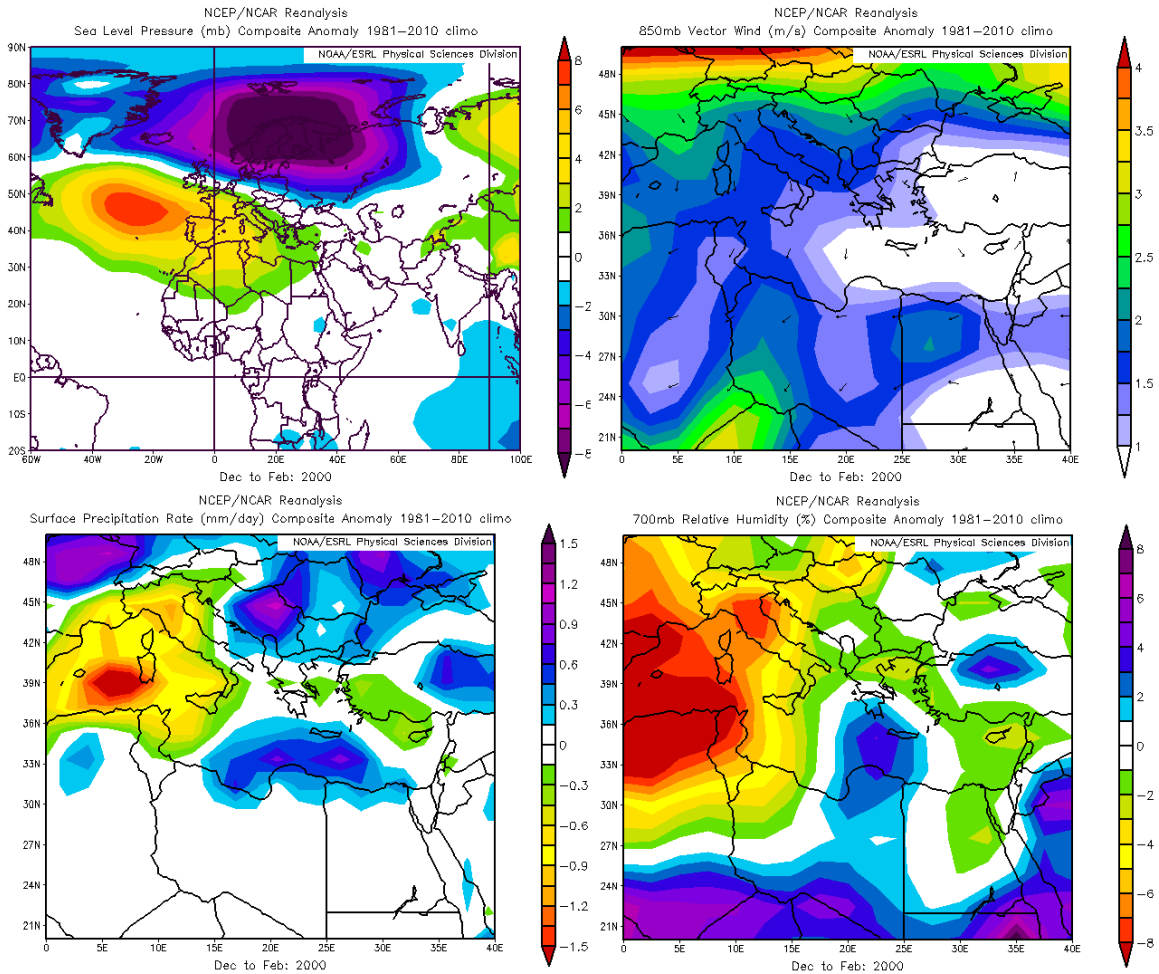
Figure 59.   Winter anomaly maps for the year 2000. The top panes show the SLP composite anomaly (left map) and VW at 850 hPa composite anomaly (right map). The bottom panes show the PR anomaly (left map) and the RH at 700 hPa composite anomaly (right map). Figures created at: NOAA/ESRL Physical Sciences Division website, available online at http://www.esrl.noaa.gov/psd/ , accessed February 2012.

(2) Summer. Correlation maps between Frequency at Izmir and selected climatic system variables follow for the summer. As for the winter, only the more significant correlations, with a physical linkage between ducting and meteorological conditions, are demonstrated.

Figure 60 shows the correlation map for SLP. Comparing this figure with its counterpart for Athens, one can see that the positive correlation over the Indian subcontinent remains, although weaker, but the pattern over Europe and the E.

Mediterranean has changed, demonstrating weak positive correlation instead of strong positive. Another distinguishable feature in this map is the dipole observed over the N. Atlantic Ocean. This dipole suggests significant relations between the Frequency at Izmir and NAO mode. Indeed, the correlation we computed between these two indices is $r = 0.67$ with significance level $p = 97\%$.
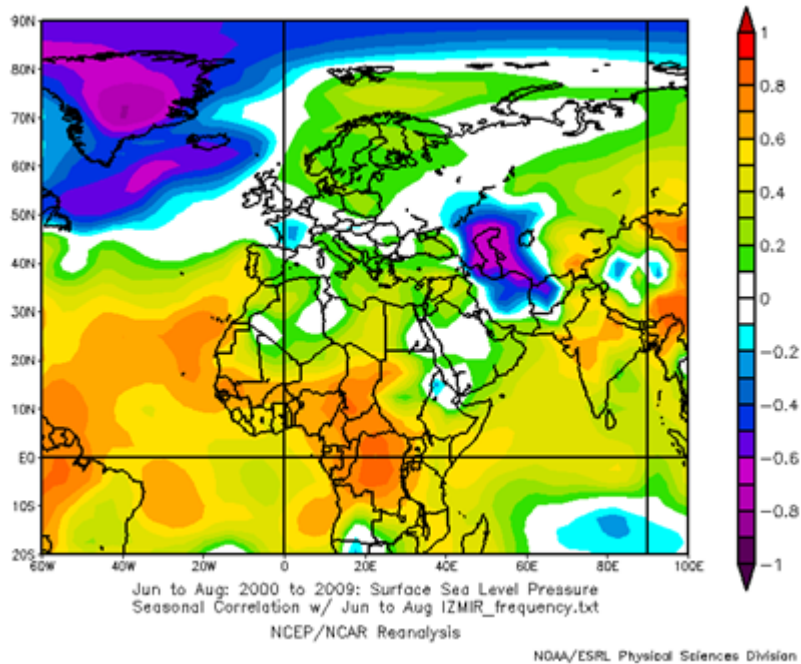
Figure 60.   Linear correlations in summer between SLP and Frequency at Izmir for the period 2000-2009, based on 1981–2010 NCEP reanalysis dataset. Correlation magnitudes ≥ 0.30 and greater indicate significance at the 95% level or greater. Figure created at: NOAA/ESRL Physical Sciences Division website, available online at http://www.esrl.noaa.gov/psd/ , accessed January 2012.

In Figure 61, the correlation maps for ZW and MW, at 850 hPa level, are depicted. Very weak positive correlation develops over the Aegean Sea for the ZW and a weak negative develops for the MW, in contrast to Athens wind patterns (Figure 37), where the correlations for both the wind components were positive and stronger.
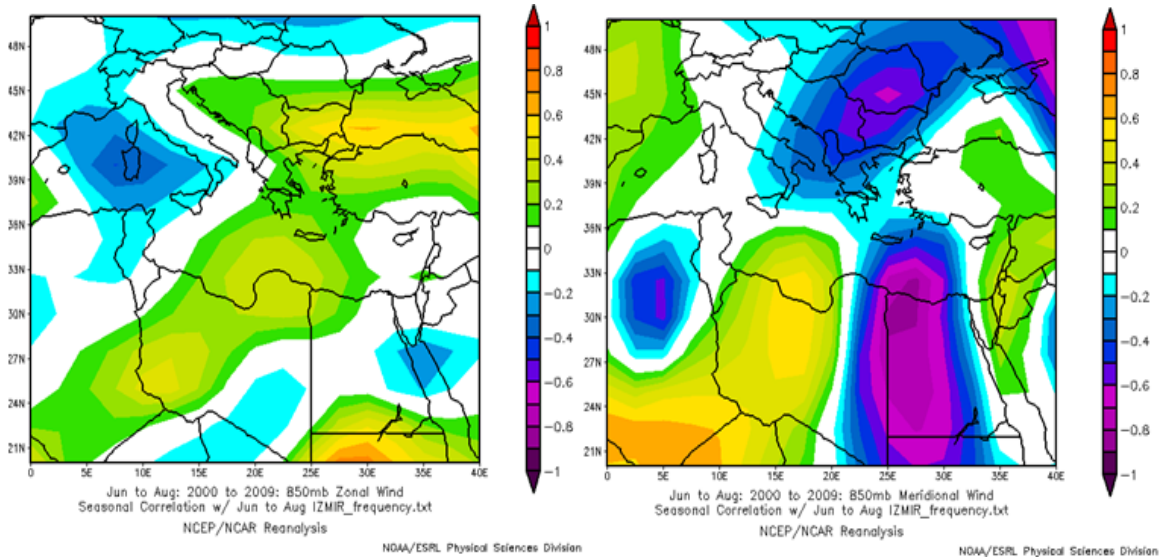
Figure 61.   Linear correlations in summer between Frequency at Izmir and the: (a) ZW at 850 hPa (left panel); and (b) MW at 850 hPa (right panel) for the period 2000-2009, based on 1981–2010 NCEP reanalysis dataset. Correlation magnitudes ≥ 0.30 and greater indicate significance at the 95% level or greater. Figures created at: NOAA/ESRL Physical Sciences Division website, available online at http://www.esrl.noaa.gov/psd/ , accessed January 2012.

Figure 62 shows correlation maps for SST. Both concurrent and lagging correlations have been plotted. Although there is consistency between the correlation patterns depicted in this maps the respective ones for Athens (Figure 38), nevertheless, they appear to be more blurred.
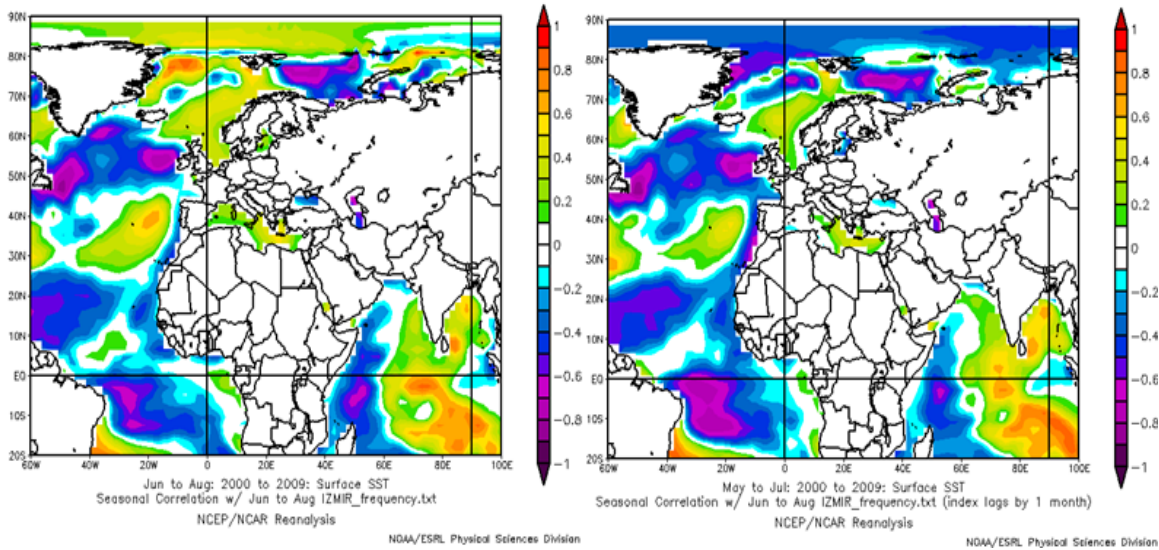
Figure 62.   Linear correlations in summer between Frequency at Izmir and the: (a) SST hPa (left panel); and (b) SST leading by one month (right panel) for the period 2000-2009, based on 1981–2010 NCEP reanalysis dataset. Correlation magnitudes ≥ 0.30 and greater indicate significance at the 95% level or greater. Figures created at: NOAA/ESRL Physical Sciences Division website, available online at http://www.esrl.noaa.gov/psd/ , accessed January 2012.

In general, summer correlations do not reveal any strong signal, with the exception of the NAO correlation, which is the unique statistically significant one. Moreover, an inconsistency is exposed, as far as correlations with wind patterns are concerned, between Izmir and Athens stations.

As described for Athens, Izmir lies under the regime of a background northeasterly flow at lower levels of the atmosphere, due to the relative position between the Azores High and the Indian Thermal Low. The geography around the station amplifies the meridional component of that flow, producing a clear northerly wind over the city of Izmir, which dominates during summer (Komusku et al., 1998). Rare, but not unusual, are situations in which this flow obtains a zonal component and shifts northwesterly or northeasterly. Even more rarely, a southwesterly flow is recorded.

The prevailing northerly flow constitutes the main mechanism that regulates the moisture levels over Izmir. Figure 63 shows the geography of the area. From the relative position of the land and water masses, it is evident that the northerly flow, before reaching the Izmir station, travels over warm sea, getting enriched in water

vapor (Sayin 2003). This results in increasing the amounts of moisture over Izmir, and consequently, in enhanced ducting conditions.
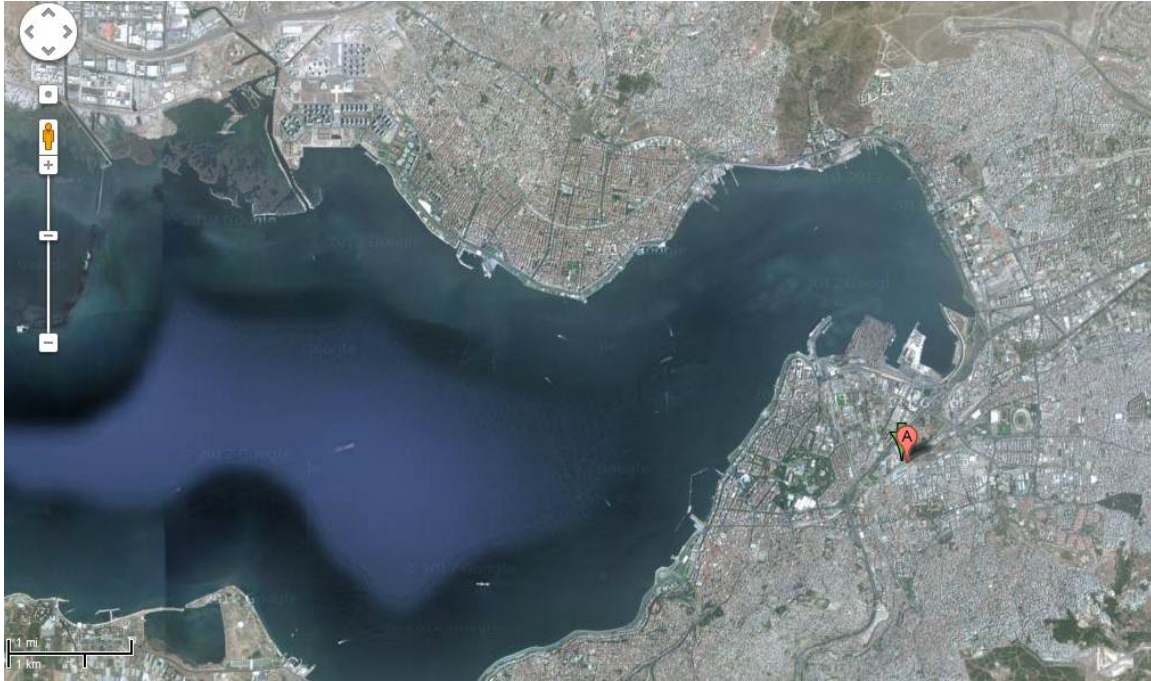
Figure 63.   Izmir Bay and the surrounding land masses. Izmir radiosonde station is denoted with the red balloon. (From Google Maps)

On the other hand, a little shift of the flow from directly northerly to northeasterly is enough to change significantly the advected amount of moisture. Northeasterly wind does not flow anymore over the sea and, therefore, it advects dry air from continental origin, reducing the total amount of moisture over Izmir. Comparing the coastlines of Izmir and Athens (Figure 39), one can see that the Izmir coastline is more rugged with a west-east orientation, whereas Athens' coastline has a nearly north-south orientation. This means that the northerly flow for Izmir has an onshore character, while the northerly flow for Athens has an offshore character. Moreover Izmir is situated on the border where two major, completely different air masses clash—one of a marine nature originating from Mediterranean Sea, and the other of a continental nature originating from Anatolia plateau (Unal et al. 2010). These differences are crucial and explain sufficiently the observed discrepancies on correlation patterns between Athens and Izmir for the summer season.

In conclusion, the wind correlation patterns in Figure 61 are justified by the fact that the northerly flow improves ducting conditions over Izmir by advecting more moisture, while an easterly component of the winds deteriorates ducting conditions. The reverse scheme is established with southerly flow and a westerly component. In general, we repeat that the complex topography around Izmir station enables local mechanisms to develop and blend with the ducting effects that the large-scale phenomena impose. This may be the main reason for the resultant weaker correlations, in comparison with the respective ones in Athens.

Quite peculiar is the situation concerning the correlations associated with the SLP presented in Figure 60, and the correlations associated with the SST presented in Figure 62. The correlations patterns seem to be blurry, without allowing for sufficient interpretation. We consider that the particularity of the terrain surrounding Izmir is the main reason for this. Little variation of the isobars orientation cause alterations in the wind patterns over Izmir bay, which in turn are capable of generating remarkable changes in ducting conditions, as discussed previously. Therefore, we believe that even small changes in the relative positions of the Azores High and Indian Low, without necessary changes of their magnitudes, can have a large impact on ducting conditions at Izmir station. This situation cannot be reflected by the correlation maps, and this may be the reason for the weak signal that we obtained.

Following the same practice we applied for Athens, we also present anomaly maps, which help us to better understand the influence of the large-scale weather upon ducting conditions. Following the same routine, we selected the four years out of the 2002–2009 period with the most anomalous behavior in terms of ducting frequency. The years 2002 and 2003 are those with the highest Frequency, and 2006 and 2009 are those with the lowest Frequency. By using seasonal composites of the anomalies of the meteorological variables under question, we have tried to verify the correlation patterns that we met before.

In Figure 64, the SLP anomaly maps do not give a clear signal between the two anomalous for the Frequency periods. No tendency of the pressure gradient over the E. Mediterranean is uncovered, in accordance with the Azores High and

the Indian Low behavior. Despite that, they are in agreement with the respective correlation map for summer (Figure 60), which also demonstrate an uncertain signal. The same ambiguity holds for the SST anomaly maps in Figure 65, as happens with the corresponding correlation map. In Figure 66, the VW at 850 hPa anomaly maps portray a general northerly flow over the E. Mediterranean for the high Frequency years, even if not evident over the Izmir area, and a southerly flow over the Aegean for the low Frequency years. For the first case, the wind travels over the sea before reaching Izmir station and gathers moisture from the evaporating water mass below. In the second case, of the low Frequency years, the wind travels over warm land and mixes with dryer air before arriving at Izmir. All in all, the anomaly maps are consistent with the correlation maps and the explanations that we have given before.
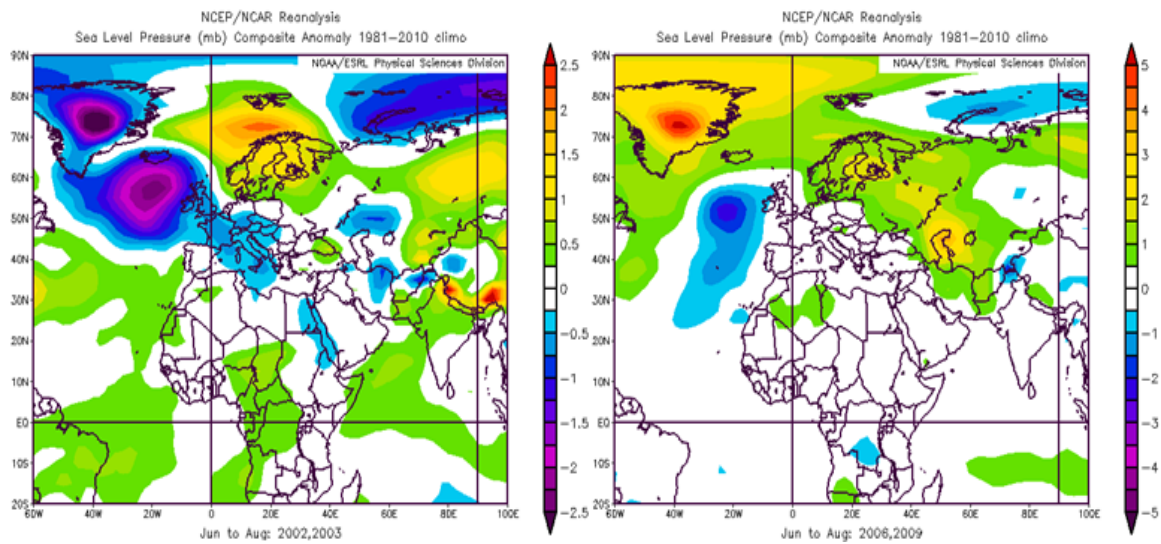
Figure 64.   SLP composite anomaly maps for the two summers with the highest Frequency at Izmir (left panel) and the lowest Frequency at Izmir (right panel). Figures created at: NOAA/ESRL Physical Sciences Division website, available online at http://www.esrl.noaa.gov/psd/ , accessed February 2012.
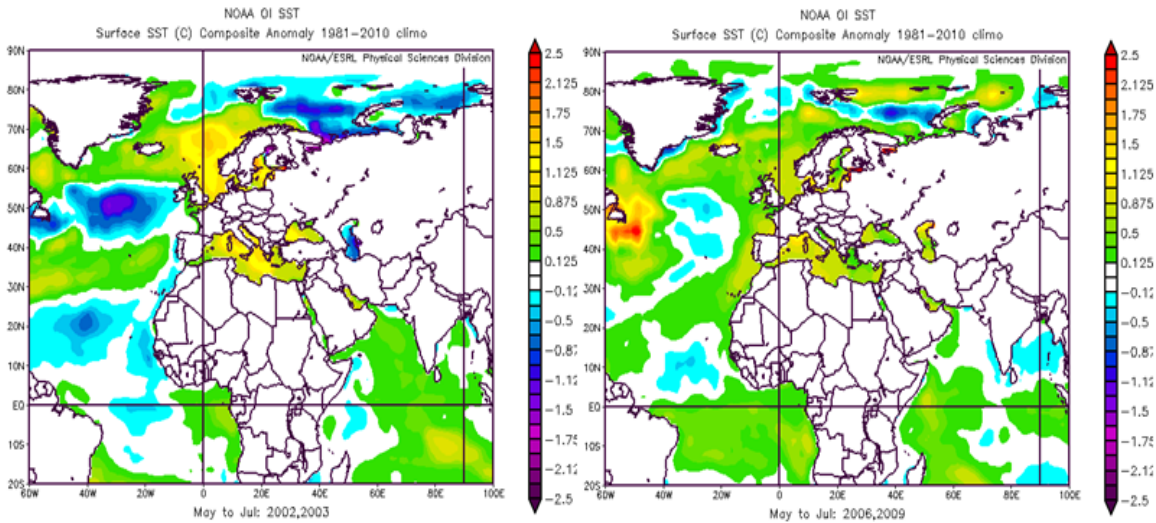
Figure 65.   SST composite anomaly maps for the two summers with the highest Frequency at Izmir (left panel) and the lowest Frequency at Izmir (right panel). The SST leads by one month. Figures created at: NOAA/ESRL Physical Sciences Division website, available online at http://www.esrl.noaa.gov/psd/ , accessed February 2012.
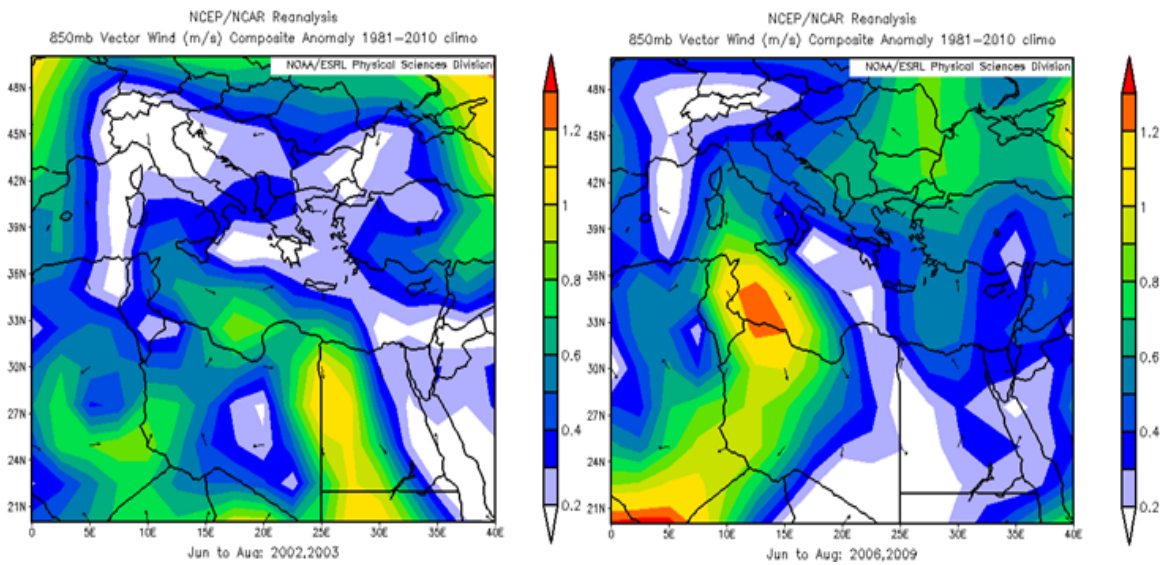
Figure 66.   VW at 850 hPa composite anomaly maps for the two summers with the highest Frequency at Izmir (left panel) and the lowest Frequency at Izmir (right panel).   Figures created at: NOAA/ESRL Physical Sciences Division website, available online at http://www.esrl.noaa.gov/psd/ , accessed February 2012.

D. ANALYSIS OF DUCTING CONDITIONS OVER HERAKLION STATION

1. Derived Statistics

Initially, we examined the variation of the ducting parameters over an entire year. Figure 67 shows the yearly distribution of these parameters. Summer has the highest Frequency, highest Height and highest Strength gradient, suggesting that favorable conditions for ducting formation prevail during summer months. In contrast, winter exhibits the lowest values of Frequency, Height and Strength gradient.
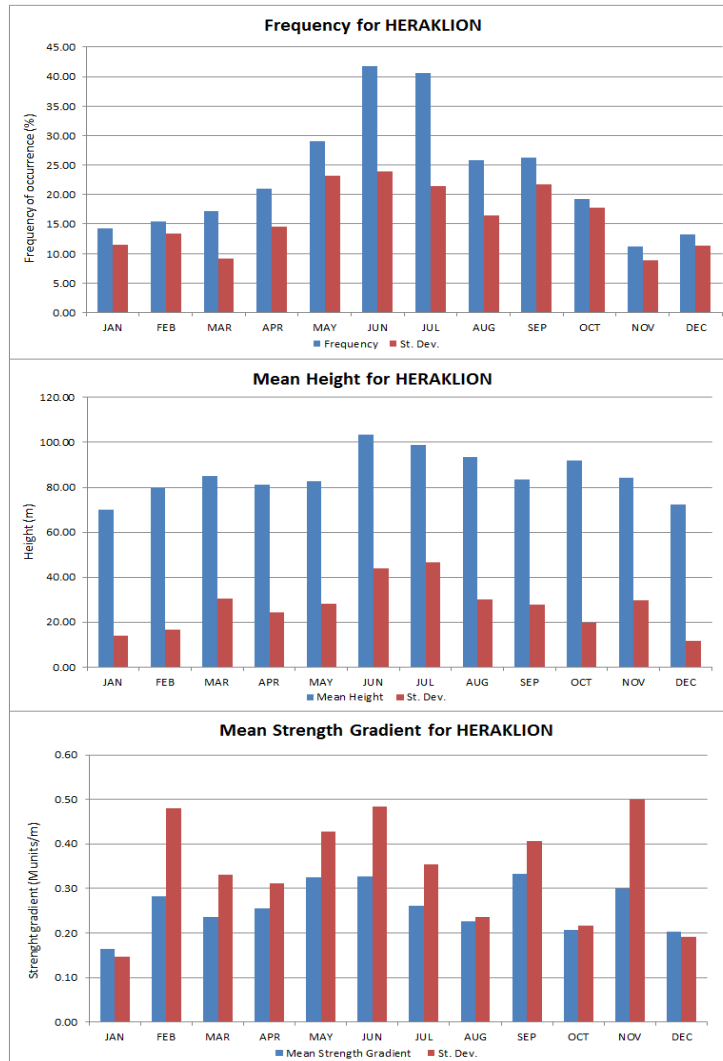
Figure 67.   Distribution plots of ducting parameters for HERAKLION station. The values used for this plot have been derived by averaging the monthly means over the 1991–2010 period. For the years 1994, 1995, 1997, 2008, and 2009, no data was available.

The variability of these parameters is quantified by the standard deviation. The same patterns as for the two previous stations appear here, which lead to the same conclusions. Summer seems to be the season with more robust ducting conditions. Another conclusion, deducted from the winter's large variability in Frequency (compared to the mean values), is that ducting conditions during winter follow the variability of atmosphere, imposed by the synoptic scale circulation. In contrast, summer's low variability in Frequency can be attributed to the more stable weather during this season.

Next, we examined the interannual variability of ducting parameters throughout the 1991–2010 period, taking into consideration the resolution issue that we had confronted with the two other stations. By applying the same methodology as for Athens, we calculated the critical levels, below which the major volume of surface ducts are expected to be. For winter, we determined a critical level of 91 m from mean SLP altitude and for summer, with a critical level of 101 m from mean SLP altitude.

In Figure 68, the resultant plots for the winter season are presented and linear trend lines for the ducting parameters have been added to each plot. A similar situation is encountered here, with trends over the ducting parameters revealing statistical biases that favor the ducting conditions during the second half of the 1991–2010 period. The additional characteristic here on the resolution graph, is that one more shift is recorded throughout the 20-year period. The first one happens after 1998, as was the case for the other stations. The second one occurs after 2007, giving rise to substantially better ducting conditions in 2010. We are not able to define exactly which year this shift on resolution emerges, because there are no data for 2008 and 2009.

Significant positive correlation occur between Height and vertical resolution with a value of $r = -0.74$ and significance level $p > 99\%$. The correlations with the other two ducting parameters are not significant, but a careful look at the relevant plots uncovers an unambiguous dependence between them and the resolution. In general, regarding the correlation coefficients along with the relevant plots, we deduce that the observed biases are due to the long-term variation of the vertical resolution.
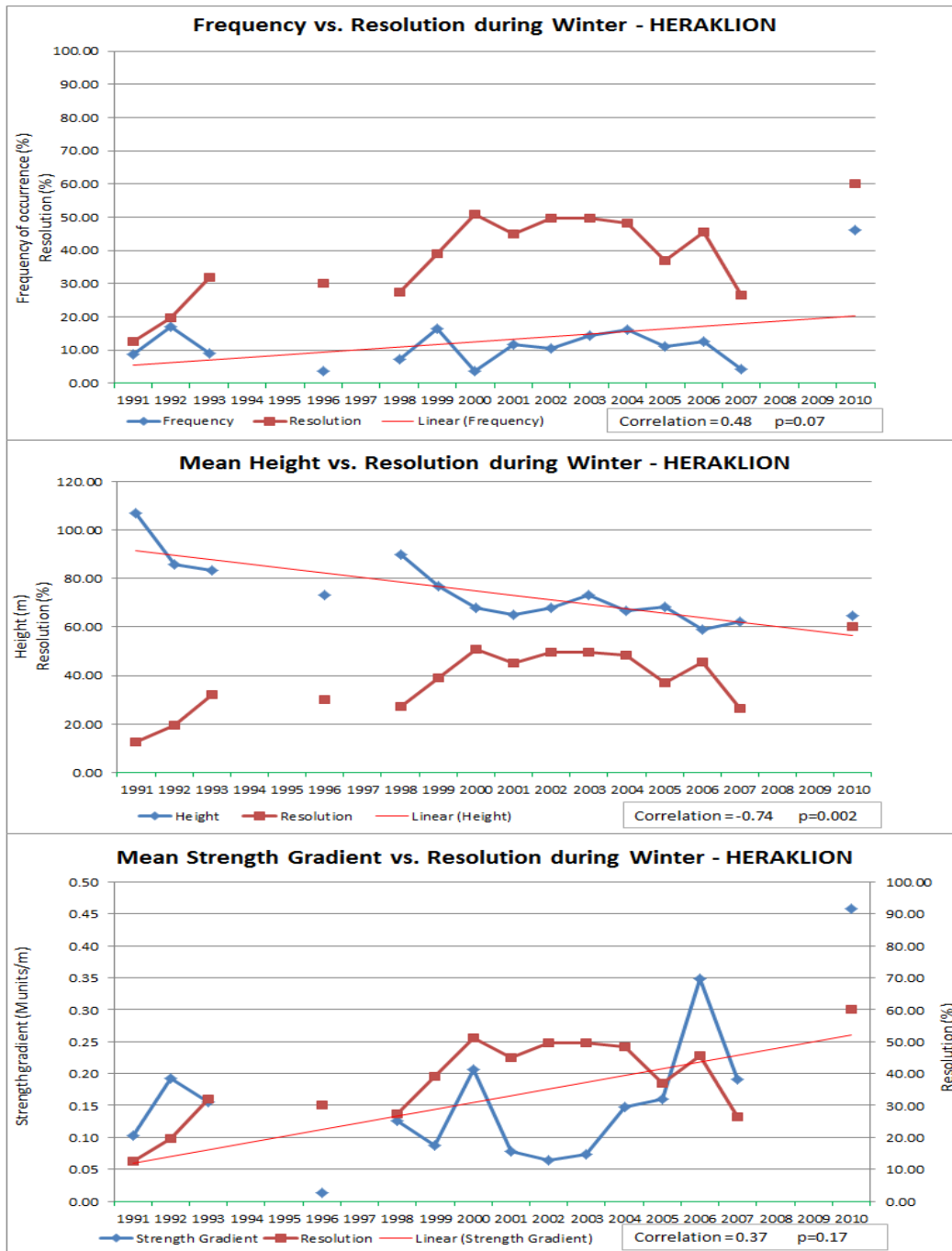
Figure 68.   Time series of ducting parameters during winter for Heraklion. The blue line (rhombus markers) connects the seasonal means of ducting parameters for each year. The red line (square markers) connects the seasonal means of the resolution, expressed in %. The red straight line depicts the linear trend of the ducting parameters series. For the years 1994, 1995, 1997, 2008, and 2009, there were no data available.

Figure 69 shows the respective plots for summer. It can be noticed that the same connection between resolution and ducting parameters statistics holds during summer. Similar features with the other stations are notable here. The correlation between Frequency and resolution is much weaker than during winter, although remaining positive. The same explanation previously given for the other stations applies to this differentiation. The first shift after 1998 is evident here too, but the second shift, which is observed for the winter season after 2007, does not exist.
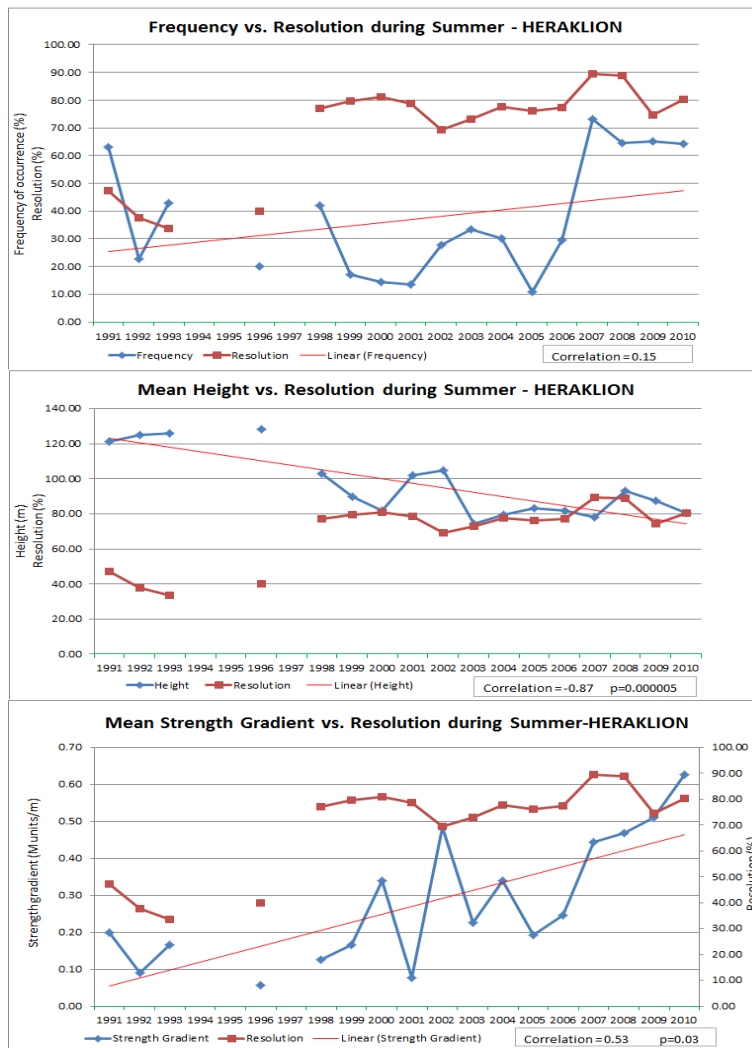
Figure 69.   Time series of ducting parameters during summer for Heraklion. The blue line (rhombus markers) connects the seasonal means of ducting parameters for each year. The red line (square markers) connects the seasonal means of the resolution, expressed in %. The red straight line depicts the linear trend of the ducting parameters series. For the years 1994, 1995, and 1997, no data was available.

2. Ducting Variability

The derived statistics described on the previous subsection are based on the averaging of the seasonal means for the 1991–2010 period. Unfortunately the existing data sets regarding radiosonde soundings are incomplete. A few years are missing completely and some other years' seasonal means have been derived by averaging only one or two months, instead of the necessary three, because of lack of data. Furthermore, the data before 2003 have been collected, based on only once-a-day measurements, sometimes during daytime only (12Z soundings), and other times during nighttime only (00Z soundings).

All these discrepancies make the available datasets for the Heraklion station unreliable for correlating with meteorological variations. We consider that the biases are large, and we cannot trust any resultant correlation accounting for the yearly variation of the ducting parameters. For this reason, we have confined our research to only the mere reference of the derived statistics, described in the previous subsection.

E. CONSOLIDATION

1. Comparisons Among the Stations

Figure 70 shows the annual cycle of the ducting parameters for all the three stations together. The seasonal variations are similar for all the three stations, which gives extra creditability to the derived statistics and supports the physical interpretations given in the previous sections. For all three stations: (1) the summer Frequency of surface ducting is approximately twice that in the winter; and (2) the summer Height and Strength gradient are generally greater than in the winter. These similarities were expected, since all the three stations belong to an area with relatively uniform climate patterns, and are influenced by the similar weather systems and climate variations. The relatively small differences between the stations are due to the particularities of each individual station, dictated by specific geography and local effects..
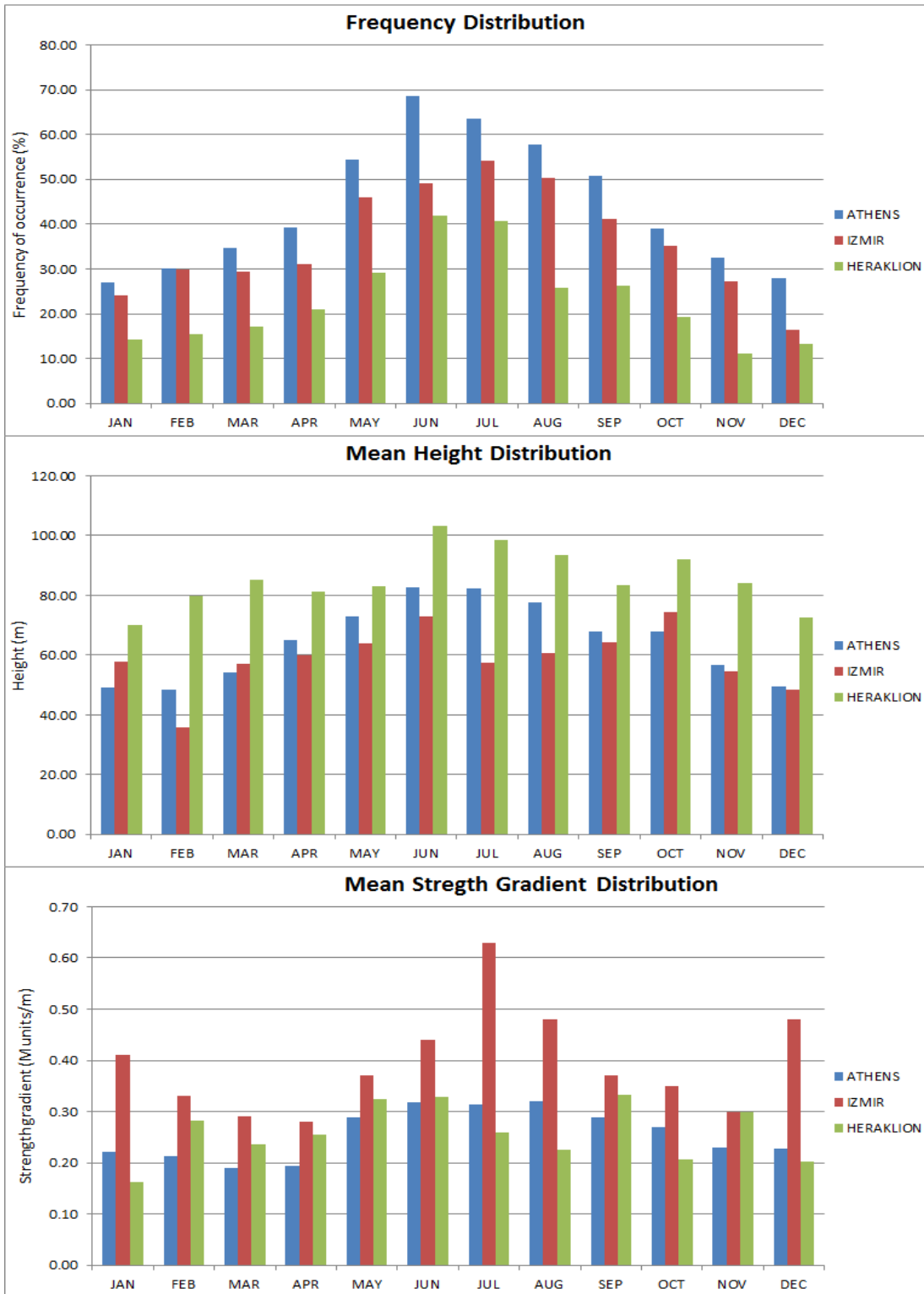
Figure 70.   Annual cycle of ducting parameters for all the three stations based on averaging the monthly means for the 1991–2010 period.

Figures 71 and 72 show the interannual variations in the ducting parameters for the winter and summer for all three stations. Table 9 summarizes the correlations between Athens and Izmir. Correlations between Heraklion and the other stations are not presented due to the incompleteness of the Heraklion datasets. Together, Figures 71-72 and Table 9 indicate a low to high degree of interannual correlation between the stations. Visual inspection of the previous plots, along with the corresponding correlations, reveals some notable ambiguities, but some important conclusions can still be drawn. Frequency correlations are stronger during winter and nonexistent to negative during summer, which is consistent with the earlier analyses concerning the differences in the processes that determine ducting conditions during winter and summer. Winter ducting conditions are governed by synoptic scale weather conditions, which tend to be very similar for all three stations. But summer ducting conditions are significantly influenced by local mechanisms due to the relative absence of synoptic scale weather events in the summer.
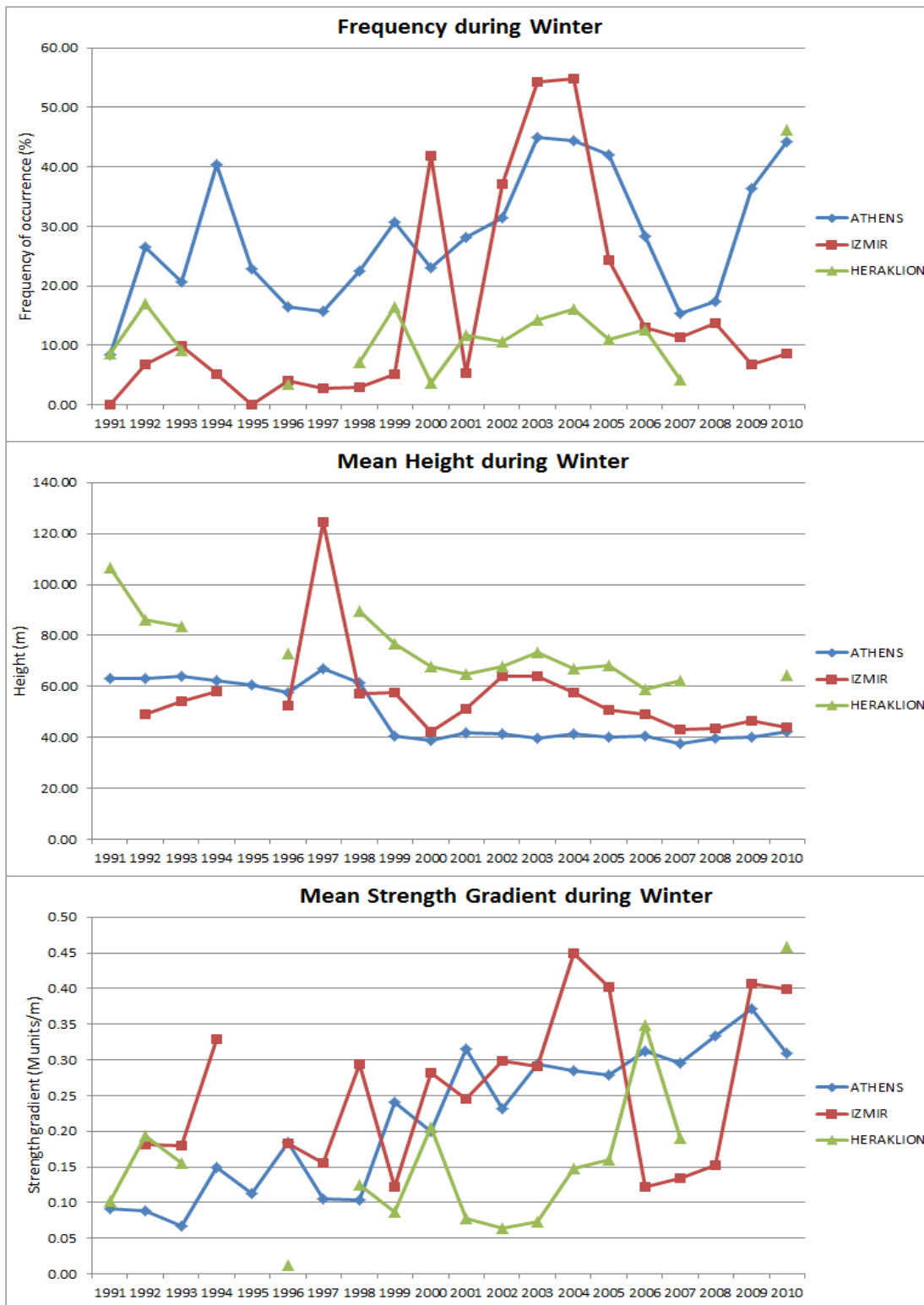
Figure 71.   Time series of ducting parameters during winter. The markers represent the
seasonal means of ducting parameters for each year. The gaps denote years with
missing data.
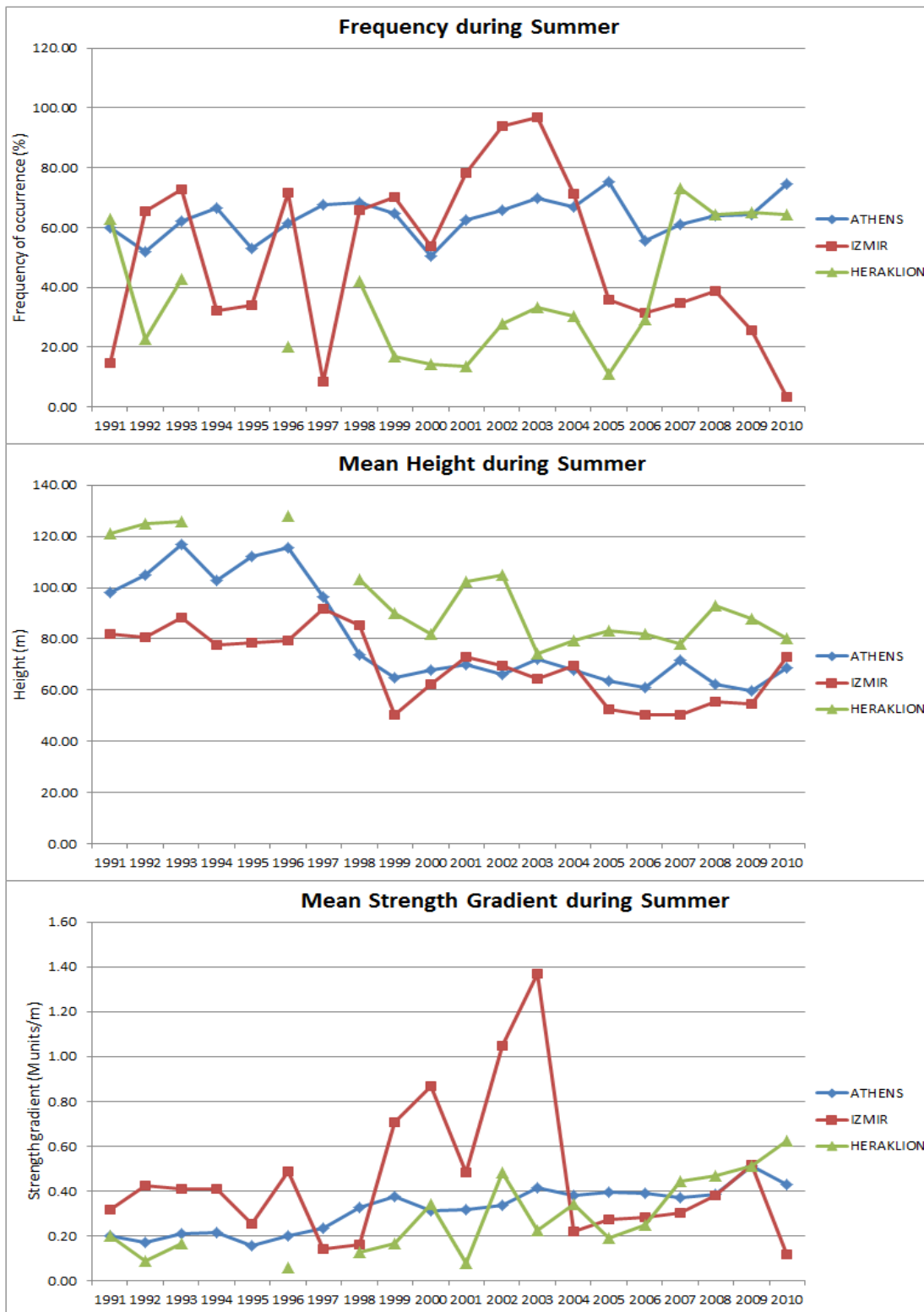
Figure 72.   Time series of ducting parameters during summer. The markers represent the seasonal means of ducting parameters for each year. The gaps denote years with missing data.

103

Table 9.   Correlation coefficients and significance levels between Athens and Izmir. Significance levels lower than 95% are not included.

ATHENS - IZMIR	Frequency	Height	Strength Gradient
Winter	r = 0.47 p = 95%	r = 0.49 p = 96%	r = 0.27
Summer	r = -0.07	r = 0.75 p > 99%	r = 0.19

2.   Measurements Errors and Statistics Uncertainties

This study was based on data derived from the processing of radiosonde measurements. In particular, our results were based on the recorded sounding measurements at the first few levels in the lower atmosphere, including the ground level. Significant biases can be caused by temporal variations in the number and elevation of these levels. Other biases can result from the use of different instruments for the measurements of the very first two levels. It is important to highlight that the measurements at the first level, the ground level, are always taken from the ground station and not from the radiosonde itself. This means that biases can ensue, due to the use of different instruments. This can produce misleading results, especially concerning reversals at the base of the M profile. However, M reversals can be substantiated if they are indicated by the data from more than two levels (i.e., one on the ground and at least two more above).

During winter, the majority of the surface ducts were determined based on data from only two measured levels — the first one being on the ground and the second one being several meters above. During summer, the majority of them were determined based on data from at least three levels. This calculation of the summer M profiles indicates that our summer results are relatively free from biases induced by the use of different instruments. This conclusion is supported by the similar annual cycles in the ducting parameters for all three stations (Figure 70).

We calculated many correlation coefficients. From a probabilistic perspective, a few of the correlations coefficients would be large, just by chance. Therefore, we recommend focusing on the correlations with a significance level greater than or equal to

99%. However, for many of the correlations with lower significance levels, the composite anomaly results indicated that the correlations represented physically plausible dynamical relationships that were physically consistent with the relationships indicated by the correlations with higher significance levels.

THIS PAGE INTENTIONALLY LEFT BLANK

IV. CONCLUSIONS AND RECOMMENDATIONS

A. SUMMARY

The purpose of this study was to establish how climatological factors affect the surface ducting conditions in the Aegean Sea Region. In order to accomplish our task, we used radiosonde soundings as a primary source of data. By analyzing this data, we were able to identify major spatial and temporal characteristics of surface ducting in the Aegean region. We did so for three different radiosonde stations in the Aegean region for a period of 20 consecutive years, 1991-2010.

We used the NCEP reanalysis dataset as the main source of data on regional and large scale climate patterns and variations. Based on these datasets and with the aid of the ESRL/PSD online tools, we were able to create seasonal mean time series for selected climate system variables and to correlate them with time a series of ducting parameters. We investigated links between the ducting and regional and large scale conditions, with a focus on seasonal and interannual variations in the ducting and correlated climate variations.

Many important relationships were identified, and even more important biases were uncovered. In our effort to interpret these relationships, we came up with explanations that are governed by physical rules and refer to fundamental climate system principles. Consequently, they can have applications beyond the limits of this study. The most important results and conclusions are listed below.

- Surface ducts constitute a special class of ducts with particular characteristics and relationships to local and regional environmental conditions. A main reason for this is surface ducts are attached to the ground, within the surface layer of the atmosphere. Because of their shallow nature, they tend not to conform to general theories that apply to other duct categories --- for example, that ducting is strongly associated with capping inversions occurring at the top of the ABL.

- Surface ducting tends to be better developed during summer and less well developed during winter. The major reason for this is that there are higher

amounts of low-level atmospheric moisture in the summer. Large-scale subsidence forced by anticyclones seems not to significantly affect surface ducting.

- The amounts of moisture at the lower atmosphere are similarly responsible for the interannual variability of the ducting conditions. Moist conditions in the lower atmosphere leads to enhanced surface ducting, while dry conditions lead to the reduced surface effect.

- For the Aegean, the main source of moist air is the Mediterranean Sea, and the main source of dry air is the surrounding land, especially continental areas to the north and northeast of the Aegean. Moist and dry air advection into the Aegean region plays a major role in determining the moisture conditions that strongly affect surface ducting in the region.

- Winter ducting conditions are strongly influenced by the occurrence or absence of mid-latitude depressions over or near the Aegean. Their occurrence (absence) leads to increased (decreased) moisture in the Aegean due to the moisture in the depressions and moisture advection induced by the depressions. The AO and NAO influence the presence of these atmospheric disturbances and thus impact ducting in the Aegean region.

- Summer ducting conditions are governed by the dry and moist air advection associated with persistent large-scale circulations features, especially the Azores High and the thermal low over southwest and south-cental Asia. These features tend to produce dry air advection from the northeast over the Aegean. Intraseasonal to interannual variations in these features can cause corresponding variations in surface ducting in the Aegean region. The relative lack of synoptic weather systems in summer allows mesoscale and local effects to manifest themselves, modulate the effects of large-scale circulation features, and thereby affect surface ducting conditions. The geography, coastline orientation, and topography are all important factors affecting summer surface ducting conditions.

- Substantial biases were discovered in our analyses due to temporal variations in the vertical resolution of the radiosonde data. The lower the resolution, the higher the divergence of the statistics from the real ducting conditions appeared to be. Extra care is required in the analysis of ducting statistics based on radiosonde datasets.

In conclusion, we believe that through this work we have set solid foundations for ducting studies from a climatological perspective in the Aegean Sea region and other regions. We expect that the results of our study will be useful, not only for ducting climatology studies in other regions, but also in investigations of the nature of surface ducting.

B.   RECOMMENDATIONS

We recommend that analogous research to ours be conducted in the near future for other regions of the globe but with similar geographic characteristics. Potentially similar results with ours will give rise to the development of surface ducting climatology for coastal areas. Moreover, future research should investigate the elevated ducting conditions for the same region in order to identify whether the same relationships hold between climate system variables and ducting parameters. Highly beneficial would be the conducting of a similar study employing other methods, than the use of radiosonde data, for determining surface ducts. In this way, an extremely useful validation would result providing more accurate and valid knowledge around the surface ducting conditions.

THIS PAGE INTENTIONALLY LEFT BLANK

APPENDIX A

The seasonal statistics of ducting parameters, in tabular format, are contained in this appendix. All the values represent seasonal means that were derived from averaging the respective monthly means.

Table 10. Winter ducting statistics for Athens, between 1991 and 2000. Besides the ducting parameters that have been analyzed in this thesis, Strength, M deficit, Maximum and Minimum Heights were calculated and are displayed in this table.

ATHENS / DEC - JAN - FEB	1991	1992	1993	1994	1995	1996	1997	1998	1999	2000
Throughout the Day (Frequency of duct - percentage)	8.33	26.54	20.72	40.35	22.86	16.53	15.78	22.58	30.78	23.07
Radiosonde Resolution % (measurements below 61m)	4.00	8.67	6.67	22.33	23.67	6.33	9.67	16.67	51.00	54.00
Daytime (Frequency of duct - percentage)	6.67	15.05	14.41	30.89	13.08	11.09	10.12	15.00	34.29	33.28
Nighttime (Frequency of duct - percentage)	13.06	38.10	26.67	50.08	33.11	21.90	22.61	31.49	27.78	12.57
Mean Heihgt (m)	63.13	63.05	63.81	62.28	60.68	57.69	67.12	61.24	40.73	39.00
Lower Quartile of Duct's Heights	57.50	60.17	60.00	54.83	50.17	47.67	61.50	54.67	29.17	30.00
Median of Duct's Heights	63.25	65.17	65.50	61.67	54.33	57.33	71.33	62.17	37.83	41.67
Higher Quartile of Duct's Heights	68.75	68.00	70.67	67.17	71.33	69.17	74.50	69.33	53.00	49.33
Std. D. of Duct's Heights	8.23	13.80	11.01	13.24	16.58	18.22	12.57	15.99	15.55	12.04
Mean of Strength of Ducts	4.53	3.74	3.06	6.29	4.45	3.89	4.22	3.72	3.71	3.01
Lower Q. Strength of Ducts	2.91	1.94	1.16	3.31	2.33	1.61	1.63	1.57	1.28	0.98
Median of Strength of Ducts	4.05	2.96	3.00	5.60	4.25	2.81	4.01	3.04	2.89	2.87
Higher Q. of Strength of Ducts	6.15	4.68	4.57	8.99	6.65	5.67	5.84	5.79	4.89	3.78
Std.D. of Strength of Ducts	2.16	2.76	2.35	3.72	2.48	3.13	2.98	2.81	3.45	2.72
Mean of Strength Gradient of Ducts	0.09	0.09	0.07	0.15	0.11	0.19	0.10	0.10	0.24	0.20
Lower Q. Strength Gradient of Ducts	0.06	0.04	0.02	0.07	0.05	0.04	0.04	0.03	0.06	0.05
Median of Strength Gradient of Ducts	0.08	0.06	0.07	0.13	0.11	0.08	0.08	0.07	0.13	0.09
Higher Q. of Strength Gradient of Ducts	0.12	0.13	0.10	0.21	0.17	0.32	0.14	0.16	0.36	0.31
Std.D. of Strength Gradient of Ducts	0.04	0.08	0.05	0.10	0.08	0.24	0.12	0.09	0.30	0.24
Min Height of Ducts	15.00	15.00	15.00	15.00	15.00	15.00	15.00	15.00	15.00	15.00
Max Height of Ducts	70.50	93.33	80.67	102.00	104.00	85.67	81.00	91.33	73.33	55.67
Mean of Mdeficit	4.53	3.74	3.06	6.29	4.45	3.89	4.22	3.72	3.71	3.01
Lower Quartile of Mdeficit	2.91	1.94	1.16	3.31	2.33	1.61	1.63	1.57	1.28	0.98
Median of Mdeficit	4.05	2.96	3.00	5.60	4.25	2.81	4.01	3.04	2.89	2.87
Higher Quartile of Mdeficit	6.15	4.68	4.57	8.99	6.65	5.67	5.84	5.79	4.89	3.78
Std. D. of Mdeficit	2.16	2.76	2.35	3.72	2.48	3.13	2.98	2.81	3.45	2.72

Table 11.   Winter ducting statistics for Athens, between 2001 and 2010. Besides the ducting parameters that have been analyzed in this thesis, Strength, M deficit, Maximum and Minimum Heights were calculated and are displayed in this table.

ATHENS / DEC - JAN - FEB	2001	2002	2003	2004	2005	2006	2007	2008	2009	2010	Average '91-'10
Throughout the Day (Frequency of duct - percentage)	28.16	31.40	44.87	44.42	42.09	28.40	15.35	17.43	36.39	44.17	33.27
Radiosonde Resolution % (measurements below 61m)	43.00	54.67	55.33	55.33	58.00	43.33	39.33	41.67	51.67	55.67	49.80
Daytime (Frequency of duct - percentage)	23.65	34.24	52.15	55.70	39.35	24.34	8.26	11.32	33.64	40.60	32.32
Nighttime (Frequency of duct - percentage)	32.70	28.75	38.06	33.07	44.82	30.86	21.46	23.65	39.13	48.85	34.13
Mean Heihgt (m)	41.85	41.58	39.63	41.38	40.31	40.75	37.74	39.54	39.93	42.10	40.48
Lower Quartile of Duct's Heights	27.00	26.00	25.33	25.67	28.33	30.33	25.00	28.00	27.00	25.33	26.80
Median of Duct's Heights	37.50	33.50	35.00	36.83	36.33	34.83	36.33	39.83	36.83	38.17	36.52
Higher Quartile of Duct's Heights	52.17	47.00	49.17	52.83	49.33	54.00	52.50	48.67	49.33	55.00	51.00
Std. D. of Duct's Heights	16.44	21.43	15.93	18.51	14.90	16.88	11.35	14.15	16.84	19.84	16.63
Mean of Strength of Ducts	4.71	3.68	4.10	4.28	4.44	4.92	4.21	4.43	5.31	4.39	4.45
Lower Q. Strength of Ducts	2.03	2.31	1.67	2.01	1.39	1.69	0.79	1.67	1.93	1.86	1.74
Median of Strength of Ducts	4.22	3.41	3.48	3.49	3.18	2.93	3.63	3.58	3.52	3.91	3.53
Higher Q. of Strength of Ducts	7.06	5.05	6.18	6.14	5.36	5.14	7.62	6.30	7.80	6.44	6.31
Std.D. of Strength of Ducts	3.27	2.11	3.14	2.97	5.69	6.45	3.67	4.01	4.69	3.34	3.93
Mean of Strength Gradient of Ducts	0.32	0.23	0.29	0.29	0.28	0.31	0.30	0.33	0.37	0.31	0.30
Lower Q. Strength Gradient of Ducts	0.07	0.06	0.09	0.07	0.05	0.07	0.03	0.06	0.07	0.05	0.06
Median of Strength Gradient of Ducts	0.19	0.16	0.15	0.16	0.17	0.16	0.15	0.14	0.18	0.16	0.16
Higher Q. of Strength Gradient of Ducts	0.41	0.33	0.41	0.38	0.34	0.34	0.58	0.42	0.50	0.47	0.42
Std.D. of Strength Gradient of Ducts	0.40	0.23	0.35	0.33	0.35	0.50	0.36	0.46	0.45	0.38	0.38
Min Height of Ducts	15.00	15.00	15.00	15.00	15.00	15.00	15.00	15.00	15.00	15.00	15.00
Max Height of Ducts	76.67	99.00	88.33	93.00	82.67	109.00	57.67	66.00	82.33	143.00	89.77
Mean of Mdeficit	4.67	3.68	4.07	4.25	4.44	4.52	4.20	4.43	5.31	4.15	4.37
Lower Quartile of Mdeficit	1.80	2.31	1.61	1.95	1.39	1.52	0.75	1.67	1.93	1.86	1.68
Median of Mdeficit	4.22	3.41	3.47	3.49	3.18	2.93	3.63	3.58	3.52	3.40	3.48
Higher Quartile of Mdeficit	7.06	5.05	6.18	6.14	5.36	5.14	7.62	6.30	7.80	6.02	6.27
Std. D. of Mdeficit	3.31	2.11	3.16	2.99	5.69	5.26	3.68	4.01	4.69	3.12	3.80

113

Table 12. Summer ducting statistics for Athens, between 1991 and 2000. Besides the ducting parameters that have been analyzed in this thesis, Strength, M deficit, Maximum and Minimum Heights were calculated and are displayed in this table.

ATHENS / JUN - JUL - AUG	1991	1992	1993	1994	1995	1996	1997	1998	1999	2000
Throughout the Day (Frequency of duct - percentage)	60.10	51.97	62.18	66.52	53.00	61.55	67.45	68.19	64.82	50.48
Radiosonde Resolution % (measurements below 91m)	39.33	37.00	36.00	36.67	35.00	32.67	38.67	81.00	87.33	75.67
Daytime (Frequency of duct - percentage)	60.54	51.16	56.30	55.53	47.42	58.25	67.23	68.89	65.95	55.78
Nighttime (Frequency of duct - percentage)	59.76	52.46	68.21	76.61	59.27	66.12	67.67	67.30	63.74	45.12
Mean Heihgt (m)	98.13	104.94	116.85	102.60	112.31	115.77	96.55	73.67	64.65	67.72
Lower Quartile of Duct's Heights	64.83	72.50	68.50	66.00	78.67	66.00	65.67	51.00	38.83	38.00
Median of Duct's Heights	96.17	105.17	107.33	101.00	107.00	117.83	88.83	68.50	59.33	59.33
Higher Quartile of Duct's Heights	117.67	127.67	143.50	127.00	124.33	139.17	122.83	89.67	84.83	92.17
Std. D. of Duct's Heights	39.76	37.61	61.45	43.36	54.45	50.11	41.07	33.29	37.10	37.79
Mean of Strength of Ducts	12.94	12.30	14.98	13.60	11.59	14.64	14.12	13.78	12.13	12.03
Lower Q. Strength of Ducts	4.38	3.85	4.33	3.97	4.12	6.76	4.61	5.17	4.78	3.90
Median of Strength of Ducts	10.24	10.06	14.15	11.33	10.68	14.01	10.83	11.20	10.30	10.81
Higher Q. of Strength of Ducts	19.50	18.36	22.70	20.19	17.99	21.66	21.77	20.95	16.99	17.75
Std.D. of Strength of Ducts	10.69	9.89	11.23	11.50	8.51	9.92	11.56	10.70	9.04	9.94
Mean of Strength Gradient of Ducts	0.20	0.17	0.21	0.22	0.16	0.20	0.23	0.33	0.38	0.31
Lower Q. Strength Gradient of Ducts	0.05	0.05	0.05	0.04	0.05	0.05	0.06	0.08	0.12	0.09
Median of Strength Gradient of Ducts	0.13	0.12	0.13	0.13	0.10	0.13	0.14	0.20	0.23	0.19
Higher Q. of Strength Gradient of Ducts	0.30	0.25	0.34	0.31	0.21	0.31	0.36	0.44	0.42	0.41
Std.D. of Strength Gradient of Ducts	0.21	0.17	0.20	0.25	0.15	0.19	0.25	0.37	0.44	0.35
Min Height of Ducts	15.00	15.00	15.00	15.00	15.00	15.00	15.00	15.00	15.00	15.00
Max Height of Ducts	241.67	222.67	359.33	296.00	346.33	259.33	214.33	229.67	253.67	218.00
Mean of Mdeficit	12.91	11.92	14.97	13.40	11.57	14.60	13.88	13.72	11.88	11.57
Lower Quartile of Mdeficit	4.25	3.16	4.33	3.97	4.12	6.58	4.61	5.17	4.60	3.48
Median of Mdeficit	10.24	9.59	14.15	11.33	10.68	14.01	10.83	11.20	9.55	10.47
Higher Quartile of Mdeficit	19.50	18.02	22.70	19.61	17.99	21.66	21.29	20.81	16.99	16.95
Std. D. of Mdeficit	10.72	9.81	11.25	11.33	8.54	9.97	11.33	10.74	9.09	9.97

Table 13. Summer ducting statistics for Athens, between 2001 and 2010. Besides the ducting parameters that have been analyzed in this thesis, Strength, M deficit, Maximum and Minimum Heights were calculated and are displayed in this table.

ATHENS / JUN - JUL - AUG	2001	2002	2003	2004	2005	2006	2007	2008	2009	2010	Average '91-'10
Throughout the Day (Frequency of duct - percentage)	62.42	65.63	69.71	66.97	75.15	55.68	60.95	64.06	64.50	74.53	65.96
Radiosonde Resolution % (measurements below 91m)	86.67	80.67	82.67	82.00	83.33	84.33	92.67	88.00	83.67	73.33	83.73
Daytime (Frequency of duct - percentage)	67.08	72.53	72.20	76.73	84.29	67.43	76.48	87.50	87.50	85.49	77.72
Nighttime (Frequency of duct - percentage)	57.79	59.52	67.38	56.67	66.34	44.31	52.07	61.77	64.17	72.58	60.26
Mean Heihgt (m)	70.05	66.19	71.89	67.70	63.48	60.89	71.70	62.31	59.66	68.53	66.24
Lower Quartile of Duct's Heights	42.33	44.50	42.50	34.67	37.33	38.17	39.83	39.00	36.00	42.67	39.70
Median of Duct's Heights	67.17	58.33	58.67	52.83	59.17	54.00	51.33	53.83	54.17	66.67	57.62
Higher Quartile of Duct's Heights	93.50	87.33	101.00	92.83	79.83	72.50	88.83	77.67	71.17	86.00	85.07
Std. D. of Duct's Heights	34.29	31.23	38.93	40.27	30.66	35.50	50.35	37.19	37.26	33.58	36.93
Mean of Strength of Ducts	12.09	11.94	14.65	12.13	11.91	11.93	13.58	11.86	10.88	12.47	12.34
Lower Q. Strength of Ducts	5.60	4.94	6.65	5.25	3.57	4.78	5.35	5.50	5.03	5.21	5.19
Median of Strength of Ducts	9.67	9.19	12.78	9.88	9.91	8.95	10.64	9.27	9.84	10.36	10.05
Higher Q. of Strength of Ducts	16.72	16.14	19.32	17.08	19.81	17.92	20.58	18.86	14.64	17.20	17.83
Std.D. of Strength of Ducts	10.12	10.12	10.61	9.41	9.28	9.74	10.15	8.22	7.56	10.48	9.57
Mean of Strength Gradient of Ducts	0.32	0.33	0.41	0.38	0.40	0.39	0.37	0.38	0.51	0.43	0.39
Lower Q. Strength Gradient of Ducts	0.10	0.10	0.10	0.11	0.09	0.12	0.10	0.11	0.12	0.10	0.11
Median of Strength Gradient of Ducts	0.21	0.23	0.23	0.24	0.23	0.25	0.22	0.24	0.29	0.23	0.24
Higher Q. of Strength Gradient of Ducts	0.36	0.44	0.47	0.45	0.49	0.46	0.37	0.44	0.61	0.46	0.45
Std.D. of Strength Gradient of Ducts	0.39	0.32	0.53	0.51	0.49	0.48	0.52	0.44	0.73	0.61	0.50
Min Height of Ducts	15.00	15.00	15.00	15.00	15.00	15.00	15.00	15.00	15.00	15.00	15.00
Max Height of Ducts	261.00	171.00	233.00	193.33	202.00	181.00	232.00	226.33	168.00	188.00	205.57
Mean of Mdeficit	11.66	11.79	14.09	11.81	11.80	11.44	13.06	11.22	10.67	12.40	12.00
Lower Quartile of Mdeficit	5.34	4.83	6.64	4.89	3.57	4.35	4.35	4.14	5.03	5.00	4.81
Median of Mdeficit	8.86	9.20	12.27	9.46	9.91	8.51	10.44	9.20	9.73	10.36	9.79
Higher Quartile of Mdeficit	15.91	15.84	17.83	16.67	19.70	17.29	19.43	18.08	14.26	17.20	17.22
Std. D. of Mdeficit	10.21	10.09	10.19	9.49	9.23	9.52	10.03	7.78	7.47	10.52	9.45

Table 14.   Winter ducting statistics for Izmir, between 1991 and 2000. Besides the ducting parameters that have been analyzed in this thesis, Strength, M deficit, Maximum and Minimum Heights were calculated and are displayed in this table.

IZMIR / DEC - JAN - FEB	1991	1992	1993	1994	1995	1996	1997	1998	1999	2000
Throughout the Day (Frequency of duct - percentage)	0.00	6.69	9.80	5.09	0.00	4.12	2.77	2.92	5.05	41.83
Radiosonde Resolution % (measurements below 71m)	5.00	10.67	13.33	16.33	9.00	11.00	11.33	8.67	28.33	87.67
Daytime (Frequency of duct - percentage)	0.00	8.90	9.21	8.02	0.00	6.00	5.17	7.02	5.19	51.31
Nighttime (Frequency of duct - percentage)	0.00	4.42	10.35	2.34	0.00	2.27	2.15	1.19	4.94	32.10
Mean Heihgt (m)	NaN	49.18	54.12	58.22	NaN	52.42	124.50	57.13	57.64	42.26
Lower Quartile of Duct's Heights	NaN	42.00	45.33	40.17	NaN	49.50	46.00	40.00	37.00	37.00
Median of Duct's Heights	NaN	49.83	54.50	57.67	NaN	52.33	123.00	56.50	58.00	42.50
Higher Quartile of Duct's Heights	NaN	57.67	63.67	76.83	NaN	53.75	62.00	46.50	46.50	47.67
Std. D. of Duct's Heights	NaN	8.02	11.81	23.80	NaN	1.69	5.23	2.39	1.65	5.52
Mean of Strength of Ducts	NaN	3.44	3.51	8.12	NaN	3.90	3.73	10.00	3.64	3.21
Lower Q. Strength of Ducts	NaN	1.10	1.10	3.25	NaN	2.79	1.98	0.44	0.61	1.48
Median of Strength of Ducts	NaN	3.20	3.59	6.55	NaN	3.83	2.25	9.18	3.48	2.35
Higher Q. of Strength of Ducts	NaN	5.94	5.58	12.99	NaN	6.31	9.02	5.79	2.71	4.58
Std.D. of Strength of Ducts	NaN	2.85	2.64	6.64	NaN	1.69	3.32	2.05	0.50	2.42
Mean of Strength Gradient of Ducts	NaN	0.18	0.18	0.33	NaN	0.18	0.15	0.29	0.12	0.28
Lower Q. Strength Gradient of Ducts	NaN	0.05	0.04	0.15	NaN	0.13	0.06	0.03	0.03	0.10
Median of Strength Gradient of Ducts	NaN	0.19	0.16	0.31	NaN	0.17	0.07	0.27	0.13	0.18
Higher Q. of Strength Gradient of Ducts	NaN	0.30	0.30	0.51	NaN	0.32	0.53	0.34	0.16	0.47
Std.D. of Strength Gradient of Ducts	NaN	0.14	0.19	0.25	NaN	0.09	0.20	0.10	0.03	0.24
Min Height of Ducts	NaN	29.00	29.00	29.00	NaN	29.00	29.00	29.00	29.00	29.00
Max Height of Ducts	NaN	58.67	120.00	167.00	NaN	54.00	131.50	60.50	59.00	53.67
Mean of Mdeficit	NaN	3.44	3.18	6.18	NaN	3.90	3.73	10.00	3.64	3.21
Lower Quartile of Mdeficit	NaN	1.10	1.10	3.09	NaN	2.79	1.98	0.44	0.61	1.48
Median of Mdeficit	NaN	3.20	3.59	5.49	NaN	3.83	2.25	9.18	3.48	2.35
Higher Quartile of Mdeficit	NaN	5.94	4.77	9.28	NaN	6.31	9.02	5.79	2.71	4.58
Std. D. of Mdeficit	NaN	2.85	2.19	4.08	NaN	1.69	3.32	2.05	0.50	2.42

116

Table 15. Winter ducting statistics for Izmir, between 2001 and 2010. Besides the ducting parameters that have been analyzed in this thesis, Strength, M deficit, Maximum and Minimum Heights were calculated and are displayed in this table.

IZMIR / DEC - JAN - FEB	2001	2002	2003	2004	2005	2006	2007	2008	2009	2010	Average '91-10
Throughout the Day (Frequency of duct - percentage)	5.32	37.14	54.22	54.78	24.26	12.91	11.39	13.72	6.83	8.59	15.37
Radiosonde Resolution % (measurements below 71m)	18.33	33.33	37.67	45.67	43.33	39.33	40.67	46.33	35.67	26.67	28.42
Daytime (Frequency of duct - percentage)	6.04	41.86	63.82	57.60	30.87	17.63	19.81	22.10	9.21	13.49	19.16
Nighttime (Frequency of duct - percentage)	4.57	32.41	44.62	51.87	17.68	8.00	3.26	5.49	4.53	3.71	11.80
Mean Heihgt (m)	51.00	64.06	64.07	57.78	50.75	48.89	43.20	43.53	46.47	43.97	56.07
Lower Quartile of Duct's Heights	41.50	42.67	45.33	37.17	36.00	36.75	36.75	34.33	42.33	37.00	40.38
Median of Duct's Heights	50.17	56.83	62.67	50.17	39.50	46.67	42.33	41.00	46.00	39.50	53.84
Higher Quartile of Duct's Heights	73.50	72.00	74.50	74.00	62.00	57.17	55.33	51.83	50.50	53.50	59.94
Std. D. of Duct's Heights	14.57	29.52	21.90	23.06	20.25	11.44	8.34	9.32	5.54	9.29	11.85
Mean of Strength of Ducts	3.20	5.50	5.15	5.54	4.31	1.42	1.42	1.82	6.51	6.91	4.52
Lower Q. Strength of Ducts	2.55	2.35	2.94	2.48	2.00	0.43	0.46	0.51	1.02	1.29	1.60
Median of Strength of Ducts	2.63	4.82	4.65	4.43	3.87	1.37	1.41	1.64	3.32	2.66	3.62
Higher Q. of Strength of Ducts	8.11	8.30	7.14	8.65	6.00	2.29	2.16	2.95	11.43	12.78	6.82
Std.D. of Strength of Ducts	2.20	4.17	3.38	3.97	3.22	1.22	1.05	1.32	8.31	8.51	3.30
Mean of Strength Gradient of Ducts	0.25	0.30	0.29	0.45	0.40	0.12	0.13	0.15	0.41	0.40	0.26
Lower Q. Strength Gradient of Ducts	0.08	0.08	0.07	0.08	0.07	0.03	0.04	0.04	0.09	0.09	0.07
Median of Strength Gradient of Ducts	0.17	0.15	0.17	0.25	0.34	0.08	0.10	0.14	0.22	0.34	0.19
Higher Q. of Strength Gradient of Ducts	0.63	0.48	0.38	0.83	0.66	0.20	0.19	0.33	0.70	0.57	0.44
Std.D. of Strength Gradient of Ducts	0.22	0.33	0.34	0.49	0.39	0.14	0.13	0.17	0.50	0.37	0.24
Min Height of Ducts	29.00	29.00	29.00	29.00	29.00	29.00	29.00	29.00	29.00	29.00	29.00
Max Height of Ducts	65.33	168.00	120.00	110.00	99.00	71.00	62.67	61.33	112.33	131.50	94.75
Mean of Mdeficit	3.20	5.50	5.15	5.54	4.31	1.42	1.41	1.82	5.25	5.02	4.22
Lower Quartile of Mdeficit	2.55	2.35	2.94	2.48	2.00	0.43	0.46	0.51	1.01	1.29	1.59
Median of Mdeficit	2.63	4.82	4.65	4.43	3.87	1.37	1.41	1.64	3.32	2.47	3.55
Higher Quartile of Mdeficit	8.11	8.30	7.14	8.65	6.00	2.29	2.16	2.95	8.30	6.59	6.05
Std. D. of Mdeficit	2.20	4.17	3.38	3.97	3.22	1.22	1.06	1.32	7.27	5.93	2.94

117

Table 16.   Summer ducting statistics for Izmir, between 1991 and 2000. Besides the ducting parameters that have been analyzed in this thesis, Strength, M deficit, Maximum and Minimum Heights were calculated and are displayed in this table.

IZMIR / JUN - JUL - AUG	1991	1992	1993	1994	1995	1996	1997	1998	1999	2000
Throughout the Day (Frequency of duct - percentage)	14.56	65.53	72.91	32.29	34.10	71.52	8.44	65.80	70.34	53.83
Radiosonde Resolution % (measurements below 81m)	51.67	61.67	49.33	65.67	76.00	71.67	40.33	52.00	95.67	82.00
Daytime (Frequency of duct - percentage)	17.02	80.32	83.41	83.33	54.52	74.77	6.13	74.13	83.00	65.41
Nighttime (Frequency of duct - percentage)	12.22	50.50	62.69	28.84	12.42	28.57	10.45	57.63	57.80	41.85
Mean Heihgt (m)	81.79	80.43	88.31	77.61	78.37	79.16	91.57	85.48	50.15	62.29
Lower Quartile of Duct's Heights	59.17	63.17	66.33	59.00	56.00	57.33	67.50	75.33	38.33	46.83
Median of Duct's Heights	82.67	82.17	87.50	74.00	72.17	72.00	96.50	84.83	46.50	56.83
Higher Quartile of Duct's Heights	97.00	96.50	111.67	95.00	89.50	97.00	116.00	94.00	56.33	71.67
Std. D. of Duct's Heights	29.19	24.84	29.37	24.64	33.70	25.69	25.90	15.24	14.03	22.59
Mean of Strength of Ducts	10.44	11.31	12.95	13.39	8.54	14.32	7.34	7.45	10.66	14.35
Lower Q. Strength of Ducts	3.21	3.80	4.99	6.30	2.78	5.94	0.87	3.29	4.37	6.65
Median of Strength of Ducts	11.11	7.82	10.73	12.38	7.37	14.66	5.12	6.54	8.75	11.73
Higher Q. of Strength of Ducts	15.11	18.30	19.70	20.77	12.22	20.48	11.59	10.95	15.28	20.47
Std.D. of Strength of Ducts	8.70	9.73	9.36	8.68	7.04	10.16	7.66	5.05	9.04	11.51
Mean of Strength Gradient of Ducts	0.32	0.43	0.41	0.41	0.25	0.49	0.14	0.16	0.71	0.87
Lower Q. Strength Gradient of Ducts	0.05	0.07	0.08	0.12	0.06	0.09	0.02	0.07	0.18	0.23
Median of Strength Gradient of Ducts	0.18	0.15	0.19	0.35	0.14	0.27	0.09	0.13	0.47	0.60
Higher Q. of Strength Gradient of Ducts	0.47	0.34	0.44	0.71	0.38	0.79	0.15	0.23	0.87	0.99
Std.D. of Strength Gradient of Ducts	0.50	0.75	0.65	0.34	0.29	0.54	0.22	0.13	0.77	0.98
Min Height of Ducts	29.00	29.00	29.00	29.00	29.00	29.00	29.00	29.00	29.00	29.00
Max Height of Ducts	126.67	211.67	164.67	126.33	185.67	137.33	120.00	116.33	93.67	124.00
Mean of Mdeficit	10.44	11.01	12.93	13.34	8.54	14.24	7.34	7.45	10.66	14.35
Lower Quartile of Mdeficit	3.21	3.80	4.99	5.99	2.78	5.71	0.87	3.29	4.37	6.65
Median of Mdeficit	11.11	7.62	10.73	12.38	7.37	14.66	5.12	6.54	8.75	11.73
Higher Quartile of Mdeficit	15.11	17.02	19.70	20.77	12.22	20.48	11.59	10.95	15.28	20.47
Std. D. of Mdeficit	8.70	9.58	9.38	8.73	7.04	10.25	7.66	5.05	9.04	11.51

Table 17. Summer ducting statistics for Izmir, between 2001 and 2010. Besides the ducting parameters that have been analyzed in this thesis, Strength, M deficit, Maximum and Minimum Heights were calculated and are displayed in this table.

IZMIR / JUN - JUL - AUG	2001	2002	2003	2004	2005	2006	2007	2008	2009	2010	Average '91-'10
Throughout the Day (Frequency of duct - percentage)	78.11	94.02	96.70	71.19	35.76	31.56	34.72	38.60	25.63	3.26	50.96
Radiosonde Resolution % (measurements below 81m)	79.33	82.33	86.00	75.00	81.00	81.00	87.00	85.67	77.00	66.00	80.03
Daytime (Frequency of duct - percentage)	86.88	100.00	100.00	79.76	60.24	58.06	63.03	62.63	45.98	6.56	66.31
Nighttime (Frequency of duct - percentage)	69.05	88.14	93.41	62.58	12.08	6.53	6.67	14.34	5.67	0.00	35.85
Mean Heihgt (m)	72.88	69.65	64.40	69.41	52.38	50.48	50.18	55.47	54.57	72.78	61.22
Lower Quartile of Duct's Heights	58.00	49.50	41.33	52.33	44.33	40.83	39.17	44.00	41.17	41.50	45.22
Median of Duct's Heights	73.67	67.00	58.33	67.67	50.83	48.17	46.33	51.50	51.33	74.33	58.92
Higher Quartile of Duct's Heights	87.67	84.00	84.83	83.00	61.33	58.50	53.00	62.83	64.00	79.50	71.87
Std. D. of Duct's Heights	19.46	27.59	25.27	24.58	12.97	13.39	15.80	18.01	14.88	15.72	18.77
Mean of Strength of Ducts	14.25	22.85	22.73	6.86	4.08	4.37	4.21	6.16	13.31	5.37	10.42
Lower Q. Strength of Ducts	6.06	12.95	13.86	3.26	1.92	1.69	1.85	2.68	1.33	1.27	4.69
Median of Strength of Ducts	13.39	22.37	21.04	6.18	3.93	3.92	3.82	4.96	4.13	2.78	8.65
Higher Q. of Strength of Ducts	20.89	30.92	31.08	9.46	6.08	6.68	5.60	7.72	23.17	12.05	15.36
Std.D. of Strength of Ducts	9.79	12.29	12.62	5.22	2.59	3.22	3.16	5.79	18.76	6.59	8.00
Mean of Strength Gradient of Ducts	0.48	1.05	1.37	0.22	0.27	0.28	0.30	0.38	0.52	0.12	0.50
Lower Q. Strength Gradient of Ducts	0.13	0.28	0.28	0.07	0.08	0.10	0.10	0.10	0.06	0.02	0.12
Median of Strength Gradient of Ducts	0.29	0.64	0.83	0.17	0.18	0.18	0.20	0.19	0.19	0.08	0.30
Higher Q. of Strength Gradient of Ducts	0.64	1.46	2.03	0.35	0.34	0.35	0.35	0.46	1.05	0.25	0.73
Std.D. of Strength Gradient of Ducts	0.55	1.08	1.47	0.25	0.30	0.28	0.36	0.61	0.71	0.13	0.57
Min Height of Ducts	29.00	29.00	29.00	29.00	29.00	29.00	29.00	29.00	29.00	29.00	29.00
Max Height of Ducts	115.00	169.00	140.33	162.67	83.67	89.00	105.33	152.33	223.00	120.33	136.07
Mean of Mdeficit	14.25	22.85	22.73	6.86	4.08	4.36	4.21	6.13	9.41	5.03	9.99
Lower Quartile of Mdeficit	6.06	12.95	13.86	3.26	1.92	1.63	1.85	2.66	1.33	1.27	4.68
Median of Mdeficit	13.39	22.37	21.04	6.18	3.93	3.92	3.82	4.96	3.95	2.72	8.63
Higher Quartile of Mdeficit	20.89	30.92	31.08	9.46	6.08	6.68	5.60	7.72	17.01	11.10	14.65
Std. D. of Mdeficit	9.79	12.29	12.62	5.22	2.59	3.22	3.16	5.81	11.66	6.02	7.24

Table 18. Winter ducting statistics for Heraklion, between 1991 and 2000. Besides the ducting parameters that have been analyzed in this thesis, Strength, M deficit, Maximum and Minimum Heights were calculated and are displayed in this table. Missing values mean that no data were available.

HERAKLION / DEC - JAN - FEB	1991	1992	1993	1994	1995	1996	1997	1998	1999	2000
Throughout the Day (Frequency of duct - percentage)	8.59	17.02	9.09			3.52		7.23	16.43	3.62
Radiosonde Resolution % (measurements below 91m)	12.50	19.67	32.00			30.00		27.33	39.00	51.00
Daytime (Frequency of duct - percentage)	8.59	17.02	9.09							
Nighttime (Frequency of duct - percentage)						3.59		6.14	16.43	3.62
Mean Heihgt (m)	106.75	86.00	83.50			73.00		89.67	76.73	67.75
Lower Quartile of Duct's Heights	81.00	78.00	80.00					73.00	63.33	47.00
Median of Duct's Heights	108.75	84.50	83.50			73.00		88.33	75.00	67.75
Higher Quartile of Duct's Heights	90.00	93.50	87.00					94.00	95.00	64.00
Std. D. of Duct's Heights	4.17	8.12	4.95			0.00		7.81	17.13	6.01
Mean of Strength of Ducts	5.21	8.93	6.60			0.43		5.74	2.67	1.82
Lower Q. Strength of Ducts	2.77	5.32	3.47					2.09	1.03	0.07
Median of Strength of Ducts	3.83	8.32	6.60			0.43		5.05	2.07	1.82
Higher Q. of Strength of Ducts	13.55	10.46	9.73					7.64	4.02	6.41
Std.D. of Strength of Ducts	3.94	4.08	4.42			0.00		2.15	2.26	2.24
Mean of Strength Gradient of Ducts	0.10	0.19	0.15			0.01		0.13	0.09	0.21
Lower Q. Strength Gradient of Ducts	0.05	0.12	0.07					0.04	0.02	0.00
Median of Strength Gradient of Ducts	0.08	0.20	0.15			0.01		0.09	0.09	0.21
Higher Q. of Strength Gradient of Ducts	0.30	0.24	0.24					0.26	0.15	0.80
Std.D. of Strength Gradient of Ducts	0.08	0.08	0.12			0.00		0.08	0.06	0.28
Min Height of Ducts	39.00	39.00	39.00			39.00		39.00	39.00	39.00
Max Height of Ducts	109.00	98.50	87.00			73.00		97.33	104.00	72.00
Mean of Mdeficit	5.21	8.93	6.60			0.43		5.74	2.67	1.82
Lower Quartile of Mdeficit	2.77	5.32	3.47					2.09	1.03	0.07
Median of Mdeficit	3.83	8.32	6.60			0.43		5.05	2.07	1.82
Higher Quartile of Mdeficit	13.55	10.46	9.73					7.64	4.02	6.41
Std. D. of Mdeficit	3.94	4.08	4.42			0.00		2.15	2.26	2.24

Table 19. Winter ducting statistics for Heraklion, between 2001 and 2010. Besides the ducting parameters that have been analyzed in this thesis Strength, M deficit, Maximum and Minimum Heights were calculated and are displayed in this table. Missing values mean that no data were available.

HERAKLION / DEC - JAN - FEB	2001	2002	2003	2004	2005	2006	2007	2008	2009	2010	Average '91-'10
Throughout the Day (Frequency of duct - percentage)	11.67	10.63	14.32	16.11	10.97	12.64	4.24			46.17	15.84
Radiosonde Resolution % (measurements below 91m)	45.00	49.67	49.67	48.33	37.00	45.67	26.50			60.00	45.23
Daytime (Frequency of duct - percentage)			20.58	21.13	10.73	13.96	6.90			48.50	20.30
Nighttime (Frequency of duct - percentage)	11.67	10.63	12.39	9.58	11.33	6.67	1.67			43.51	13.43
Mean Heihgt (m)	65.00	67.92	73.37	66.87	68.19	58.78	62.40			64.48	65.88
Lower Quartile of Duct's Heights	47.00	61.17	52.67	51.17	51.00	49.33	56.00			50.17	52.31
Median of Duct's Heights	67.00	69.17	72.83	56.83	53.00	55.33	64.00			58.50	62.08
Higher Quartile of Duct's Heights	99.00	74.67	86.33	80.67	83.75	71.67	72.00			71.00	79.89
Std. D. of Duct's Heights	13.11	10.16	26.06	24.17	24.80	14.09	6.69			18.01	17.14
Mean of Strength of Ducts	1.80	1.90	2.20	3.00	2.02	5.18	3.72			6.10	3.24
Lower Q. Strength of Ducts	1.12	1.15	0.33	0.98	0.74	2.03	0.91			2.80	1.26
Median of Strength of Ducts	1.32	1.88	1.52	1.98	1.74	4.67	2.06			5.35	2.56
Higher Q. of Strength of Ducts	5.27	2.65	2.87	4.02	3.37	8.33	7.36			9.75	5.45
Std.D. of Strength of Ducts	1.12	1.05	2.93	3.04	1.66	4.57	3.72			4.36	2.81
Mean of Strength Gradient of Ducts	0.08	0.06	0.07	0.15	0.16	0.35	0.19			0.46	0.19
Lower Q. Strength Gradient of Ducts	0.03	0.04	0.01	0.05	0.03	0.14	0.04			0.13	0.06
Median of Strength Gradient of Ducts	0.09	0.06	0.04	0.09	0.10	0.24	0.10			0.32	0.13
Higher Q. of Strength Gradient of Ducts	0.14	0.08	0.12	0.16	0.32	0.56	0.38			0.69	0.31
Std.D. of Strength Gradient of Ducts	0.03	0.03	0.09	0.17	0.18	0.33	0.22			0.47	0.19
Min Height of Ducts	39.00	39.00	39.00	39.00	39.00	39.00	39.00			39.00	39.00
Max Height of Ducts	77.00	74.67	133.67	118.33	115.50	84.33	72.00			147.00	102.81
Mean of Mdeficit	1.80	1.90	1.81	3.00	2.02	4.08	3.72			6.04	3.04
Lower Quartile of Mdeficit	1.12	1.15	0.33	0.98	0.74	1.68	0.91			2.64	1.19
Median of Mdeficit	1.32	1.88	1.29	1.98	1.74	3.97	2.06			5.35	2.45
Higher Quartile of Mdeficit	5.27	2.65	2.71	4.02	3.37	6.48	7.36			9.51	5.17
Std. D. of Mdeficit	1.12	1.05	2.25	3.04	1.66	3.31	3.72			4.38	2.57

Table 20.   Summer ducting statistics for Heraklion, between 1991 and 2000. Besides the ducting parameters that have been analyzed in this thesis Strength, M deficit, Maximum and Minimum Heights were calculated and are displayed in this table. Missing values mean that no data were available.

HERAKLION / JUN - JUL - AUG	1991	1992	1993	1994	1995	1996	1997	1998	1999	2000
Throughout the Day (Frequency of duct - percentage)	63.02	22.82	42.73			20.12		42.10	16.94	14.47
Radiosonde Resolution % (measurements below 101m)	47.33	37.67	33.67			40.00		77.00	79.67	81.00
Daytime (Frequency of duct - percentage)	63.02	22.82	42.73							
Nighttime (Frequency of duct - percentage)						20.12		42.10	17.10	14.47
Mean Heihgt (m)	121.13	125.11	125.93			128.03		103.07	89.93	81.83
Lower Quartile of Duct's Heights	95.67	78.75	91.25			86.83		78.67	74.00	70.50
Median of Duct's Heights	108.50	128.67	109.67			119.33		89.50	85.67	83.00
Higher Quartile of Duct's Heights	125.67	167.50	186.25			147.33		133.50	103.67	94.17
Std. D. of Duct's Heights	48.00	34.36	45.78			62.14		40.44	19.78	16.57
Mean of Strength of Ducts	12.22	9.42	9.03			5.50		6.14	5.29	8.38
Lower Q. Strength of Ducts	4.41	3.82	6.26			2.15		2.37	3.18	2.35
Median of Strength of Ducts	9.02	9.03	7.25			3.83		4.95	4.64	5.83
Higher Q. of Strength of Ducts	17.20	20.76	16.94			6.73		8.37	7.70	9.41
Std.D. of Strength of Ducts	10.73	6.92	7.19			5.96		5.11	2.81	9.48
Mean of Strength Gradient of Ducts	0.20	0.09	0.17			0.06		0.13	0.17	0.34
Lower Q. Strength Gradient of Ducts	0.07	0.05	0.04			0.03		0.06	0.09	0.05
Median of Strength Gradient of Ducts	0.10	0.07	0.06			0.05		0.08	0.11	0.11
Higher Q. of Strength Gradient of Ducts	0.25	0.13	0.19			0.09		0.15	0.18	0.25
Std.D. of Strength Gradient of Ducts	0.24	0.07	0.35			0.04		0.13	0.13	0.66
Min Height of Ducts	39.00	39.00	39.00			39.00		39.00	39.00	39.00
Max Height of Ducts	271.33	251.67	294.67			260.00		198.00	141.33	164.33
Mean of Mdeficit	11.98	8.98	8.64			5.25		6.10	5.06	6.18
Lower Quartile of Mdeficit	4.41	3.82	6.18			1.21		2.37	3.18	2.02
Median of Mdeficit	9.02	8.96	6.67			3.58		4.89	4.57	3.06
Higher Quartile of Mdeficit	17.20	19.54	15.84			6.73		8.37	6.85	6.12
Std. D. of Mdeficit	10.00	6.27	7.21			6.11		5.12	2.55	8.25

Table 21.   Summer ducting statistics for Heraklion, between 2001 and 2010. Besides the ducting parameters that have been analyzed in this thesis, Strength, M deficit, Maximum and Minimum Heights were calculated and are displayed in this table. Missing values mean that no data were available.

HERAKLION / JUN - JUL - AUG	2001	2002	2003	2004	2005	2006	2007	2008	2009	2010	Average '91-'10
Throughout the Day (Frequency of duct - percentage)	13.52	27.68	33.33	30.26	10.91	29.39	73.23	64.41	65.02	64.37	41.21
Radiosonde Resolution % (measurements below 101m)	78.67	69.33	73.00	77.67	76.00	77.33	89.50	89.00	74.50	80.33	78.53
Daytime (Frequency of duct - percentage)			53.33	47.70	17.86	40.79	89.00	73.46	82.61	95.00	62.47
Nighttime (Frequency of duct - percentage)	13.52	27.68	13.33	14.27	3.70	18.26	57.47	55.75	59.59	55.34	31.89
Mean Heihgt (m)	102.14	104.74	74.20	79.30	83.17	81.82	78.11	92.95	87.65	80.39	86.45
Lower Quartile of Duct's Heights	70.33	55.33	58.00	59.00	74.00	59.67	63.25	65.00	60.75	59.17	62.45
Median of Duct's Heights	100.83	71.33	66.00	67.67	77.50	72.00	72.75	80.50	78.00	78.33	76.49
Higher Quartile of Duct's Heights	137.00	95.50	81.00	82.33	97.00	92.33	92.50	96.50	105.00	91.33	97.05
Std. D. of Duct's Heights	36.97	93.75	20.15	43.26	12.61	34.55	23.13	65.77	37.38	29.26	39.68
Mean of Strength of Ducts	4.46	7.89	5.78	9.40	10.24	8.18	11.02	13.48	11.44	11.55	9.34
Lower Q. Strength of Ducts	1.86	2.38	2.08	2.67	3.54	1.84	4.40	5.70	4.64	5.34	3.44
Median of Strength of Ducts	4.71	7.82	4.62	7.29	7.69	3.94	9.05	9.59	8.70	9.90	7.33
Higher Q. of Strength of Ducts	6.66	12.52	6.99	12.89	15.53	11.85	15.74	17.48	17.30	14.81	13.18
Std.D. of Strength of Ducts	2.71	5.75	4.81	8.35	9.17	10.06	9.13	12.67	8.59	8.16	7.94
Mean of Strength Gradient of Ducts	0.08	0.48	0.23	0.34	0.19	0.25	0.44	0.47	0.51	0.63	0.36
Lower Q. Strength Gradient of Ducts	0.04	0.06	0.06	0.08	0.07	0.04	0.09	0.09	0.08	0.13	0.07
Median of Strength Gradient of Ducts	0.08	0.16	0.18	0.23	0.11	0.10	0.26	0.21	0.23	0.26	0.18
Higher Q. of Strength Gradient of Ducts	0.10	0.77	0.34	0.47	0.31	0.35	0.60	0.48	0.50	0.62	0.45
Std.D. of Strength Gradient of Ducts	0.04	0.71	0.21	0.35	0.17	0.32	0.49	0.63	0.72	0.92	0.46
Min Height of Ducts	39.00	39.00	39.00	39.00	39.00	39.00	39.00	39.00	39.00	39.00	39.00
Max Height of Ducts	160.33	313.00	244.00	275.67	229.00	348.67	235.00	422.00	262.50	166.33	265.65
Mean of Mdeficit	2.97	7.89	4.91	8.11	6.57	6.07	10.88	12.68	11.01	11.52	8.26
Lower Quartile of Mdeficit	1.28	2.38	1.98	2.30	2.62	1.84	3.57	5.29	4.42	5.31	3.10
Median of Mdeficit	2.29	7.82	4.38	6.34	4.53	3.58	9.05	9.51	8.58	9.90	6.60
Higher Quartile of Mdeficit	4.74	12.52	6.72	12.45	7.78	8.39	15.74	16.52	16.72	14.81	11.64
Std. D. of Mdeficit	2.09	5.75	3.83	7.40	6.53	6.48	9.24	12.22	8.27	8.19	7.00

123

THIS PAGE INTENTIONALLY LEFT BLANK

This appendix contains the MATLAB codes that were used for the extraction of the necessary variables from the raw data and the computation of statistical quantities.

A. MATLAB CODE TO PREPROCESS THE RAW DATA FILES

```matlab
function preprocess(filename)
%
% Purpose: Adds a blank line in between individual soundings so that
%          the "load_sounding" program will work without any
%          modifications.
% Written 5/26/11 by Arlene Guest
%
% Output filename is same as input filename, but with an 'm' at the
% beginning, so ATHENS_MAY_2010.txt becomes mATHENS_MAY2010.txt
%
% format:
% LGIR Observations at 00Z 01 Jan 2005
% -----------------------------------------------------------------
%    PRES   HGHT   TEMP   DWPT   RELH   MIXR   DRCT   SKNT   THTA
%     hPa     m      C      C      %    g/kg    deg   knot    K
% -----------------------------------------------------------------
%  1016.0    39    9.6    7.0     84   6.22    160      6  281.5
%  1009.0    95   12.0    8.5     79   6.94    184      6  284.4
%  1000.0   168   12.2    6.2     67   5.98    215      6  285.4
%   987.0   277   11.6    6.6     71   6.23    234      6  285.8
% Station information and sounding indices
%                        Station identifier: LGIR
%                            Station number: 16754
%                          Observation time: 050101/0000
%                          Station latitude: 35.33
%                         Station longitude: 25.18
%                         Station elevation: 39.0
%                          Showalter index: 11.02
%                             Lifted index: 9.45
%     LIFT computed using virtual temperature: 9.38
%                              SWEAT index: 72.32
%                                 K index: -11.20
%                       Cross totals index: 17.20
%                    Vertical totals index: 19.10
%                      Totals totals index: 36.30
%      Convective Available Potential Energy: 7.46
%            CAPE using virtual temperature: 12.88
%                     Convective Inhibition: -14.83
%            CINS using virtual temperature: -13.39
%                          Equilibrum Level: 803.48
%  Equilibrum Level using virtual temperature: 800.10
%                  Level of Free Convection: 870.17
%             LFCT using virtual temperature: 877.40
```

```matlab
%                       Bulk Richardson Number: 0.11
%            Bulk Richardson Number using CAPV: 0.18
%   Temp [K] of the Lifted Condensation Level: 278.77
% Pres [hPa] of the Lifted Condensation Level: 921.85
%       Mean mixed layer potential temperature: 285.35
%                 Mean mixed layer mixing ratio: 6.24
%                 1000 hPa to 500 hPa thickness: 5472.00
% Precipitable water [mm] for entire sounding: 13.18
%
% LGIR Observations at 12Z 01 Jan 2005
% -----------------------------------------------------------------
%    PRES   HGHT   TEMP   DWPT   RELH   MIXR   DRCT   SKNT   THTA
%    hPa     m      C      C      %     g/kg    deg   knot    K
% -----------------------------------------------------------------
%  1016.0     39   15.8    9.8     68   7.54    350      4  287.6
%  1014.0     56   13.4    6.4     63   5.98    349      4  285.4
%
%
% -----------------------------------------------------------------
fid_in=fopen(filename,'r');
if fid_in > 0
    disp(['Sounding file opened: '  filename])
end

% Create a filenumber for the output:
fid_out=fopen(['m' filename],'wt');

% counter for all soundings
nsoundings = 0;

flag = 1;
while flag
% get a line from the file:
  line = fgetl(fid_in);
if line==-1  % Exit the while loop if we're at the end of the file
break
end

% write out the line of data plus a line break:
  fprintf(fid_out,line);
  fprintf(fid_out,'\n');

% Check to see if we're at the last line of the sounding.  If so,
% write a blank line, count the sounding and go back up to the
% beginning of the while loop
if line(1:12)=='Precipitable'
     fprintf(fid_out,'\n');
     nsoundings = nsoundings + 1;
end

end% end of while loop
%
% this is the end.  If we get here, we hit the end of the original
% file.
```

126

```matlab
  fprintf('Wrote out %f soundings \n',nsoundings)
end
```

B. MATLAB CODE TO READ THE RAW DATA AND DETERMINE DUCTING CONDITIONS

```matlab
function load_sounding(filename)
%
% Purpose:  decodes for files with format below.  MUST, MUST have
% a blank line between soundings.
%
% format:
% LGIR Observations at 00Z 01 Jan 2005
% -----------------------------------------------------------------
%    PRES   HGHT   TEMP   DWPT   RELH   MIXR   DRCT   SKNT   THTA
%    hPa     m      C      C      %     g/kg   deg    knot    K
% -----------------------------------------------------------------
%  1016.0    39    9.6    7.0    84    6.22    160      6   281.5
%  1009.0    95   12.0    8.5    79    6.94    184      6   284.4
%  1000.0   168   12.2    6.2    67    5.98    215      6   285.4
%   987.0   277   11.6    6.6    71    6.23    234      6   285.8
% Station information and sounding indices
%                          Station identifier: LGIR
%                              Station number: 16754
%                             Observation time: 050101/0000
%                             Station latitude: 35.33
%                            Station longitude: 25.18
%                            Station elevation: 39.0
%                             Showalter index: 11.02
%                                 Lifted index: 9.45
%     LIFT computed using virtual temperature: 9.38
%                                 SWEAT index: 72.32
%                                      K index: -11.20
%                           Cross totals index: 17.20
%                        Vertical totals index: 19.10
%                           Totals totals index: 36.30
%        Convective Available Potential Energy: 7.46
%                CAPE using virtual temperature: 12.88
%                       Convective Inhibition: -14.83
%            CINS using virtual temperature: -13.39
%                            Equilibrum Level: 803.48
%  Equilibrum Level using virtual temperature: 800.10
%                     Level of Free Convection: 870.17
%             LFCT using virtual temperature: 877.40
%                      Bulk Richardson Number: 0.11
%           Bulk Richardson Number using CAPV: 0.18
%    Temp [K] of the Lifted Condensation Level: 278.77
% Pres [hPa] of the Lifted Condensation Level: 921.85
%       Mean mixed layer potential temperature: 285.35
%                Mean mixed layer mixing ratio: 6.24
%                 1000 hPa to 500 hPa thickness: 5472.00
% Precipitable water [mm] for entire sounding: 13.18
%
```

```matlab
% LGIR Observations at 12Z 01 Jan 2005
% -----------------------------------------------------------------
%    PRES    HGHT    TEMP    DWPT    RELH    MIXR    DRCT    SKNT    THTA
%     hPa      m       C       C       %      g/kg    deg    knot     K
% -----------------------------------------------------------------
%  1016.0      39    15.8     9.8      68    7.54     350       4   287.6
%  1014.0      56    13.4     6.4      63    5.98     349       4   285.4
%
% -------------------------------------------
% Modified 5/9/11 by M. Jordan, NPS/MR
% Last modified 10/26/11 by K. Raptis
% -------------------------------------------------------------
fid_in=fopen(filename,'r');
if fid_in > 0
    disp(['Sounding file opened: '  filename])
end


% counter for all soundings ie: 700 soundings/year or
% 60 soundings/month
bigcounter = 0;


% initialize matrices to store Date/Time and Station ID
YYMMDD_HHMM_matrix = [];
STATION_ID_matrix = []; % to be commented out for IZMIR



while 1     %This loop for each sounding

% clear variables before start to read next sounding
    clear preshghttmpcdwpcrelhmixrdrctsknt
    clear thtaqMN

% Skip first five rows header
for ihead = 1:5;
        line = fgetl(fid_in);
end
%
%initialize a line counter
    iline=0;
%
%This loop reads each line
while 1
%Read each line as a character string
        line=fgetl(fid_in);
%This loop finds missing value for dwpt
while line (22:28) == '       '
            line=fgetl(fid_in);
end
%This is statement for reading headers
if line (1:7) == 'Station'
            line=fgetl(fid_in);
            station_ID_str = line(46:49);
            line=fgetl(fid_in);
            station = str2num(line(46:50));
```

128

```matlab
                station_number = str2num(line(46:50));
                line=fgetl(fid_in);
                date_time_str = line(45:56);
                date=str2num(line(46:51));
                time=str2num(line(53:56));
                line=fgetl(fid_in);
%This loop skip other lines
while ~isempty(line) %line(44) == ':'
                line=fgetl(fid_in);
%Check for the effective "end-of-file"
if line == -1
break
end
end
end

% Check for the end of one data set (one sounding)...
% ...this means MUST have a blank line between soundings
if isempty(line)
break
end
%Check for the effective "end-of-file"
if line == -1
break
end

% Increment line counter.  This is the index for each
% data array
        iline = iline+1;
%Reads data from file
        pres(iline) = str2num(line(1:7));
        hght(iline) = str2num(line(8:14));
        tmpc(iline) = str2num(line(15:21));
        dwpc(iline) = str2num(line(22:28));
        relh(iline) = str2num(line(29:35));
        mixr(iline) = str2num(line(36:42));

if line(48:56) =='          '
            drct(iline) = NaN;
            sknt(iline) = NaN;
else
            drct(iline) = str2num(line(47:49));
            sknt(iline) = str2num(line(54:56));
end

end% This is the end of the WHILE Loop

% This is the end of reading and decoding its sounding separetely
% ATTENTION: Only those values of the very final sounding's
% parameters are saved. The values of the previous soundings are
% overwritten by the next each time the while loop runs.

%------------------------------------------------------------------
```

129

```matlab
% This is the begining of the part which computes all the necessary
% parameters for ducts calculation
% Calculate theta & q
    [thta,q] = theta_q(pres,tmpc,relh);


% Calculate M and N
    [M,N] = m_n_profile(pres,tmpc,relh,hght);


% increment counter
    bigcounter = bigcounter + 1;

    STATION_ID_matrix = char(STATION_ID_matrix, station_ID_str);
    STATION_NUMBER_matrix(bigcounter,1) = station_number;
    YYMMDD_HHMM_matrix = char(YYMMDD_HHMM_matrix,date_time_str);


%     % plot refractivity its optional
%     plot_refractivity


% Calculates the Modified Refractivity gradient
    Mgrad=NaN;
for n=1:iline-1 ;
     Mgrad(n,1)=(M(n+1) - M(n)) /(hght(n+1) - hght(n));
end


% This portion finds the first three ducts, if
% they exist
    ducttop=[0 0 0];
    ductmiddle=[0 0 0];
    ductbottom=[0 0 0];
    Ttop=NaN;
    Dewtop=NaN;
    Presstop=NaN;
    Mtop=NaN;
    Tmid=NaN;
    Dewmid=NaN;
    Pressmid=NaN;
    Mmid=NaN;
    Mtop2=NaN;
    Mmid2=NaN;
    Mtop3=NaN;
    Mmid3=NaN;


% Find tops and mids of ducts....
    topcounter=0;
    midcounter=0;
    topindex=[0 0 0];
    midindex=[0 0 0];
for m=2:length(Mgrad)
if ((Mgrad(m-1) < 0) && (Mgrad (m) > 0))
         topcounter=topcounter+1;
         topindex(topcounter)=m;
end
if ((Mgrad(m-1) > 0) && (Mgrad (m) < 0))
```

130

```matlab
            midcounter=midcounter+1;
            midindex(midcounter)=m;
end
end

% Align these depending on case.....
% If the gradient starts negative from the surface,
% the subsequent indexing is different that for the
% case if the gradient starts positive from the
% surface.
if (Mgrad(1) <  0)
if (topindex(1) > 0)
            ducttop(1)=hght(topindex(1));
            ductmiddle(1)=hght(1);
            ductbottom(1)=hght(1);
end
if (topindex(2) > 0) && (midindex(1) > 0)
            ducttop(2)=hght(topindex(2));
            ductmiddle(2)=hght(midindex(1));
if M(midindex(1)-1) < M(topindex(2))
                ductbottom(2)=ductmiddle(2) - ...
                    (M(midindex(1))-M(topindex(2)))/...
                    (M(midindex(1))-M(midindex(1)-1))*...
                    (hght(midindex(1)) - hght(midindex(1)-1));
elseif M(midindex(1)-1) > M(topindex(2))&& M(midindex(1)-
2)>M(midindex(1)-1)
                ductbottom(2)=hght(midindex(1)-1);
elseif M(midindex(1)-2) > M(topindex(2))&& M(midindex(1)-
3)>M(midindex(1)-2)
                ductbottom(2)=hght(midindex(1)-2);
elseif M(midindex(1)-1) > M(topindex(2))
                counterindex = 1;
while M(midindex(1)-counterindex)>M(topindex(2))&&...
                    (midindex(1)-counterindex)~=1
                counterindex = counterindex+1;
end
                ductbottom(2)=hght(midindex(1)-counterindex+2) - ...
                    (M(midindex(1)-counterindex+2)-M(topindex(2)))/...
                    (M(midindex(1)-counterindex+2)-M(midindex(1)-
counterindex))*...
                    (hght(midindex(1)-counterindex+2) -
hght(midindex(1)-counterindex));
end
            Mtop2=M(topindex(2));
            Mmid2=M(midindex(1));
end
if (topindex(3) > 0) && (midindex(2) > 0)
            ducttop(3)=hght(topindex(3));
            ductmiddle(3)=hght(midindex(2));
if M(midindex(2)-1) < M(topindex(3))
                ductbottom(3)=ductmiddle(3) - ...
                    (M(midindex(2))-M(topindex(3)))/...
                    (M(midindex(2))-M(midindex(2)-1))*...
                    (hght(midindex(2)) - hght(midindex(2)-1));
elseif M(midindex(2)-1) > M(topindex(3))
```

```matlab
                 counterindex = 1;
while M(midindex(2)-counterindex)>M(topindex(3))
                 counterindex = counterindex+1;
end
                 ductbottom(3)=hght(midindex(2)-counterindex+2) - ...
                     (M(midindex(2)-counterindex+2)-M(topindex(3)))/...
                     (M(midindex(2)-counterindex+2)-M(midindex(2)-
counterindex))*...
                     (hght(midindex(2)-counterindex+2) -
hght(midindex(2)-counterindex));
end
           Mtop3=M(topindex(3));
           Mmid3=M(midindex(2));
end
       Ttop=tmpc(topindex(1));
       Dewtop=dwpc(topindex(1));
       Presstop=pres(topindex(1));
       Mtop=M(topindex(1));
       Tmid=tmpc(1);
       Dewmid=dwpc(1);
       Pressmid=pres(1);
       Mmid=M(1);
end

% These are for the cases when the gradient starts
% positive, and there is a duct present somewhere in
% the profile
if (Mgrad(1) > 0) & (topindex(1) > 0)
if (topindex(1) > 0) & (midindex(1) > 0) &...
               (M(topindex(1)) < M(1))
           ducttop(1)=hght(topindex(1));
           ductmiddle(1)=hght(midindex(1));
           ductbottom(1)=hght(1);
end

if (topindex(1) > 0) & (midindex(1) > 0) &...
               (M(topindex(1)) > M(1))
           ducttop(1)=hght(topindex(1));
           ductmiddle(1)=hght(midindex(1));
if M(midindex(1)-1)<M(topindex(1))
               ductbottom(1)=ductmiddle(1) - ...
                   (M(midindex(1))-M(topindex(1)))/...
                   (M(midindex(1))-M(midindex(1)-1))*...
                   (hght(midindex(1)) - hght(midindex(1)-1));
elseif M(midindex(1)-1)>M(topindex(1))
               counterindex = 1;
while M(midindex(1)-counterindex)>M(topindex(1))
               counterindex = counterindex+1;
end
               ductbottom(1)=hght(midindex(1)-counterindex+2) - ...
                   (M(midindex(1)-counterindex+2)-M(topindex(1)))/...
                   (M(midindex(1)-counterindex+2)-M(midindex(1)-
counterindex))*...
                   ((hght(midindex(1)-counterindex+2)) -
hght(midindex(1)-counterindex));
```

132

```matlab
            end

    end

if (topindex(2) > 0) & (midindex(2) > 0)
            ducttop(2)=hght(topindex(2));
            ductmiddle(2)=hght(midindex(2));
            ductbottom(2)=ductmiddle(2) - ...
                (M(midindex(2))-M(topindex(2)))/...
                (M(midindex(2))-M(midindex(2)-1))*...
                (hght(midindex(2)) - hght(midindex(2)-1));
if M(midindex(2)-1)<M(topindex(2))
                ductbottom(2)=ductmiddle(2) - ...
                    (M(midindex(2))-M(topindex(2)))/...
                    (M(midindex(2))-M(midindex(2)-1))*...
                    (hght(midindex(2)) - hght(midindex(2)-1));
elseif M(midindex(2)-1)>M(topindex(2))
                counterindex = 1;
while M(midindex(2)-counterindex)>M(topindex(2))&&...
                        (midindex(2)-counterindex)~=1
                    counterindex = counterindex+1;
end
                ductbottom(2)=hght(midindex(2)-counterindex+2) - ...
                    (M(midindex(2)-counterindex+2)-M(topindex(2)))/...
                    (M(midindex(2)-counterindex+2)-M(midindex(2)-
counterindex))*...
                    ((hght(midindex(2)-counterindex+2)) -
hght(midindex(2)-counterindex));
end
            Mtop2=M(topindex(2));
            Mmid2=M(midindex(2));
    end

if (topindex(3) > 0) & (midindex(3) > 0)
            ducttop(3)=hght(topindex(3));
            ductmiddle(3)=hght(midindex(3));
            ductbottom(3)=ductmiddle(3) - ...
                (M(midindex(3))-M(topindex(3)))/...
                (M(midindex(3))-M(midindex(3)-1))*...
                (hght(midindex(3)) - hght(midindex(3)-1));
if M(midindex(3)-1)<M(topindex(3))
                ductbottom(3)=ductmiddle(3) - ...
                    (M(midindex(3))-M(topindex(3)))/...
                    (M(midindex(3))-M(midindex(3)-1))*...
                    (hght(midindex(3)) - hght(midindex(3)-1));
elseif M(midindex(3)-1)>M(topindex(3))
                counterindex = 1;
while M(midindex(3)-counterindex)>M(topindex(3))
                    counterindex = counterindex+1;
end
                ductbottom(3)=hght(midindex(3)-counterindex+2) - ...
                    (M(midindex(3)-counterindex+2)-M(topindex(3)))/...
                    (M(midindex(3)-counterindex+2)-M(midindex(3)-
counterindex))*...
```

```matlab
                        ((hght(midindex(3)-counterindex+2))-
hght(midindex(3)-counterindex));
end

            Mtop3=M(topindex(3));
            Mmid3=M(midindex(3));
end

        Ttop=tmpc(topindex(1));
        Dewtop=dwpc(topindex(1));
        Presstop=pres(topindex(1));
        Mtop=M(topindex(1));
        Tmid=tmpc(midindex(1));
        Dewmid=dwpc(midindex(1));
        Pressmid=pres(midindex(1));
        Mmid=M(midindex(1));

if topindex(2)~=0 && midindex(2)~=0
            Mtop2=M(topindex(2));
            Mmid2=M(midindex(2));
else
            Mtop2=NaN;
            Mmid2=NaN;
end
if topindex(3)~=0 && midindex(3)~=0
            Mtop3=M(topindex(3));
            Mmid3=M(midindex(3));
else
            Mtop3=NaN;
            Mmid3=NaN;
end


end
if ductbottom(1) < 0
        ductbottom(1)=ductmiddle(1)-[ducttop(1)-ductmiddle(1)];
end
if ductbottom(2) < 0
        ductbottom(2)=ductmiddle(2)-[ducttop(2)-ductmiddle(2)];
end
if ductbottom(1) < 0
        ductbottom(1) =0;
end
if ductbottom(2) < 0
        ductbottom(2) =0;
end

% This will assign a true/false value if the lowest duct is
% "attached" to (Surface Duct) or "elevated" from the surface
if [ducttop(1) > 0] & [ductbottom(1) > hght(1)]
        sfcduct=0; %elevated
elseif ([ducttop(1) > 0] & [ductbottom(1) == hght(1)]) |...
            ([ducttop(1) > 0] & [ductbottom(1) == 0])
        sfcduct=1; %attached
else
```

```matlab
        sfcduct=NaN; %technically, it means no duct at all
end
% Assigns needed data to the Plotdata matrix
    Plotdata(bigcounter,1)=station;
    Plotdata(bigcounter,2)=date;
    Plotdata(bigcounter,3)=time;
    Plotdata(bigcounter,4)=Ttop;  %Temp at the top of the first duct
    Plotdata(bigcounter,5)=Dewtop; %Dewp at the top of the first duct
%----------------------------------------------------------------
    Plotdata(bigcounter,6)=ducttop(1); %Height of the duct's top
    Plotdata(bigcounter,7)=ductmiddle(1); %First duct from the surface
    Plotdata(bigcounter,8)=ductbottom(1); %Height of the duct's bottom
%----------------------------------------------------------------
    Plotdata(bigcounter,9)=ducttop(2);
    Plotdata(bigcounter,10)=ductmiddle(2); %Next duct up above
    Plotdata(bigcounter,11)=ductbottom(2);
%----------------------------------------------------------------
    Plotdata(bigcounter,12)=ducttop(3);
    Plotdata(bigcounter,13)=ductmiddle(3); %Next duct up above
    Plotdata(bigcounter,14)=ductbottom(3);
%----------------------------------------------------------------
    Plotdata(bigcounter,15)=sfcduct; % surface duct or elevated

%All the following parameters concern the surface duct. If it
% doesn't exist,then no value is assigned to them.
    Plotdata(bigcounter,16)=Presstop;
    Plotdata(bigcounter,17)=Pressmid;
    Plotdata(bigcounter,18)=Tmid;
    Plotdata(bigcounter,19)=Dewmid;
    Plotdata(bigcounter,20)=Mtop;
    Plotdata(bigcounter,21)=Mmid;
%----------------------------------------------------------------
    Plotdata(bigcounter,22)=pres(1); %All these parameters give
    Plotdata(bigcounter,23)=drct(1); %surface values regardless of
    Plotdata(bigcounter,24)=sknt(1); %the existance of ducts
%----------------------------------------------------------------
% Duct's thickness
    Plotdata(bigcounter,25)=ducttop(1)-ductbottom(1);
    Plotdata(bigcounter,26)=ducttop(2)-ductbottom(2);
    Plotdata(bigcounter,27)=ducttop(3)-ductbottom(3);
%----------------------------------------------------------------
% Duct's M at the top and at the midle for the second and
% third duct
    Plotdata(bigcounter,28)=Mtop2;
    Plotdata(bigcounter,29)=Mmid2;
    Plotdata(bigcounter,30)=Mtop3;
    Plotdata(bigcounter,31)=Mmid3;
    Plotdata(bigcounter,32)=Mmid-Mtop;
    Plotdata(bigcounter,33)=Mmid2-Mtop2;
    Plotdata(bigcounter,34)=Mmid3-Mtop3;
%----------------------------------------------------------------
% Gradient of M - Duct's strength
    Plotdata(bigcounter,35)=(Mmid-Mtop)/(ducttop(1)-ductmiddle(1));
    Plotdata(bigcounter,36)=(Mmid2-Mtop2)/(ducttop(2)-ductmiddle(2));
    Plotdata(bigcounter,37)=(Mmid3-Mtop3)/(ducttop(3)-ductmiddle(3));
```

135

```matlab
%----------------------------------------------------------------

    Plotdata(bigcounter,38)=M(1); % The M of the very first segment
% (measurment) of the sounding


%finds M deficit
if Plotdata(bigcounter,15)==1 % = if there is surface duct

        Plotdata(bigcounter,39) = M(1)-Mtop; % it should be positive
else% or zero
        Plotdata(bigcounter,39) = NaN;
end
%------------------------------------------------------------------------
%Check for the effective "end-of-file"
if line == -1
break
end
end


fclose(fid_in); % --- end of sounding "decoder" portion

% remove extra lines & columns in data matrices
STATION_ID_matrix(1,:) = [];  % to be commented out for IZMIR
YYMMDD_HHMM_matrix(1,:) = [];

% add a variable
number_of_soundings = bigcounter;

%  prepare the name for the ".mat" file
%  Logic:  find the "/"s and ".", so we can use the first part of
%  the name.
index1=find(filename == '/');        %  find the "/" in the name
if length(index1) == 0               %  if no "/" in name
    first=1;
else
    iend=length(index1);             %  the last "/"
    first=index1(iend)+1;            %  first character in matfile
end%  name
index2=find(filename == '.');
last=index2-1;                       %  use characters before the "."
matfile= [filename(1,first:last)  '_statistics.mat'];

% clear variables before saving MAT file
clear preshghttmpcdwpcrelhmixrdrctsknt
clear thtaqMNstation_ID_strstation_number
clear date_time_strone_P
clear ansiheadilineindex1index2lastlinefid_in
clear indexindex1index2firstlastiendansfilename
clear time_str_UTCidate_str_YYMMDD
clear *top*mid*bottom

% save MAT file ... with variables listed
```

136

```matlab
eval(['save ' matfile ' Plotdata STATION_ID_matrix
STATION_NUMBER_matrix YYMMDD_HHMM_matrix number_of_soundings'])

disp(['MAT file written to current directory: ' matfile ])

% ----- end of function ----------------------------------
```

1. This Is the Function to Compute Θ and Q.

```matlab
function [thta,q] = theta_q(pres,tmpc,relh)
%
%  function [thta,q] = theta_q(pres,tmpc,relh)
%
%  written by:  Mary Jordan, NPS Meteorology Dept, 10/9/96
%
%  Purpose: Calculates Potential Temperature (thta) and
%       Specific Humidity (q)
%
%  Reference:  Atmospheric Science by Wallace & Hobbs, 1977,
%  Academic Press
%
%  Input:   pres = Pressure (mb)
%       tmpc = Air Temperature (C)
%       relh = Relative Humidity (%)
%
%  Output:  thta = Potential Temperature (K)
%           q = Specific Humidity (g/kg)
%
% ------------------------------------------------------------


%
% define local constants for thermodynamic equations:
    p0=1000.;R=287.;cp=1004.;L=2.5e6;
%
tmpk = tmpc+273.155;              % convert to tmpc to Kelvin
%
e_s = 6.1078*exp((17.26939.*tmpc)./(tmpc+237.3));% saturation vapor
% pressure
ee = (relh ./ 100.) .* e_s;                      % vapor pressure
%
w = 0.622 * (ee ./ (pres - ee));       % mixing ratio (kg/kg)
q_kg = w ./ (1.0 + w);                 % specific humidity (kg/kg)
%
q=q_kg*1000;                           % specific humidity (g/kg)
%
thta = tmpk .* ((p0 ./ pres).^(R/cp));  % Potential Temperature (K)

%--------------------     END    ----------------------------
```

2. This Is the Function to Compute the Profile of M.

```matlab
function [M,N] = m_n_profile(pres,tmpc,relh,hght)
%
%  Purpose: Calculates the vertical profiles of Refractive Index, N,
%           and the Modified Refractive Index, M, for input vertical
%           profiles of Pressure, Temperature Relative Humidity and
%           Height.
%
%  Input:   pres = pressure (millibars)
%           tmpc = air temperature (Celsius)
%           relh = relative humidity (percent, %)
%           hght = height (meters)
%
%  Output:  M = Modified Refractive Index (dimensionless refractivity
%                                          units)
%           N = Refractive Index (dimensionless refractivity units)
%
%  Local Variables:
%
%           tmpk = air temperature (Kelvin)
%           e_s  = saturation vapor pressure (millibars)
%           ee   = vapor pressure (millibars)
%
% References
%  Bean and Dutton, 1968, Equation 1.16.  ... for N
%  Patterson, et al. (1994), Equation 5, p. 9.  ... for M
%  Bolton, Monthly Weather Review, 1980...for saturation vapor pres.
%  Huschke, Glossary of Meteorology, 1959, p. 477...for vapor pres.
%
%  History
%   Version 1.0  17 July 2001
%   Mary S. Jordan
%   Dept. of Meteorology, Naval Postgraduate School, Monterey, CA
%  ----------------------------------------------------------------

%    ... convert to temperature to Kelvin
tmpk = tmpc+273.15;

%    ... compute saturation vapor pressure, e_s
e_s = 6.112*exp((17.67 .* tmpc)./(tmpc+243.5));

%    ... compute vapor pressure, ee
ee = (relh ./ 100.) .* e_s;

%  ... compute Refractive Index, N, and Modified Refractive Index, M
%
N = (77.6*pres./tmpk) - (5.6*ee./tmpk) + (3.75e5*ee./(tmpk.^2));
M = N + 157*hght./1000;

% ---------------------- end of function -------------------------
```

C. MATLAB CODE TO CALCULATE THE RELEVANT STATISTICS

```
% Purpose: To calculate the basic statistics modes (mean, stdev,
%          quartiles) for ducting parameters
%
% Input: The Plotdata table (derived from the load_sounding
%        program) must be loaded first and then run this program.
%
% Output: Statistics. The derived variable "table" gives all the
%          computed statistics in tabular form
%
% Last modified 9/15/11 by Kostas Raptis NPS/MR
%_____

x=length(Plotdata(:,1)); % number of rows = number of soundings

temp1=0;%temporary variables
temp2=0;
temp3=0;
tmp1=0;
tmp2=0;
tmp3=0;
tempmin1=0;
tempmin2=0;
tempmin3=0;
temp=0;

%_____FREQUENCY OF OCCURANCE_____(line 1 to 3 of table)__
%finds duct frequencies of occurance
%Duct 1
counter = 1;
ducts1=0;
for i=1:x
if Plotdata(counter,6)>0 %=if top's height of 1st duct>0
        ducts1=ducts1+1;
end
    counter=counter+1;
end

percent1duct=(ducts1/x)*100;

table=[];
table(1,1)=percent1duct;

%Duct 2
counter = 1;
ducts2=0;
for i=1:x
if Plotdata(counter,9)>0 %=if top's height of 2nd duct>0
        ducts2=ducts2+1;
end
    counter=counter+1;
end
```

```matlab
percent2duct=(ducts2/x)*100;

table(1,2)=percent2duct; %it appears on the 2nd column of the 1st line

%Duct 3
counter = 1;
ducts3=0;

for i=1:x
if Plotdata(counter,12)>0
        ducts3=ducts3+1;
end
    counter=counter+1;
end

percent3duct=(ducts3/x)*100;

table(1,3)=percent3duct; %it appears on the 3d column of the 1st line

%finds frequency of daytime duct1
counter=1;
dayduct1=0;
day=0;
for i=1:x
if Plotdata(counter,3)==1200
        day=day+1;
end
if Plotdata(counter,3)==1200 && Plotdata(counter,6)>0
        dayduct1=dayduct1+1;
end
    counter=counter+1;
end
percent1ductday=(dayduct1/day)*100;
table(2,1)=percent1ductday; % it appears on the 1st column of the
% 2nd line

%finds frequency of nighttime duct1
counter=1;
nightduct1=0;
night=0;
for i=1:x
if Plotdata(counter,3)==0
        night=night+1;
end
if Plotdata(counter,3)==0 && Plotdata(counter,6)>0
        nightduct1=nightduct1+1;
end
    counter=counter+1;
end
percent1ductnight=(nightduct1/night)*100;
table(3,1)=percent1ductnight;

%finds frequency of daytime duct2
counter=1;
```

```matlab
dayduct2=0;
day=0;
for i=1:x
if Plotdata(counter,3)==1200
        day=day+1;
end
if Plotdata(counter,3)==1200 && Plotdata(counter,9)>0
        dayduct2=dayduct2+1;
end
    counter=counter+1;
end
percent2ductday=(dayduct2/day)*100;
table(2,2)=percent2ductday;

%finds frequency of nighttime duct2
counter=1;
nightduct2=0;
night=0;
for i=1:x
if Plotdata(counter,3)==0
        night=night+1;
end
if Plotdata(counter,3)==0 && Plotdata(counter,9)>0
        nightduct2=nightduct2+1;
end
    counter=counter+1;
end
percent2ductnight=(nightduct2/night)*100;
table(3,2)=percent2ductnight;

%finds frequency of daytime duct3
counter=1;
dayduct3=0;
day=0;
for i=1:x
if Plotdata(counter,3)==1200
        day=day+1;
end
if Plotdata(counter,3)==1200 && Plotdata(counter,12)>0
        dayduct3=dayduct3+1;
end
    counter=counter+1;
end
percent3ductday=(dayduct3/day)*100;
table(2,3)=percent3ductday;

%finds frequency of nighttime duct3
counter=1;
nightduct3=0;
night=0;
for i=1:x
if Plotdata(counter,3)==0
        night=night+1;
end
if Plotdata(counter,3)==0 && Plotdata(counter,12)>0
```

```
            nightduct3=nightduct3+1;
end
    counter=counter+1;
end
percent3ductnight=(nightduct3/night)*100;
table(3,3)=percent3ductnight;
%_____HEIGHTS_____(line 4 to 8 of table)_____
%finds mean height of duct 1
counter = 1;
j=1;
for i=1:x
if Plotdata(counter,6)>0
        temp1(j)=Plotdata(counter,6);
        j=j+1;
end
    counter=counter+1;
end
table(4,1)=mean(temp1);

%finds mean height of duct 2

counter = 1;
j=1;
for i=1:x
if Plotdata(counter,9)>0
        temp2(j)=Plotdata(counter,9);
        j=j+1;
end
    counter=counter+1;
end
table(4,2)=mean(temp2);

%finds mean height of duct 3

counter = 1;
j=1;
for i=1:x
if Plotdata(counter,12)>0
        temp3(j)=Plotdata(counter,12);
        j=j+1;
end
    counter=counter+1;
end
table(4,3)=mean(temp3);

% find medians of duct's heights

table(6,1)=median(temp1); %Duct 1
table(6,2)=median(temp2); %Duct 2
table(6,3)=median(temp3); %Duct 3

% compute 25th percentile (first quartile) for duct1
table(5,1) = median(temp1(find(temp1<median(temp1))));
```

```matlab
% compute 75th percentile (third quartile) for duct1
table(7,1) = median(temp1(find(temp1>median(temp1))));

% compute 25th percentile (first quartile) for duct2
table(5,2) = median(temp2(find(temp2<median(temp2))));

% compute 75th percentile (third quartile) for duct2
table(7,2) = median(temp2(find(temp2>median(temp2))));

% compute 25th percentile (first quartile) for duct3
table(5,3) = median(temp3(find(temp3<median(temp3))));

% compute 75th percentile (third quartile) for duct3
table(7,3) = median(temp3(find(temp3>median(temp3))));


% standard deviations of duct's heights

table(8,1)=std(temp1); %Duct 1
table(8,2)=std(temp2); %Duct 2
table(8,3)=std(temp3); %Duct 3

%_____THICKNESS_____(line 9 to 13 of table)_____
% find mean, median and std. dev. of duct's thickness
% Duct1
counter = 1;
j=1;
temp1=0;
for i=1:x
if Plotdata(counter,25)>0
        temp1(j)=Plotdata(counter,25);
        j=j+1;
end
    counter=counter+1;
end
table(9,1)=mean(temp1);
table (11,1)=median(temp1);
table(13,1)=std(temp1);

% compute 25th percentile (first quartile) for duct1
table(10,1) = median(temp1(find(temp1<median(temp1))));

% compute 75th percentile (third quartile) for duct1
table(12,1) = median(temp1(find(temp1>median(temp1))));

%Duct2
counter = 1;
j=1;
temp2=0;
for i=1:x
if Plotdata(counter,26)>0
        temp2(j)=Plotdata(counter,26);
        j=j+1;
```

```matlab
end
    counter=counter+1;
end
table(9,2)=mean(temp2);
table (11,2)=median(temp2);
table(13,2)=std(temp2);

% compute 25th percentile (first quartile) for duct2
table(10,2) = median(temp2(find(temp2<median(temp2))));

% compute 75th percentile (third quartile) for duct2
table(12,2) = median(temp2(find(temp2>median(temp2))));

%Duct3
counter = 1;
j=1;
temp3=0;
for i=1:x
if Plotdata(counter,27)>0
        temp3(j)=Plotdata(counter,27);
        j=j+1;
end
    counter=counter+1;
end
table(9,3)=mean(temp3);
table (11,3)=median(temp3);
table(13,3)=std(temp3);

% compute 25th percentile (first quartile) for duct3
table(10,3) = median(temp3(find(temp3<median(temp3))));

% compute 75th percentile (third quartile) for duct3
table(12,3) = median(temp3(find(temp3>median(temp3))));

%---------------SURFACE DUCTS------(column 4 of table)-------

%M starting negative

%_____Frequency of Occurance__(line 1 to 3)_____

clear temp
counter=1;
j=1;
temp=0;
for i=1:x
if Plotdata(counter,7)==Plotdata(counter,8) && Plotdata(counter,7)>0
    temp(j)=Plotdata(counter,6); %height of duct's top
    j=j+1;
end
    counter=counter+1;
end
if temp>0
a=length(temp);
else
```

```matlab
a=0;
end
table(1,4)=(a/x)*100; % occurance throughout the day

%_____Heights Statistics_____(line 4 to 8)_____
table(4,4)=mean(temp);
table (6,4)=median(temp);
table(8,4)=std(temp);
% compute 25th percentile (first quartile) for duct1
table(5,4) = median(temp(find(temp<median(temp))));

% compute 75th percentile (third quartile) for duct1
table(7,4) = median(temp(find(temp>median(temp))));


%M starting positive

%_____Thickness Statistics_____(line 9 to 13)_____
% find mean, median and std. dev. of thickness
% surface duct
counter = 1;
j=1;
temp=0;
for i=1:x
if Plotdata(counter,15)==1 && Plotdata(counter,25)>0
% if attached but M does not start negative
        temp(j)=Plotdata(counter,25);
        j=j+1;
end
    counter=counter+1;
end
table(9,4)=mean(temp);
table (11,4)=median(temp);
table(13,4)=std(temp);

% compute 25th percentile (first quartile) for surface duct
table(10,4) = median(temp1(find(temp1<median(temp))));

% compute 75th percentile (third quartile) for surface duct
table(12,4) = median(temp1(find(temp1>median(temp))));
%_____
counter=1;
j=1;
temp=0;
for i=1:x
if Plotdata(counter,3)==1200.... %sounding taken at 1200z
&& Plotdata(counter,7)==Plotdata(counter,8) && Plotdata(counter,7)>0
    temp(j)=Plotdata(counter,7);
    j=j+1;
end
    counter=counter+1;
end
if temp>0
a=length(temp);
else
```

```matlab
a=0;
end
table(2,4)=(a/day)*100; % occurance during daytime


counter=1;
j=1;
temp=0;
for i=1:x
if Plotdata(counter,3)==0.... % sounding taken at 0000z
&& Plotdata(counter,7)==Plotdata(counter,8) && Plotdata(counter,7)>0
    temp(j)=Plotdata(counter,7);
    j=j+1;
end
    counter=counter+1;
end
if temp>0
a=length(temp);
else
a=0;
end
table(3,4)=(a/night)*100; % occurance during nighttime




%------This the end of surface ducts statistics-----------------

%-----------STRENGTH OF DUCTS-----(line 14 to 23)---------------

% First duct M strength
counter = 1;
j=1;
for i=1:x
if Plotdata(counter,32)>0   %indeed, there is a duct
        tmp1(j)=Plotdata(counter,32);
        j=j+1;
end
    counter=counter+1;
end
table(14,1)=mean(tmp1);
table (16,1)=median(tmp1);
table(18,1)=std(tmp1);
% compute 25th percentile (first quartile) for duct1
table(15,1) = median(tmp1(find(tmp1<median(tmp1))));

% compute 75th percentile (third quartile) for duct1
table(17,1) = median(tmp1(find(tmp1>median(tmp1))));


% Second duct M strength
counter = 1;
j=1;
```

```matlab
for i=1:x
if Plotdata(counter,33)>0         %indeed, there is a duct
        tmp2(j)=Plotdata(counter,33);
        j=j+1;
end
    counter=counter+1;
end
table(14,2)=mean(tmp2);
table (16,2)=median(tmp2);
table(18,2)=std(tmp2);
% compute 25th percentile (first quartile) for duct2
table(15,2) = median(tmp2(find(tmp2<median(tmp2))));

% compute 75th percentile (third quartile) for duct2
table(17,2) = median(tmp2(find(tmp2>median(tmp2))));


% Third duct M strength
counter = 1;
j=1;
temp3=0;
for i=1:x
if Plotdata(counter,34)>0          %indeed, there is a duct
        tmp3(j)=Plotdata(counter,34);
        j=j+1;
end
    counter=counter+1;
end
table(14,3)=mean(tmp3);
table (16,3)=median(tmp3);
table(18,3)=std(tmp3);
% compute 25th percentile (first quartile) for duct3
table(15,3) = median(tmp3(find(tmp3<median(tmp3))));

% compute 75th percentile (third quartile) for duct3
table(17,3) = median(tmp3(find(tmp3>median(tmp3))));

% First duct M gradient
counter = 1;
j=1;
tmp1=0;
for i=1:x
if Plotdata(counter,35)>0          %indeed, there is a duct
        tmp1(j)=Plotdata(counter,35);
        j=j+1;
end
    counter=counter+1;
end
table(19,1)=mean(tmp1);
table (21,1)=median(tmp1);
table(23,1)=std(tmp1);
% compute 25th percentile (first quartile) for duct1
table(20,1) = median(tmp1(find(tmp1<median(tmp1))));
% compute 75th percentile (third quartile) for duct1
```

```matlab
table(22,1) = median(tmp1(find(tmp1>median(tmp1))));


% Second duct M gradient
counter = 1;
j=1;
tmp2=0;
for i=1:x
if Plotdata(counter,36)>0          %indeed, there is a duct
        tmp2(j)=Plotdata(counter,36);
        j=j+1;
end
    counter=counter+1;
end
table(19,2)=mean(tmp2);
table (21,2)=median(tmp2);
table(23,2)=std(tmp2);
% compute 25th percentile (first quartile) for duct2
table(20,2) = median(tmp2(find(tmp2<median(tmp2))));

% compute 75th percentile (third quartile) for duct2
table(22,2) = median(tmp2(find(tmp2>median(tmp2))));


% Third duct M gradient
counter = 1;
j=1;
tmp3=0;
for i=1:x
if Plotdata(counter,37)>0          %indeed, there is a duct
        tmp3(j)=Plotdata(counter,37);
        j=j+1;
end
    counter=counter+1;
end
table(19,3)=mean(tmp3);
table (21,3)=median(tmp3);
table(23,3)=std(tmp3);
% compute 25th percentile (first quartile) for duct3
table(20,3) = median(tmp3(find(tmp3<median(tmp3))));

% compute 75th percentile (third quartile) for duct3
table(22,3) = median(tmp3(find(tmp3>median(tmp3))));


% surface ducts = attached to the surface

% M strength
counter = 1;
j=1;
tmp1=0;
for i=1:x
if Plotdata(counter,15)==1
if Plotdata(counter,32)>0 %indeed, there is a duct
```

```matlab
        tmp1(j)=Plotdata(counter,32);
        j=j+1;
end
end
    counter=counter+1;

end
table(14,4)=mean(tmp1);
table (16,4)=median(tmp1);
table(18,4)=std(tmp1);
% compute 25th percentile (first quartile) for duct1
table(15,4) = median(tmp1(find(tmp1<median(tmp1))));

% compute 75th percentile (third quartile) for duct1
table(17,4) = median(tmp1(find(tmp1>median(tmp1))));

% M gradient
counter = 1;
j=1;
tmp1=0;
for i=1:x
if Plotdata(counter,15)==1
if Plotdata(counter,35)>0          %indeed, there is a duct
        tmp1(j)=Plotdata(counter,35);
        j=j+1;
end
end
    counter=counter+1;

end
table(19,4)=mean(tmp1);
table (21,4)=median(tmp1);
table(23,4)=std(tmp1);
% compute 25th percentile (first quartile) for duct1
table(20,4) = median(tmp1(find(tmp1<median(tmp1))));

% compute 75th percentile (third quartile) for duct1
table(22,4) = median(tmp1(find(tmp1>median(tmp1))));

%----This is the end of strength of ducts--------------------------

%------------------------------------------------------------------
% find mins and maxs heights of first duct (line 24,25)
counter = 1;
j=1;
tempmin1=0;
tempmax1=0;
for i=1:x
if Plotdata(counter,8)~=0

        tempmin1(j)=Plotdata(counter,8);
        tempmax1(j)=Plotdata(counter,6);
        j=j+1;
```

```
end
    counter=counter+1;

end
table(24,1)=min(tempmin1); %minimum of lower boundary height
table(25,1)=max(tempmax1); %maximum of upper boundary height

% find mins and maxs heights of second duct (line 24,25)
counter = 1;
j=1;
tempmin2=0;
tempmax2=0;
for i=1:x
if Plotdata(counter,11)~=0

        tempmin2(j)=Plotdata(counter,11);
        tempmax2(j)=Plotdata(counter,9);
        j=j+1;

end
    counter=counter+1;

end
table(24,2)=min(tempmin2); %minimum of lower boundary height
table(25,2)=max(tempmax2); %maximum of upper boundary height

% find mins and maxs heights of third duct (line 24,25)
counter = 1;
j=1;
tempmin3=0;
tempmax3=0;
for i=1:x
if Plotdata(counter,14)~=0

        tempmin3(j)=Plotdata(counter,14);
        tempmax3(j)=Plotdata(counter,12);
        j=j+1;

end
    counter=counter+1;

end
table(24,3)=min(tempmin3); %minimum of lower boundary height
table(25,3)=max(tempmax3); %maximum of upper boundary height

% find mins and maxs heights of surface duct (line 24,25)
counter = 1;
j=1;
tempmin=0;
tempmax=0;
for i=1:x
if Plotdata(counter,15)==1 && Plotdata(counter,8)~=0
```

```matlab
        tempmin(j)=Plotdata(counter,8);
        tempmax(j)=Plotdata(counter,6);
        j=j+1;

end
    counter=counter+1;

end
table(24,4)=min(tempmin);
table(25,4)=max(tempmax);

%------------------------------------------------------------------------
----

% finds mean, median, first and second quartiles, std. deviation of
% Mdeficit of surface ducts (line 26 to 30)
counter = 1;
j=1;
tempdeficit=0;
for i=1:x
if Plotdata(counter,39)> 0
        tempdeficit(j)=Plotdata(counter,39);
        j=j+1;
end

    counter=counter+1;

end
table(26,4)=mean(tempdeficit);
table (28,4)=median(tempdeficit);
table(30,4)=std(tempdeficit);
% compute 25th percentile (first quartile) for duct1
table(27,4) =
median(tempdeficit(find(tempdeficit<median(tempdeficit))));

% compute 75th percentile (third quartile) for duct1
table(29,4) =
median(tempdeficit(find(tempdeficit>median(tempdeficit))));

%--------SURFACE PRESSURE STATISTICS (line 31 to 35)----------------

%Finds mean, median, lower and higher quartile and std. deviation of
%surface Plotdata pressure if there is a duct (column 1)
counter = 1;
j=1;
temp=0;
for i=1:x
if Plotdata(counter,6)> 0
        temp(j)=Plotdata(counter,22);
        j=j+1;
end

    counter=counter+1;
```

151

```matlab
end

table(31,1)=mean(temp);
table (33,1)=median(temp);
table(35,1)=std(temp);
% compute 25th percentile (first quartile) for duct1
table(32,1) = median(temp(find(temp<median(temp))));

% compute 75th percentile (third quartile) for duct1
table(34,1) = median(temp(find(temp>median(temp))));

%Finds mean, median, lower and higher quartile and std. deviation of
%surface Plotdata pressure if there is  no duct (column 2)
counter = 1;
j=1;
temp=0;
for i=1:x
if Plotdata(counter,6)== 0
        temp(j)=Plotdata(counter,22);
        j=j+1;
end

    counter=counter+1;

end

table(31,2)=mean(temp);
table (33,2)=median(temp);
table(35,2)=std(temp);
% compute 25th percentile (first quartile) for duct1
table(32,2) = median(temp(find(temp<median(temp))));

% compute 75th percentile (third quartile) for duct1
table(34,2) = median(temp(find(temp>median(temp))));

%Finds mean, median, lower and higher quartile and std. deviation of
%surface Plotdata presssure if there is a surfaceduct (column 3)
counter = 1;
j=1;
temp=0;
for i=1:x
if Plotdata(counter,15)==1
        temp(j)=Plotdata(counter,22);
        j=j+1;
end

    counter=counter+1;

end
table(31,3)=mean(temp);
table (33,3)=median(temp);
table(35,3)=std(temp);
```

```matlab
% compute 25th percentile (first quartile) for duct1
table(32,3) = median(temp(find(temp<median(temp))));

% compute 75th percentile (third quartile) for duct1
table(34,3) = median(temp(find(temp>median(temp))));

%//end of file
```

D.   MATLAB CODE TO EXTRACT THE METEOROLOGICAL VARIABLES FROM THE SOUNDING AND COMPUTE THE VERTICAL RESOLUTION

```matlab
function decode_and_save_soundings(filename)
%
% Purpose:  decodes for files with format below.  MUST, MUST have
%           a blank line between soundings.
%
% format:
% LGIR Observations at 00Z 01 Jan 2005
% -----------------------------------------------------------------
%    PRES   HGHT   TEMP   DWPT   RELH   MIXR   DRCT   SKNT   THTA
%     hPa     m     C      C      %     g/kg    deg   knot    K
% -----------------------------------------------------------------
%  1016.0    39    9.6    7.0     84    6.22    160      6  281.5
%  1009.0    95   12.0    8.5     79    6.94    184      6  284.4
%  1000.0   168   12.2    6.2     67    5.98    215      6  285.4
%   987.0   277   11.6    6.6     71    6.23    234      6  285.8
% Station information and sounding indices
%                          Station identifier: LGIR
%                              Station number: 16754
%                            Observation time: 050101/0000
%                            Station latitude: 35.33
%                           Station longitude: 25.18
%                           Station elevation: 39.0
%                             Showalter index: 11.02
%                                Lifted index: 9.45
%     LIFT computed using virtual temperature: 9.38
%                                 SWEAT index: 72.32
%                                     K index: -11.20
%                          Cross totals index: 17.20
%                       Vertical totals index: 19.10
%                         Totals totals index: 36.30
%         Convective Available Potential Energy: 7.46
%              CAPE using virtual temperature: 12.88
%                        Convective Inhibition: -14.83
%              CINS using virtual temperature: -13.39
%                            Equilibrum Level: 803.48
%   Equilibrum Level using virtual temperature: 800.10
%                    Level of Free Convection: 870.17
%                LFCT using virtual temperature: 877.40
```

```
%                         Bulk Richardson Number: 0.11
%              Bulk Richardson Number using CAPV: 0.18
%   Temp [K] of the Lifted Condensation Level: 278.77
% Pres [hPa] of the Lifted Condensation Level: 921.85
%       Mean mixed layer potential temperature: 285.35
%                Mean mixed layer mixing ratio: 6.24
%                1000 hPa to 500 hPa thickness: 5472.00
% Precipitable water [mm] for entire sounding: 13.18
%
% LGIR Observations at 12Z 01 Jan 2005
% -----------------------------------------------------------------
%    PRES   HGHT   TEMP   DWPT   RELH   MIXR   DRCT   SKNT   THTA
%    hPa     m      C      C      %     g/kg   deg    knot    K
% -----------------------------------------------------------------
%  1016.0     39   15.8    9.8    68   7.54    350      4  287.6
%  1014.0     56   13.4    6.4    63   5.98    349      4  285.4
%
%
% ------------------------------------------------
% Modified 5/9/11 by M. Jordan, NPS/MR
% ------------------------------------------------
% Last modified at 11/15/2011 by Kostas Raptis
%_____


fid_in=fopen(filename,'r');
if fid_in > 0
    disp(['Sounding file opened: '  filename])
end


% counter for all data
bigcounter = 0;

% Preallocate Matrices
N_sounding = 1000;
N_rows_each_sounding = 200;
pres_all_soundings = NaN*ones(N_rows_each_sounding,N_sounding);
hght_all_soundings =NaN*ones(N_rows_each_sounding,N_sounding);
tmpc_all_soundings = NaN*ones(N_rows_each_sounding,N_sounding);
dwpc_all_soundings = NaN*ones(N_rows_each_sounding,N_sounding);
relh_all_soundings = NaN*ones(N_rows_each_sounding,N_sounding);
mixr_all_soundings = NaN*ones(N_rows_each_sounding,N_sounding);
drct_all_soundings = NaN*ones(N_rows_each_sounding,N_sounding);
sknt_all_soundings = NaN*ones(N_rows_each_sounding,N_sounding);
thta_all_soundings = NaN*ones(N_rows_each_sounding,N_sounding);
q_all_soundings = NaN*ones(N_rows_each_sounding,N_sounding);
M_all_soundings = NaN*ones(N_rows_each_sounding,N_sounding);
N_all_soundings = NaN*ones(N_rows_each_sounding,N_sounding);
YYMMDD_HHMM_matrix = [];
STATION_ID_matrix = [];
res=0;
%This loop for all year
while 1

% clear variables before start to read next sounding
    clear preshghttmpcdwpcrelhmixrdrctsknt
```

```matlab
    clear thtaqMN

% Skip first five rows header
for ihead = 1:5;
        line = fgetl(fid_in);
end
%
%initialize a line counter
    iline=0;
%
%This loop reads each line
while 1
%Read each line as a character string
        line=fgetl(fid_in) ;
%This loop finds missing value for dwpt
while line (22:28) == '       '
             line=fgetl(fid_in);
end
%This is statement for reading headers
if line (1:7) == 'Station'
             line=fgetl(fid_in);
             station_ID_str = line(46:49);
             line=fgetl(fid_in);
             station_number = str2num(line(46:50));
             line=fgetl(fid_in);
             date_time_str = line(46:56);
             line=fgetl(fid_in);
%This loop skip other lines
while ~isempty(line) %line(44) == ':'
                line=fgetl(fid_in);
%Check for the effective "end-of-file"
if line == -1
break
end
end
end

%Check for the end of one data set
if isempty(line)
break
end
%Check for the effective "end-of-file"
if line == -1
break
end

%Increment line counter.  This is the index for each data array
        iline = iline+1;
%Reads data from file
        pres(iline,1) = str2num(line(1:7));
%disp(pres(iline));
        hght(iline,1) = str2num(line(8:14));
        tmpc(iline,1) = str2num(line(15:21));
        dwpc(iline,1) = str2num(line(22:28));
        relh(iline,1) = str2num(line(29:35));
```
155

```matlab
        mixr(iline,1) = str2num(line(36:42));

if line(48:56) =='         '
            drct(iline,1) = NaN;
            sknt(iline,1) = NaN;
else
            drct(iline,1) = str2num(line(47:49));
            sknt(iline,1) = str2num(line(54:56));
end


end% This is the end of the WHILE Loop



% Calculate theta & q
    [thta,q] = theta_q(pres,tmpc,relh);

% Calculate M and N
    [M,N] = m_n_profile(pres,tmpc,relh,hght);

    bigcounter = bigcounter + 1;

% store each sounding variable in Matrix
    pres_all_soundings(1:length(pres),bigcounter) = pres;
    hght_all_soundings(1:length(hght),bigcounter) = hght;
    tmpc_all_soundings(1:length(tmpc),bigcounter) = tmpc;
    dwpc_all_soundings(1:length(dwpc),bigcounter) = dwpc;
    relh_all_soundings(1:length(relh),bigcounter) = relh;
    mixr_all_soundings(1:length(mixr),bigcounter) = mixr;
    drct_all_soundings(1:length(drct),bigcounter) = drct;
    sknt_all_soundings(1:length(sknt),bigcounter) = sknt;
    thta_all_soundings(1:length(thta),bigcounter) = thta;
    q_all_soundings(1:length(q),bigcounter) = q;
    M_all_soundings(1:length(M),bigcounter) = M;
    N_all_soundings(1:length(N),bigcounter) = N;

    STATION_ID_matrix = char(STATION_ID_matrix, station_ID_str);
    STATION_NUMBER_matrix(bigcounter,1) = station_number;
    YYMMDD_HHMM_matrix = char(YYMMDD_HHMM_matrix,date_time_str);

% computation of vertical resolution
if hght_all_soundings(2,bigcounter)<101 % this is the rounded up
        res=res+1;                                  % height of upper quartile
end

%Check for the effective "end-of-file"
if line == -1
break
end
end
res
percentage=(res*100)/bigcounter
fclose(fid_in); % --- end of sounding "decoder" portion
```

```matlab
% remove extra lines & columns in data matrices
STATION_ID_matrix(1,:) = [];
YYMMDD_HHMM_matrix(1,:) = [];
% remove extra columns
pres_all_soundings(:,bigcounter+1:end) = [];
hght_all_soundings(:,bigcounter+1:end) = [];
tmpc_all_soundings(:,bigcounter+1:end) = [];
dwpc_all_soundings(:,bigcounter+1:end) = [];
relh_all_soundings(:,bigcounter+1:end) = [];
mixr_all_soundings(:,bigcounter+1:end) = [];
drct_all_soundings(:,bigcounter+1:end) = [];
sknt_all_soundings(:,bigcounter+1:end) = [];
thta_all_soundings(:,bigcounter+1:end) = [];
q_all_soundings(:,bigcounter+1:end) = [];
M_all_soundings(:,bigcounter+1:end) = [];
N_all_soundings(:,bigcounter+1:end) = [];
for i = 1:bigcounter
    one_P = pres_all_soundings(:,i);
    index = ~isnan(one_P);
    number_rows_per_sounding(i) = length(one_P(index));
end
NN = max(number_rows_per_sounding)+1;
% remove extra rows
pres_all_soundings(NN:end,:) = [];
hght_all_soundings(NN:end,:) = [];
tmpc_all_soundings(NN:end,:) = [];
dwpc_all_soundings(NN:end,:) = [];
relh_all_soundings(NN:end,:) = [];
mixr_all_soundings(NN:end,:) = [];
drct_all_soundings(NN:end,:) = [];
sknt_all_soundings(NN:end,:) = [];
thta_all_soundings(NN:end,:) = [];
q_all_soundings(NN:end,:) = [];
M_all_soundings(NN:end,:) = [];
N_all_soundings(NN:end,:) = [];

% add a variable
number_of_soundings = bigcounter;

%  prepare the name for the ".mat" file
%  Logic:  find the "/"s and ".", so we can use the first part of
%  the name.
%
index1=find(filename == '/');          %  find the "/" in the name
if length(index1) == 0                 %  if no "/" in name
    first=1;
else
    iend=length(index1);               %  the last "/"
    first=index1(iend)+1;              %  first character in matfile name
end
index2=find(filename == '.');
last=index2-1;                         %  use characters before the "."
matfile= [filename(1,first:last)  '_all_soundings.mat'];

% clear variables before saving MAT file
```
157

```matlab
clear preshghttmpcdwpcrelhmixrdrctsknt
clear thtaqMNstation_ID_strstation_number
clear date_time_strone_P
clear N_rows_each_soundingN_soundingNN
clear ansiheadilineindex1index2lastlinefid_in
clear indexindex1index2firstlastiendansfilename
clear time_str_UTCidate_str_YYMMDD

% save MAT file
eval(['save ' matfile] )

disp(['MAT file written to current directory: ' matfile ])

% ----- end of function ---------------------------------
```

E.   MATLAB CODE TO GENERATE PLOTS FOR EACH SOUNDING PROFILE

```matlab
% Purpose: To generate plots for M,T and D profile, for each sounding.
% file = plot_all_soundings.m
%
clear all
close all
clc
% Any time the program needs to run it is required to load the
% particular file i.e. "ATHENS_2007_JUL_all_soundings.mat",
% which has been derived from the "decode_and_save_soundings.m"
load ATHENS_2007_JUL_all_soundings.mat

for i = 1:number_of_soundings
    hght = hght_all_soundings(:,i);   % extract i-th column
    tmpc = tmpc_all_soundings(:,i);   % extract i-th column
    dwpc = dwpc_all_soundings(:,i);   % extract i-th column
    M = M_all_soundings(:,i);         % extract i-th column
    DateTime_str = YYMMDD_HHMM_matrix(i,:);   % extract i-th row
    Station_str = STATION_ID_matrix(i,:);   % extract i-th row

    figure(i)    % use same figure window
    clf          % clear the figure
    subplot(1,2,1)
    plot(tmpc,hght,'b*-',dwpc,hght,'g+-')
    legend('Temp','DewPt')
    xlabel('Temperature (C)')
    ylabel('Height (m)')
    title([Station_str ', ' DateTime_str])
    grid on
    subplot(1,2,2)
    plot(M,hght,'bx-')
    xlabel('Modified Refractive Index (unitless)')
    ylabel('Height (m)')
    title(['Data Matrix Column number: ' int2str(i)])
```

```matlab
%eval(['print -dpng ' Station_str '_' DateTime_str(1:6) '_'
DateTime_str(8:end)])
end
```

THIS PAGE INTENTIONALLY LEFT BLANK

LIST OF REFERENCES

Aviation Meteorology, cited 2012: Related Issue 17:Climate in Europe. [Available online at http://www.aviamet.gr/cms.jsp?moduleId=022&extLang=LG]

Babin, S. M., 1996: Surface duct height distributions for Wallops Island, Virginia, 1985-1994. *J. Appl. Meteor.*, **35**, 86–93.

Bech, J., B. Codina, J. Lorente, and D. Bebbington, 2002: Monthly and daily variations of radar anomalous propagation conditions: How "normal" is normal propagation? *Proc. Second European Meteorological Radar Conf.,* Delft, Netherlands, Copernicus GmbH, 35–39.

Climate Prediction Center, cited 2012: Teleconnection Patterns, North Atlantic Oscillation. [Available online at http://www.cpc.ncep.noaa.gov/data/teledoc/nao.shtml].

COST Action 255, 2002: Radiowave Propagation Modelling for SatCom Services at Ku-Band and Above – Final Report, European Cooperation in Science and Technology, European Space Agency.

Craig, K. H., and T. G. Hayton, 1995: Climatic mapping of refractivity parameters from radiosonde data. *Proc. Conf. 567 on Propagation Assessment in Coastal Environments*, Bremerhaven, Germany, AGARD-NATO, 43-1–43-14.

Davidson, K. L., 2003. *Assessment Of Atmospheric Factors in EM/EO Propagation*. Course notes, Department of Meteorology, Naval Postgraduate School, Monterey, CA.

Guest, P., 2010: *MR3419 Course Lecture 12: Refraction Above the Surface Layer, Basic Principles.* Department of Meteorology, Naval Postgraduate School, Monterey, California, 56 pp.

Hayton, T. G., and K. H. Craig, 1996: Use of Radiosonde Data in Propagation Prediction. *Remote Sensing of the Propagation Environment (Digest No: 1996/221)*, IEE Colloquium on, doi:10.1049/ic:19961186.

Helvey, R., J. Rosenthal, L. Eddington, P. Greiman, and C. Fisk, 1995: Use of satellite imagery and other indicators to assess variability and climatology of oceanic elevated ducts. *AGARD/NATO Conf. on Propagation Assessment in Coastal Environments,* Bremerhaven, Germany, NATO, 1–14.

Isaakidis, S. A., D. T. Xenos, and A. N. Dris, 2004: Tropospheric ducting phenomena over the Hellenic region.*Int. J. Commun. Syst.*, **17**, 337–346, doi:10.1002/dac.646

ITU-R, 1999a: The radio refractive index: its formula and refractivity data.Rec. P.453-8, International Telecommunication Union.

ITU-R, 1999b: Effects of tropospheric refraction on radiowave propagation.Rec. P.834-4, International Telecommunication Union.Petty, G. W., 2006: *A First Course In Atmospheric Radiation.* 2nd. Sundog Publishing, 459 pp.

Jacobeit, J., S. Seubert, and A. Dunkeloh, 2007: Links of the Mediterranean Oscillation to mid-latitude and tropical climate dynamics. *ESF-MedCLIVAR 2nd Workshop, Connections between Mediterranean and Global Climate Variability*, Toulon, France, CNRS/IPSL, 13.

Kalnay, E., and Co-Authors, 1996: The NCEP/NCAR 40-year Reanalysis Project, *Bull Amer. Meteor. Soc.,* **77**, no. 3, 437–471.

Kistler, R., and Co-Authors, 2001: The NCEP–NCAR 50-Year Reanalysis: Monthly Means CD-ROM and Documentation. *Bull. Amer. Meteor. Soc.*, **82**, no. 2, 247–267.

Komuscu, A. M., A. Erkan, and S. Selik, 1998: Analysis of Meteorological and Terrain, Features Leading to the Izmir Flash Flood, 3–4 November 1995. *Natural Hazards*, **18**, 1–25.

Mentes, S. and Z. Kaymaz, 2007: Investigation of Surface Duct Conditions over Instanbul, Turkey, *J. Appl. Meteor. Clim.*, **46**, 318–337, doi:10.1175/JAM2452.1.

Murphree, T., 2011: *MR3610 Course Module 23: North Atlantic Oscillation and Arctic Oscillation*. Department of Meteorology, Naval Postgraduate School, Monterey, California, 62 pp.

Petty, G. W., 2006: *A First Course In Atmospheric Radiation*. 2nd ed. Sundog Publishing, 458 pp.

Robinson, A. R., W. G. Leslie, A. Theocharis, and A. Lascaratos, 2001: Mediterranean Sea Circulation, *Ocean Currents*, Indira, Eds., Academic Press, 283–298.

Romanou, A., G. Tselioudis, C. S. Zerefos, C. A. Clayson, J. A. Curry, and A. Anderson, 2010:Evaporation–Precipitation Variability over the Mediterranean and the Black Seas from Satellite and Reanalysis Estimates, *J. Clim.*, **23**, 5268–5287, doi:10.1175/2010JCLI3525.1.

Seyin, E., 2003: Physical features of the Izmir Bay. *Cont. Shelf Res.*, **23**, 957–970, doi:10.1016/S0278-4343(03)00083-9.

Skliris, N., S. S. Sofianos, A. Gkanasos, P. Axaopoulos, A. Mantziafou, and V. Vervatis, 2011: Long-term sea surface temperature. *Advances in Oceanography and Limnology*, **2:2**, 125–139.

Theocharis, A., M. Gacic, and H. Kontoyiannis, 1998: Physical and dynamical processes in the coastal and shelf areas of the Mediterranean. *The Sea*, A. R. Robinson and K. H. Brink, Eds., John Wiley and Sons, Inc., 863–886.

Turk, S., 2010: Atmospheric Effects on Communication and Electronic Warfare Systems within Turkey and Surrounding Areas. M.S. thesis, Department of Meteorology, Naval Postgraduate School, 91 pp.

Unal, Y. S., A. Deniz, H. Toros, and S. Incecik, 2010: Temporal and spatial patterns of precipitation variability for annual, wet and dry seasons in Turkey. *Int. J. Climatol.*, doi:10.1002/joc.2274.

Von Engeln, A., J. Teixeira, 2004. A ducting climatology derived from ECMWF global analysis fields. *J. Geophys. Res*. **109**: D18104, doi: 10.1029/2003JD004380.

Wallace, J. M., and P. V. Hobbs, 2006: *Atmospheric science an indroductory survey*. 2nd ed. Elsevier, 483 pp.

Zervakis,V., D. Gergopoulos, P. Karageorgis, and A. Theocharis, 2004: On the response of the Aegean Sea to climatic variability: a review. *Int. J. Climatol.*, **24**, 1845–1858, doi:10.1002/joc.1108.

Zhu, M., and B. W. Atkinson B. W., 2005: Simulated climatology of atmosphericducts over the Persian Gulf. *Boundary-Layer Meteorol,*. **115**, 433–452, doi:10.1007/s10546-004-1428-1.

THIS PAGE INTENTIONALLY LEFT BLANK

INITIAL DISTRIBUTION LIST

1.   Defense Technical Information Center
      Ft. Belvoir, VA

2.   Dudley Knox Library
      Naval Postgraduate School
      Monterey, CA

3.   Chair
      Department of Meteorology
      Naval Postgraduate School
      Monterey, CA

4.   Chair
      Department of Physical Oceanography
      Naval Postgraduate School
      Monterey, CA

5.   Professor Tom Murphree
      Department of Meteorology
      Naval Postgraduate School
      Monterey, CA

6.   Professor Peter Guest
      Department of Meteorology
      Naval Postgraduate School
      Monterey, CA

7.   Embassy of Greece
      Office of Naval Attaché
      Washington, DC

8.   Hellenic Navy General Staff
      Hellenic Navy
      Cholargos, Athens, Greece

9.   Hellenic Navy Hydrographic Service
      Hellenic Navy
      Cholargos, Athens, Greece